4-3-2009

# Novel Roles for B-Raf in Mitosis and Cancer

Meghan E. K Borysova
*University of South Florida*

# Novel Roles for B-Raf in Mitosis and Cancer

by

Meghan E. K. Borysova

A dissertation submitted in partial fulfillment
of the requirements for the degree of
Doctor of Philosophy
Department of Cancer Biology
Graduate School
University of South Florida

Major Professor: Thomas M. Guadagno, Ph.D.
Gary Reuther, Ph.D.
Alvaro Monteiro, Ph.D.
Huntington Potter, Ph.D.
Andrew Aplin, Ph.D.

Date of Approval:
April 3, 2009

Keywords: siRNA, spindle, centrosome, kinetochores, aneuploidy

*To my husband, my parents, my siblings and my children.*

*It is you who have made me who I am.*

**ACKNOWLEDGEMENTS**

I would like to thank my thesis advisor, Tom Guadagno, for a terrific project and 5 years of mentorship. Dr. Guadagno has great scientific instincts. He always knows when a project is promising and his belief in the end-point does not waiver in the face of scientific challenges. I would like to thank the present and former members of the Guadagno lab for support and assistance. I thank my committee members, Drs. Gary Reuther, Alvaro Monteiro and Huntington Potter, for their availability, guidance and support. I especially thank Gary Reuther who has not only served as my scientific advisor, but has extended himself as a friend throughout my time in graduate school. I thank Dr. Andrew Aplin for traveling to Florida and serving as the outside chairperson for my defense. I would like to thank Ken Wright, the Cancer Biology, Ph.D. program director, for his outstanding mentorship and leadership. The scientific and personal well-being of the students is always Ken's priority. I thank Cathy Gaffney for all of her kindness, support and assistance. I thank the other graduate students, particularly my classmates, for their friendship, drive and determination. I would like to thank the members of the Moffitt's microscope core facility (Ed Seijo, Mark Lloyd, Joe Johnson and Nancy Burke); they have added to the breadth and depth to my microscopy studies. I would like to thank my favorite scientist – my husband, Sergiy Borysov – for his brilliance, wit, humor and endless hours of scientific discussion and debate. And finally, I thank my children, for they have been the greatest inspiration, motivation and gratification during my time in the Cancer Biology, Ph.D. program.

**TABLE OF CONTENTS**

## LIST OF FIGURES

## LIST OF ABBREVIATIONS

| | |
|---|---|
| Apc | Adenomatosis polyposis coli |
| APC | Anaphase promoting complex |
| APC/C | Anaphase promoting complex/cyclosome |
| Bad | Bcl-xL/Bcl-2-associated death promotor |
| BCA | Bicinchoninic acid |
| BE11 | siRNA to B-Raf exon 11 |
| BE3 | siRNA to B-Raf exon 3 |
| Bim | Bcl2 interacting mediator of cell death |
| BRCA | Breast Cancer gene |
| BSA | Bovine serum albumin |
| Bub | Budding uninhibited by benzimidazoles |
| cAMP | Cyclin adenosine monophosphate |
| CAS | Cellular apoptosis susceptibility |
| Cdc | Cell division cycle |
| Cdk | Cyclin-dependent kinase |
| CENP-E | Centromere-associated protein E |
| CHAPS | 3[(3-Cholamidopropyl)dimethylammonio]-1-propanesulfonate |
| CIN | Chromosomal Instability |
| CR | Conserved region |
| CRD | Cysteine rich domain |
| CREST | Calcinosis, Raynaud phenomenon, Esophageal dysmotility, Sclerodactyly, and Telangiectasia |
| CSF | Cytostatic factor |
| DAPI | 4’,6-diamidino-2-phenylindole |

| | |
|---|---|
| DMSO | Dimethylsulfoxide |
| DNA | Deoxyribonucleic acid |
| EDTA | Ethylene diamine tetraacetic acid |
| EGF | Epidermal growth factor |
| EGFR | Epidermal growth factor receptor |
| EGTA | Ethylene glycol bis(aminoethylether)-N,N,N',N'-tetraacetic acid |
| ERK | Extracellular signal-regulated kinase |
| FISH | Fluorescence *in situ* hybridization |
| G1 | Gap 1 phase |
| G2 | Gap 2 phase |
| GDP | Guanosine diphosphate |
| GFP | Green fluorescent protein |
| GTP | Guanosine triphosphate |
| HeLa | Henrietta Lacks |
| HEM | Human epidermal melanocytes |
| HFF | Human foreskin fibroblast |
| HIF | Hypoxia inducible factor |
| HME | Human mammary epithelial |
| Hsp | Heat shock protein |
| hTERT | Human telomerase reverse transcriptase |
| IgG | Immunoglobulin G |
| JNK | Jun N-terminal kinase |
| K-fibers | Kinetochore-fibers |
| Mad | Mitotic arrest deficient |
| MAPK | Mitogen-activated protein kinase |
| MEK | MAPK/ERK kinase |
| MEKK | MAPK/ERK kinase kinase |
| MIN | Microsatellite instability |
| MKP | MAPK phosphatase |
| MMP | Matrix metalloproteinases |
| MMR | Mismatch repair |

| | |
|---|---|
| M-phase | mitosis |
| Mps | Mono-polar spindle |
| MT | Microtubules |
| MTOC | Microtubule organizing center |
| NEB | Nuclear Envelope Breakdown |
| Nek | NIMA-related kinase |
| NER | Nucleotide excision repair |
| NIH | National Institutes of Health |
| NIN | Nucleotide excision repair-associated instability |
| NGF | Neural Growth Factor |
| PAGE | Polyacrylamide gel electrophoresis |
| PBS | Phosphate buffered saline |
| Phospho | Phosphorylated |
| PMSF | Phenylmethanesulphonylfluoride |
| PTC | Papillary thyroid cancer |
| PVDF | Polyvinylidene fluoride |
| Raf | Rapidly accelerated fibrosarcoma |
| Rap | Ribosome associated protein |
| Ras | Rat sarcoma |
| RBD | Ras binding domain |
| RNA | Ribonucleic acid |
| Rsk | Ribosomal S6 kinase |
| SAC | Spindle assembly checkpoint |
| Scr | Scrambled control |
| SDS | Sodium dodecyl sulfate |
| Ser | Serine |
| shRNA | Small (short) hairpin RNA |
| siRNA | Small interfering RNA |
| S-phase | DNA synthesis phase |
| TGF | Transforming growth factor |
| Thr | Threonine |

| | |
|---|---|
| TuRC | Tubulin ring complex |
| Tyr | Tyrosine |
| UV | Ultraviolet |
| V600E | Valine-600-Glutamic acid |
| WT | Wild-type |

**Novel Roles for B-Raf in Mitosis and Cancer**

**Meghan E. K. Borysova**

## ABSTRACT

The MAP kinase pathway is well known for its key roles in regulating cell proliferation and cell cycle progression. MAP kinases have also been implicated in mitotic functions, however these functions are less-well understood. Recent studies from our laboratory used *Xenopus* egg extracts to identify B-Raf as an essential activator of the MAPK cascade during mitosis. Therefore, the first objective of my dissertation research was to determine if B-Raf has functional significance during mitosis in human somatic cells.

Using RNA interference against B-Raf and various immunofluorescence techniques, I show that B-Raf: (1) localizes to and is phosphorylated at a key mitotic structure, (2) is critical for proper mitotic spindle assembly and chromatin congression, (3) is important for the engagement of microtubules with kinetochores during mitosis, and (4) is necessary for activation of the spindle assembly checkpoint.

It has been demonstrated that B-Raf is a prominent oncogene, constitutively activated in the vast majority of melanomas and other cancers. I hypothesized that oncogenic B-Raf expression perturbs mitosis and causes aneuploidy.

First, we show that oncogenic B-Raf expression correlates with mitotic abnormalities in human melanoma cells and that spindle defects are induced when

oncogenic B-Raf is ectopically expressed. Further, using FISH and karyotype analysis, I demonstrate that oncogenic B-Raf drives aneuploidy and chromosome instability in primary, immortalized, and tumor cells.

In summary, my dissertation studies elucidate novel roles for B-Raf in mammalian mitosis. In addition, my studies show for the first time that oncogenic B-Raf disrupts mitosis causing chromosomal instability. I propose that oncogenic B-Raf-induced chromosome instability contributes to tumorigenesis.

# CHAPTER 1

# BACKGROUND AND INTRODUCTION

## Mitosis

The cell cycle is the order of processes by which a cell duplicates and divides its DNA equally into two identical daughter cells. The cell cycle consists of temporally coordinated interphase (G1, S, G2 phases) and mitosis (prophase, metaphase, anaphase and telophase). During interphase cells prepare for mitosis through cell growth, DNA duplication and nutrient accumulation. Mitosis is the ultimate stage in the cell cycle during which the cell partitions its chromosomes and subsequently divides its cytoplasmic components into two identical and distinct daughter cells.

### Stages of Mitosis

Mitosis is an irreversible process whose stages have traditionally been described by gross structural and behavior changes documented by light microscopists. Modern use of fluorescence microscopy has aided in the identification of mitotic stages (Fig. 1). Proteins and enzymatic activities which regulate these morphological changes and their transitions serve as biochemical markers for some of the mitotic phases.

Entry into mitosis directly follows the latter part of the second gap (G2) phase during which cells can be reversibly arrested in response to various stresses [1]. Passage through late G2 serves as a 'point of no return' and marks the termination of interphase

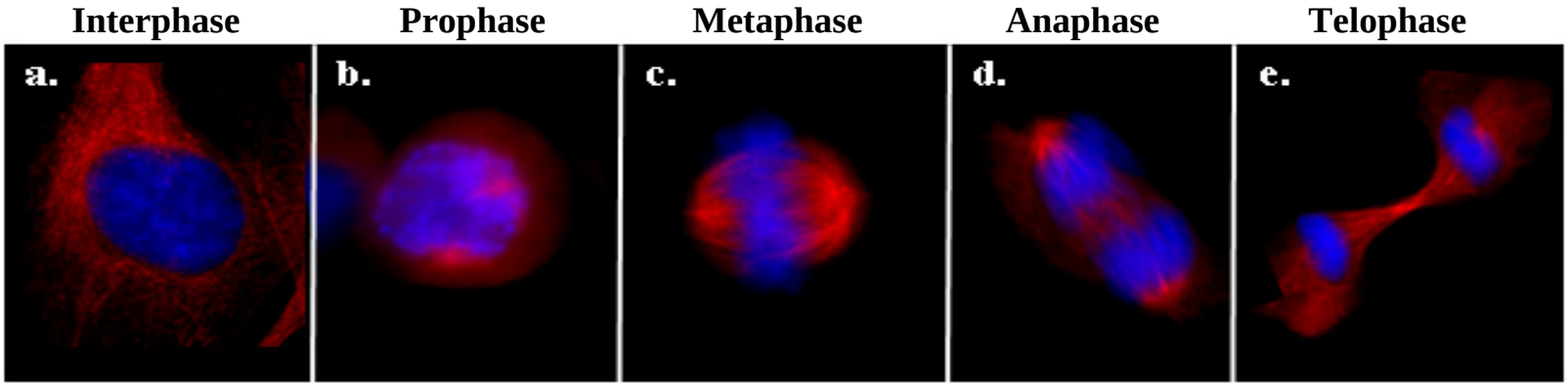


**Figure. 1 Stages of mitosis**
a. Interphase cells have polymerized microtubules, and the decondensed chromatin resides within the nucleus surrounded by a nuclear membrane. b. Prophase is the first stage of mitosis; microtubules are depolymerized from their interphase stage, the DNA begins to condense, the nuclear envelope is broken down and the two centrosomes migrate to opposite poles. c. During metaphase, condensed chromosomes align at the metaphase plate and the bipolar spindle is formed. d. In anaphase, the spindle pulls the chromosomes in a poleward directions. e. During telophase/cytokinesis, the DNA is partitioned into two distinct regions, the nuclear envelopes reform and the cell pinches off into two daughter cells.

and the beginning of mitosis. The phases of mitosis are most frequently referred to as prophase, prometaphase and metaphase – the stages of early mitosis; and anaphase and telophase - the phases of mitotic exit.

Prophase is the initiating stage of mitosis. It is traditionally defined as the point at which condensing chromosomes are first visible in the membrane-bound nucleus when observed by light or fluorescence microscopy. As well during prophase, the two centrosomes (the mother centrosome is duplicated during S-phase) move to opposite poles of the cell [2] where they initiate microtubule nucleation into focal arrays called asters[3]. Centrosomes and asters are visible via fluorescence microscopy. Prophase is accompanied by the nuclear accumulation and activation of cyclin B-Cdk1 (also termed M-phase promoting factor, MPF), the master regulator of mitosis [4-9]. Cyclin B-Cdk1 remains active throughout prophase, prometaphase and metaphase and, therefore, serves as a biochemical marker of early mitosis. It has been shown that Cyclin B-Cdk1 regulates chromosome condensation through direct phosphorylation of the condensin complexes [10-12]. Estimates reveal that DNA is compacted 1000-2000 fold over interphase chromosomes [13] and chromosome condensation is generally completed during prophase. The significance of prophase events cannot be understated. Chromosomes condensation reveals the centromeres upon which the attachment sites for spindle microtubules are assembled. Centrosome segregation is crucial for the organization of a bipolar spindle. Aster formation serves to properly position the mitotic spindle. Prophase ends and prometaphase is initiated when nuclear envelope breakdown become visible by light microscopy. Nuclear envelope breakdown is largely a consequence of phosphorylation of nuclear lamins by the Cyclin B-Cdk1 complex [14].

The nuclear membrane fragments into small vesicles which are eventually fuse during telophase to form the new intact nuclei. Breakdown of the nuclear envelope permits the chromosomes to physically associate with the polymerizing microtubules. Each chromosome has two sister kinetochores, one on each of the fused sister chromatids. During prometaphase kinetochores attach to the microtubules emanating from both poles of the developing spindle [15]. A spindle checkpoint arrest prevents anaphase onset until all kinetochores are fully engaged [16]. Following full engagement, kinetochore associated motor proteins direct the movement of attached chromosomes toward the spindle poles. Spindle microtubule growth acts as an opposing force that pulls the chromosomes toward the center of the mitotic spindle [17]. Eventually the forces balance thus aligning the chromosomes at the spindle equator, called the metaphase plate. It is at this point of chromosome congression that the cell has entered metaphase.

During metaphase chromosomes are aligned at the equator of an organized, fully formed, bipolar spindle (Fig. 2). Cyclin B-Cdk1 remains active during metaphase. Sister chromatids remain fused by cohesin complexes at the region of the centromere [18-20].

Metaphase ends and anaphase is initiated when sister chromatids are disjoined. Sister chromatid segregation results from the abrupt and synchronous degradation of the cohesin molecules that hold them together [21-23]. The onset of anaphase occurs when the anaphase promoting complex/cyclosome (APC/C) becomes active. APC/C is an E3 ubiquitin ligase which targets a number of mitotic substrates including securin and Cyclin B, for proteasome mediated destruction [24]. The destruction of securin allows for the activation of separase which subsequently cleaves the cohesin molecules [25]. After the dissolution of cohesin, kinetochore microtubules begin to shorten and kinetochore forces

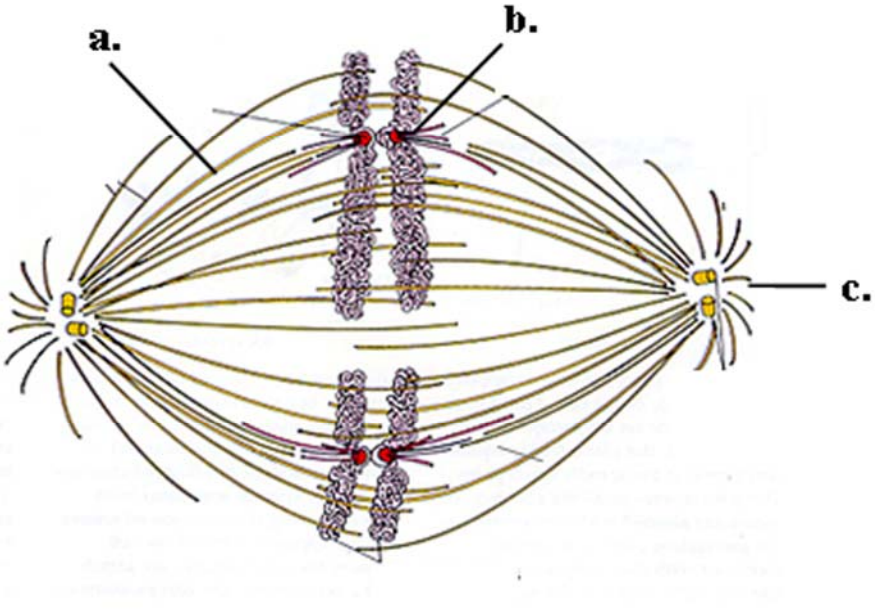


**Figure. 2 The mitotic spindle**
The bipolar spindle apparatus formed during mitosis has several key features: a. microtubules polymerize from the centrosomes to the kinetochores; b. the kinetochores are a proteinaceous structure to which the microtubules attach; c. the centrosomes are the microtubule organizing center (MTOC) of mammalian cells.

result in poleward movement of the chromatids. This movement is detectable by light microscopy and is termed early anaphase or 'anaphase A' which culminates when the chromatids reach the poles. Late anaphase or 'anaphase B' then ensues during which time poleward microtubules elongate thus the entire spindle elongates, thereby partitioning the chromatids further apart [15]. Rapid degradation of cyclin B is the most commonly used biochemical marker for anaphase and leads to the hallmarks of telophase.

Telophase is the final stage of mitosis during which the chromosomes and cytoplasm are ultimately divided [15]. It is during this stage that the nuclear envelopes reform around both sets of chromosomes, the chromosomes decondense, the microtubules return to an interphase state and the cell is divided into two daughter cells. All of these features are detectable through light and fluorescence microscopy. It is due to the destruction of cyclin B-Cdk1 that components of the nuclear envelope and chromosomes no longer undergo phosphorylation, thereby permitting the reformation of the envelope and decondensation of chromosomes. Simultaneously, an actin-myosin contractile ring positioned beneath the plasma membrane causes the membrane to invaginate at the former site of the metaphase plate creating a cleavage furrow in the cytoplasm. Following nuclear envelope reformation, the contractile ring pinches the cell in half at the furrow, thus allowing for the equal separation of the cytoplasm, a process termed cytokinesis. The completion of cytokinesis gives rise to two daughter cells both of which are in the beginning stage of interphase.

**Organization of the Mitotic Spindle**

The mitotic spindle is the structural and functional unit of the cell that is responsible for the mitotic partitioning the duplicated chromosome pairs. While the structure of the spindle apparatus changes continually throughout mitosis, the quintessential metaphase spindle is fusiform - elliptical in shape, having tapered spindle poles and a wide midzone. The basic elements of the mitotic spindle are the centrosomes and the microtubules (Fig. 2). While not primary components of the spindle, chromosomes and kinetochores are necessary for the structural formation of the spindle apparatus.

The spindle poles serve as the microtubule organizing centers (MTOC) that initiate the formation of the mitotic spindle. In animal cells, the MTOCs are centrosomes, organelles containing a pair of orthogonally arranged centrioles surrounded by protein rich pericentriolar material, including pericentrin, ninein, γ-tubulin and others [26-29]. The single centrosome of the cell is duplicated during S-phase. Early in mitosis, Nek2 kinase promotes the migration of the two centrosomes to opposite poles of the cell [30-33]. γ-tubulin and other members of the gamma complex protein family form hundreds of ring-shaped γ-tubulin ring complexes per centrosome (γ-TuRC). γ-tubulin is required for microtubule nucleation [34, 35] and, while the exact mechanism is not completely understood, γ-TuRCs are most likely the sites of microtubule nucleation [36-38].

Microtubule polymers are composed of α- and β-tubulin dimers whose orientation in the polymerized microtubule gives microtubules their polarity. The opposing ends of microtubules have different tubulin-polymerizing properties and orientations in the

mitotic spindle. The relatively static minus ends of the microtubules interact with the pericentriolar material of the centrosome and the highly dynamic plus ends extend away from the centrosome [39, 40]. These intrinsic features of polarity and dynamic instability are what give the microtubules the ability to form the mitotic spindle.

At least three types of microtubules comprise the mitotic spindle, all of which emanate from the MTOC. Astral microtubules are organized in radial arrays around both centrosomes. They connect the spindle poles to the cortex of a mitotic cell, thus, are critical for proper positioning of the mitotic spindle and mark the site for subsequent cell division [41]. Interpolar microtubules polymerize toward the poles opposite of their nucleation. They terminate in the body of the spindle where some of them interact with the plus ends of antiparallel interpolar microtubules thus giving the spindle stability [42]. During late anaphase, the interpolar microtubules polymerize and slide thereby elongating the spindle. Finally, the plus ends of kinetochore fibers (K-fiber), comprised of 20-30 microtubules [43, 44], associate with, and are captured by, the outer kinetochores of the chromosomes, thus connecting the chromosomes to the mitotic spindle [41, 45]. During early anaphase, the kinetochore microtubules shorten forcing the attached chromosomes to move in the direction of the spindle poles.

The centromeres of the chromosomes are specific regions of repetitive DNA sequences, which are critical for proper organization of the mitotic spindle. First, they are the site of fusion between the chromatids thus creating a visible constriction site in metaphase chromosomes. Secondly, they are also the sites where two identical proteinaceous structures called the kinetochores assemble and function. Kinetochores

serve as the sites of microtubule engagement as well as the location of the spindle assembly checkpoint.

Accurate positioning and function of the centrosomes, microtubules and chromosomes are necessary for the proper formation of the metaphase spindle. A properly formed spindle is fusiform in structure with sister chromatids bioriented and symmetrically arranged at the spindle equator. Achieving this arrangement prior to anaphase is critical in order to ensure equal segregation of chromosomes, thereby maintaining the genomic integrity of both daughter cells.

**Spindle Assembly Checkpoint**

In order to prevent chromosomal missegregation from occurring, anaphase must not proceed until all kinetochores are engaged in an amphitelic (bipolar) fashion. A cellular surveillance mechanism called the spindle assembly checkpoint (SAC) ensures that anaphase onset is delayed until all chromosomes have achieved bipolar attachments. [16, 46, 47].

The process by which kinetochores capture K-fibers is largely a stochastic event based on their own chance interactions. In brief, one sister kinetochore becomes engaged with K-fibers of the spindle, generating a monotelic chromosomal attachment. Subsequently the second sister kinetochore captures microtubules from the opposite pole and the chromosome becomes bioriented. This somewhat random process can result in syntelic attachments where K-fibers from one pole engage with both sister kinetochores. As well, merotelic attachments can take place in which case K-fibers from opposite poles

engage with one sister kinetochore. Therefore, monotelic attachments occur as a transitional state prior to achievement of bipolar engagement [48].

Syntelic kinetochore-microtubule attachments cause chromosomes to be positioned near one pole and such attachments elicits the SAC [49]. Merotelic attachments are bipolar by definition, cause chromosomes to align at the metaphase plate and do not elicit a SAC. The mechanism by which the syntelic chromosome orientation is reversed is not understood. However, it has been proposed that Aurora B kinase is instrumental in reversing maloriented attachments [50-54] by phosphorylating targets that cause rapid microtubule turn-over at the kinetochores [55], after which amphitelic attachments are free to take place.

On the biochemical level the metaphase-anaphase transition is driven by the E3 ubiquitin ligase activity of the APC/C which targets securin and cyclin B for proteasomal degradation. The SAC functions as a sensory mechanism by detecting unattached kinetochores and as an effector by inhibiting the activation of the anaphase promoting complex/cyclosome (APC/C) (Fig. 3). The nature of the 'wait anaphase' signal is not completely understood. However, it is widely accepted that the SAC protein complexes assembled at unattached kinetochores early in mitosis and negatively regulate activation of the APC/C, thus preventing anaphase onset [56-60].

A large complex of proteins including Mad1, Mad2, BubR1, Bub1, Bub3, Mps1 and Aurora B, comprise the core spindle checkpoint proteins in yeast [61-64] and mammalian cells [65-67]. It is evident that the proteins of SAC require kinetochore localization and function as large multi-componential protein complexes.

Aurora B [68-70] and Mps1 [71-73] are required for recruitment and localization of all other checkpoint proteins to the kinetochores. The current model for SAC activity suggests that kinetochore bound Mad1 and Mad2 form a complex which can then bind Cdc20, the activator of APC/C [74-78] and the key target of the SAC [79]. However, Cdc20 binding by the Mad1-Mad2 complex is insufficient for inactivating APC/C. BubR1/Mad3 and Bub3 are all required for full inhibition of the APC/C [80, 81]. The BubR1 complex appears to synergize [59] with the Mad1-Mad2-Cdc20 complex by forming a supercomplex that can fully inhibit the APC/C.

Several other proteins have been shown to be involved in the SAC, including the ROD-SWILCH complex [82], p31 [83-85], cyclin B-Cdk1 [86, 87], NEK2 [88] and polo-like kinase-1 (PLK1) [89]. The contribution of these proteins to the SAC is not well understood.

The activity of the spindle assembly checkpoint is essential for preventing chromosome missegregation and aneuploidy [90, 91]. The presence of a single unattached kinetochore is sufficient to activate the SAC and the SAC is not turned off until every kinetochore has formed fully saturated (25-30 microtubules) bipolar microtubule attachments.

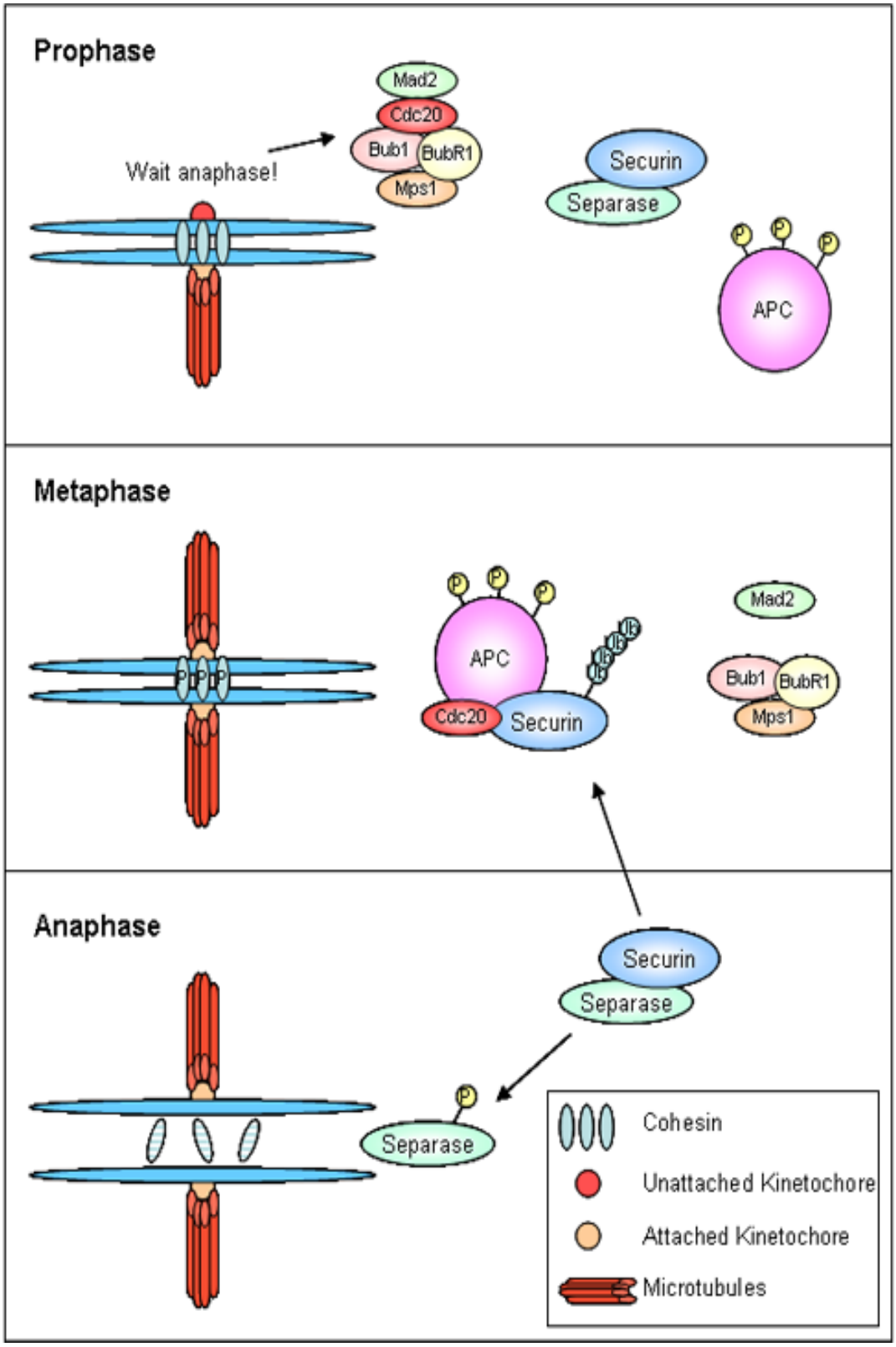


**Fig. 3 The spindle assembly checkpoint**

## MAPK Pathway

The mitogen activated protein kinase (MAPK) pathway is highly conserved from yeast to humans [92, 93]. MAPK signaling integrates a variety of extracellular and intracellular signals to control a broad spectrum of cellular processes including proliferation, survival, stress response and apoptosis [93]. A number of cooperating molecular mechanisms regulate the cascade in order to ensure signaling specificity.

### MAPK Cascade

The basic structure of the MAPK cascade is a module consisting of three kinases which sequentially activate one another through phosphorylation events. The most upstream kinases in the cascade are the serine/threonine kinases, MAP kinase kinase kinases or MAPKKK (MAP3K). Upon their own activation, MAP3Ks phosphorylate and activate the second kinase in the module, MAP kinase kinase or MAPKK (MAP2K) [93, 94]. MAP2Ks are defined as dual-specificity kinases, for upon their activation, they in turn phosphorylate a Thr-X-Tyr motif in the third cascade member, MAP kinase or MAPK [93, 95]. Substrates of MAPK include transcription factors, phospholipases and cytoskeleton-associated proteins.

The family of MAP3Ks, MAP2Ks and MAPKs is large, with at least 20 different members of the mammalian MAPK family identified to date [96]. The four most well described MAPK cascades are named for their relative MAPKs. Jun amino-terminal kinases (JNKs) primarily serve in the response to cellular stress. p38 is also activated in

response to cell stresses and plays a role in cytokine production in hematopoietic cells, cytokine-stimulated proliferation and apoptosis. ERK5 is the least well known MAPK cascade [93] and it has been suggested that ERK5 regulates cell survival and proliferation [97, 98]. The most well studied MAPK pathway is extracellular signal-regulated kinases 1 and 2 (ERK 1/2).

**Regulation and Functions of the ERK 1/2 Pathway**

The ERK 1/2 cascade is implicated primarily in cellular proliferation, differentiation, cell cycle regulation and cell survival [93]. ERK 1/2 phosphorylates many known targets including transcription factors Elk1 [99], c-Fos [100] and p53 [101], all of which play a role in cellular proliferation and transformation. As well, ERK targets include the S6 kinase p90/RSK [102], phospholipase A2 [103], EGFR [93] and several microtubule-associated proteins [103].

Activation of the ERK 1/2 cascade in response to mitogen stimulation has been well studied. During cell cycle entry activation of the ERK1/2 cascade is triggered by engagement and oligomerization of extracellular growth factor receptors [104] which in turn, stimulates the conversion of Ras, a small GTP-ase, from its GDP-bound inactive form to an active GTP-bound form [96, 105]. GTP-bound Ras mediates the translocation of the MAP3K, Raf-1, to the membrane where it is activated by a yet undefined, phosphorylation mechanism [106]. Raf-1 activates MEK which transmits the signal to ERK1/2. Activated ERK1/2 phosphorylates cytoplasmic targets or translocates into the nucleus where it phosphorylates transcription factors which promote S-phase progression [96, 105].

**Mitotic Roles of ERK 1/2**

It is well established that ERK 1/2 regulates the G1/S transition in response to mitogen stimulation [96, 105]. A large but lesser known body of evidence suggests that the ERK 1/2 pathway regulates various mitotic functions including entry and exit from mitosis, spindle assembly, the spindle assembly checkpoint and Golgi apparatus fragmentation (Fig. 4). Despite a growing body of evidence supporting mitotic roles for ERK 1/2, a firm role for ERK 1/2 in mammalian mitosis has not been established.

Early evidence supporting a mitotic role for ERK 1/2 came from studies in *Xenopus* egg extracts where it was shown that p42 (the *Xenopus* ERK 2 homologue) is activated during M-phase [107-110]. As well, ERK activity during mitosis in NIH 3T3 and HeLa cells is detectable via western blot analysis using antibodies that recognize activated ERK [111].

Importantly, reports using immunofluorescence microscopy support the early conclusions from *Xenopus* egg extracts that ERK is activated during mitosis. Several groups have demonstrated that in mammalian cells small pools of active ERK 1/2 and MEK 1/2 are localized to the kinetochores and spindle poles throughout mitosis and to midbody during cytokinesis [112-114] (Fig. 4). Activated p42 has also been shown to localize to mitotic spindles in *Xenopus* egg extracts [115] as well as in fertilized sea urchin eggs [116].

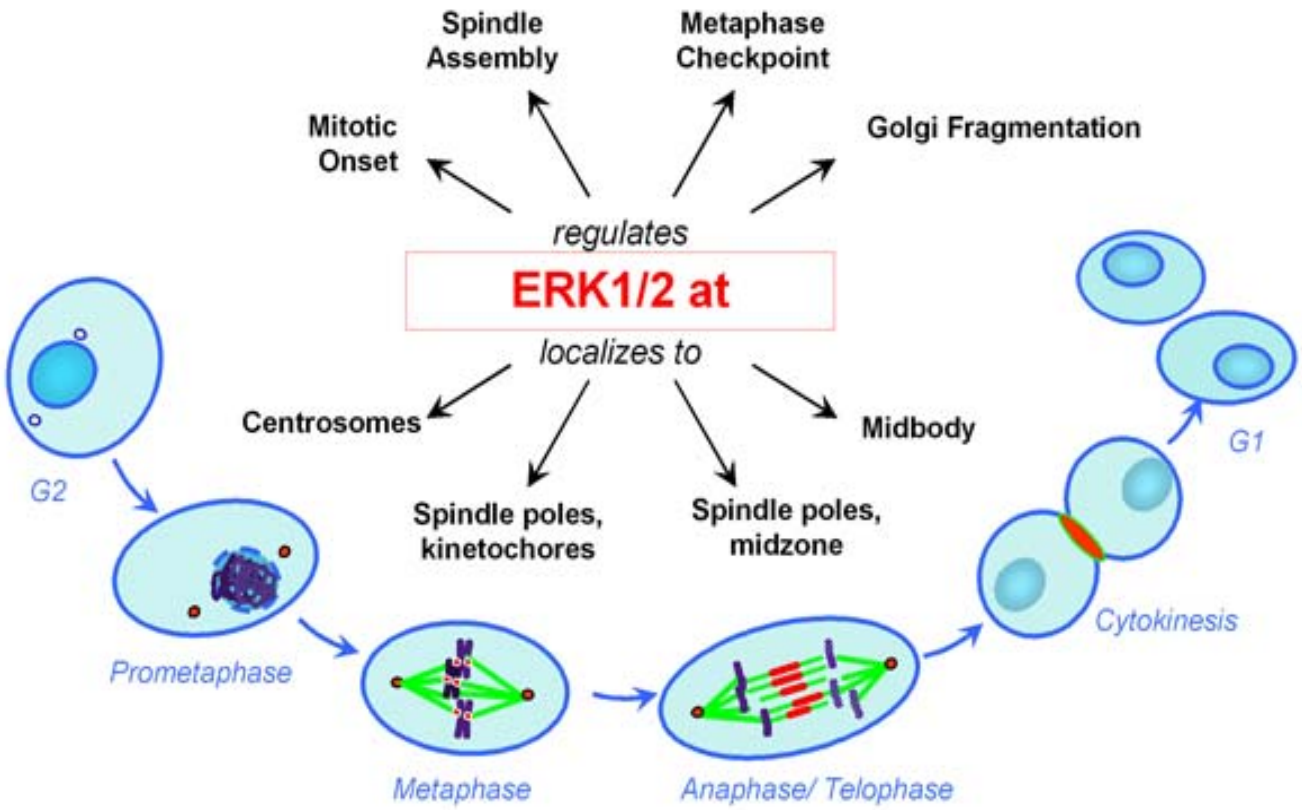


**Fig. 4 MAPK functions and localization during mitosis**

Functional studies have revealed roles for ERK 1/2 in mitotic entry in mammalian cells but not in *Xenopus* egg extracts. In mammalian cells, expression of dominant-negative MEK [117], treatment with MEK inhibitors [111, 117] and RNA interference (RNAi) of MEK 1/2 and ERK 1/2 [118] all induce a G2/M cell cycle arrest. As well, such conditions decrease nuclear translocation of cyclin B-Cdk1 and delay and reduce its activation [111, 117, 118]. Such data supports a role for ERK 1/2 in Cdk1 activation and entry into mitosis in mammalian cells. However, cyclin B-Cdk1 is not affected by the depletion of p42 from *Xenopus* egg extracts [110, 119]. To the contrary, constitutive activation of p42 in this system inhibits cyclin B-Cdk1 and delays entry into mitosis [120, 121]. Further, evidence in *Xenopus* egg extracts revealed that p42 activates Wee1 kinase which directly phosphorylates and inactivates cyclin B-Cdk1 [122]. However, differences in the requirement of MAPK activity in mitotic entry between mammalian cells and *Xenopus* egg extracts, may be explained by their inherently different cell cycles. Indeed, while the cell cycle of somatic cells follows a classic G1-S-G2-M cycle, *Xenopus* egg extracts recapitulate the embryonic cell cycle, which is comprised only of S and M phases, with no gap phases in between. Therefore, *Xenopus* egg extracts may not possess an active G2 phase molecular mechanism. Thus, a role for ERK 1/2 during mitotic entry remains disputable.

ERK 1/2 has been implicated in assembly of the mitotic spindle in several model systems. Early work in mammalian cell culture showed that ERK 1/2 associates with [123] and phosphorylates components of the cytoskeleton [124-126], and it has been demonstrated that ERK 1/2 negatively regulates tubulin polymerization in *Xenopus* egg extracts [108, 115]. Immunodepletion of p42 or pharmacological inhibition of its

activation causes abnormal mitotic spindles to form in *Xenopus* egg extracts [115]. As well, inhibition of ERK 1/2 disrupts formation of the mitotic spindle in mammalian cells [115] and in sea urchin eggs [116].

It has been suggested that ERK 1/2 regulates spindle assembly through regulation of a mitotic motor protein CENP-E. CENP-E is necessary for the establishment of chromosome-microtubule attachment and, therefore, is critical for proper spindle formation. It has been demonstrated in mammalian cells that CENP-E is a mitotic substrate of ERK2, which phosphorylates CENP-E on sites that mediate its association with kinetochores [114].

In cycling *Xenopus* egg extracts, blockade of mitotic p42 activation shortens the duration of mitosis [119]. Along with kinetochore localization of ERK 1/2 in mammalian cells, this data suggests a potential role for ERK in regulation of the SAC. Indeed, maintenance of an induced spindle assembly checkpoint arrest is compromised in p42 depleted [109] or p42 inhibited [127] *Xenopus* egg extracts. As well, loss-of-function mutations in *Drosophila*'s rolled/MAPK gene caused the abrogation of a colchicine induced mitotic arrest in *Drosophila* larvae [128].

Several reports have implicated MAPK in the regulation of SAC. As mentioned above, the SAC arrest depends on several checkpoint proteins including BubR1, Bub3 and Mad2 binding to Cdc20 to inhibit activation of the anaphase promoting complex (APC/C). Using *Xenopus* egg extracts it was shown that during mitotic arrest MAPK phosphorylates Cdc20 on sites that increase its affinity for BubR1, Bub3 and Mad2 and negatively regulate the APC/C [129]. Another report demonstrated that MAPK phosphorylates Mps1, a critical SAC kinase, and this phosphorylation is necessary for

kinetochore localization of SAC proteins in *Xenopus* egg extracts [73]. Therefore, it has been proposed that ERK 1/2 is involved in regulating the SAC.

Supportive of an ERK 1/2 mitotic role in mammalian cells are studies demonstrating that constitutive activation of MAPK via expression of v-mos or v-ras expression in mouse fibroblasts causes cells to fail cytokinesis and become binucleated [130, 131]. This indicates that ERK inactivation is necessary prior to cytokinesis. However, further studies will be necessary in order to definitively establish that ERK 1/2 regulate this critical mitotic stage.

Fragmentation of the Golgi apparatus during mitosis is an essential process and it is thought to be a method for partitioning Golgi membranes equally in both daughter cells [132]. It has been shown that mitotically activated MEK1 (the upstream activator of ERK1) localizes to Golgi membranes in late prophase [133, 134] and that Raf-1 activation of MEK1 is required for mitotic Golgi fragmentation [133, 135, 136]. Further studies demonstrated that Golgi fragmentation is mediated through an unusual, truncated ERK isoform, ERK1c [137, 138]. ERK1c is regulated in an M-phase specific manner, becoming phosphorylated and localizing to the Golgi during early mitosis [138]. These findings indicate that activation of ERK 1/2 pathway during mitosis may differ from its S-phase activation.

In summary, ERK1/2 and their activators, MEK 1/2, localize to key mitotic structures in *Xenopus* egg extracts and in cells grown in culture. Functional studies reveal that ERK 1/2 plays roles in a variety of mitotic functions. While a role for ERK 1/2 in Golgi fragmentation has been established in mammalian cells, roles in spindle assembly

formation and the spindle assembly checkpoint have primarily been studied in the system of *Xenopus* egg extracts.

## B-Raf Kinase

Raf kinases are serine/threonine kinases whose activities regulate a variety of cellular processes including growth, proliferation, survival, differentiation and apoptosis [96, 139, 140]. The Raf family consists of A-Raf, B-Raf and C-Raf (Raf-1), which function as MAP3Ks. Nearly all reported Raf functions result from activation of the MAPK cascade. Rafs share significant sequence identity and are structurally similar. In spite of some similarities, Rafs have some significant differences in their regulation, tissue distribution and developmental functions. While C-Raf is the prototypic Raf kinase, B-Raf has emerged as the most potent activator of MAPK signaling.

### B-Raf Protein Structure

B-Raf, A-Raf and C-Raf share a basic three-domain architecture including conserved domains, CR1, CR2 and CR3 (Fig. 5). CR1 and CR2 are embedded within the N-terminal regulatory portion of Rafs, and CR3 resides in the C-terminal kinase domain. CR1 contains a Ras binding domain (RBD) and a cysteine rich domain (CRD) [141, 142], both of which provide interacting sites for upstream regulators such as Ras and Rap1 [143]. The CR2 domain contains a negatively regulatory phosphorylation site [144-146] and a 14-3-3 binding phospho-epitope [147]. The CR3 domain is the kinase domain, comprised of the N-region and the activation loop, both of which contain phospho-sites

that regulate Raf activity. Unlike A-Raf and C-Raf, B-Raf contains a unique N-terminal domain, the significance of which is unknown. While A-Raf and C-Raf genes are transcribed into one transcript, B-Raf is alternatively spliced, generating several different B-Raf isoforms [148, 149]. The 95 KD isoform is the largest and most commonly studied and the significance of the smaller isoforms is not understood.

**B-Raf Activation**

Raf kinases are activated by similar and distant mechanisms. It is believed that the N-terminal regulatory domain of Rafs bind to the C-terminal kinase domain, creating a closed conformation which renders the kinase domain inaccessible for activation [150]. Phosphorylation events and protein-protein interactions disrupts the N-terminal-C-terminal interactions, opening the Raf protein which prepares it for activation [142, 143, 151-155]. However, there are unique aspects to B-Raf's regulation which explains its potent MEK kinase activity.

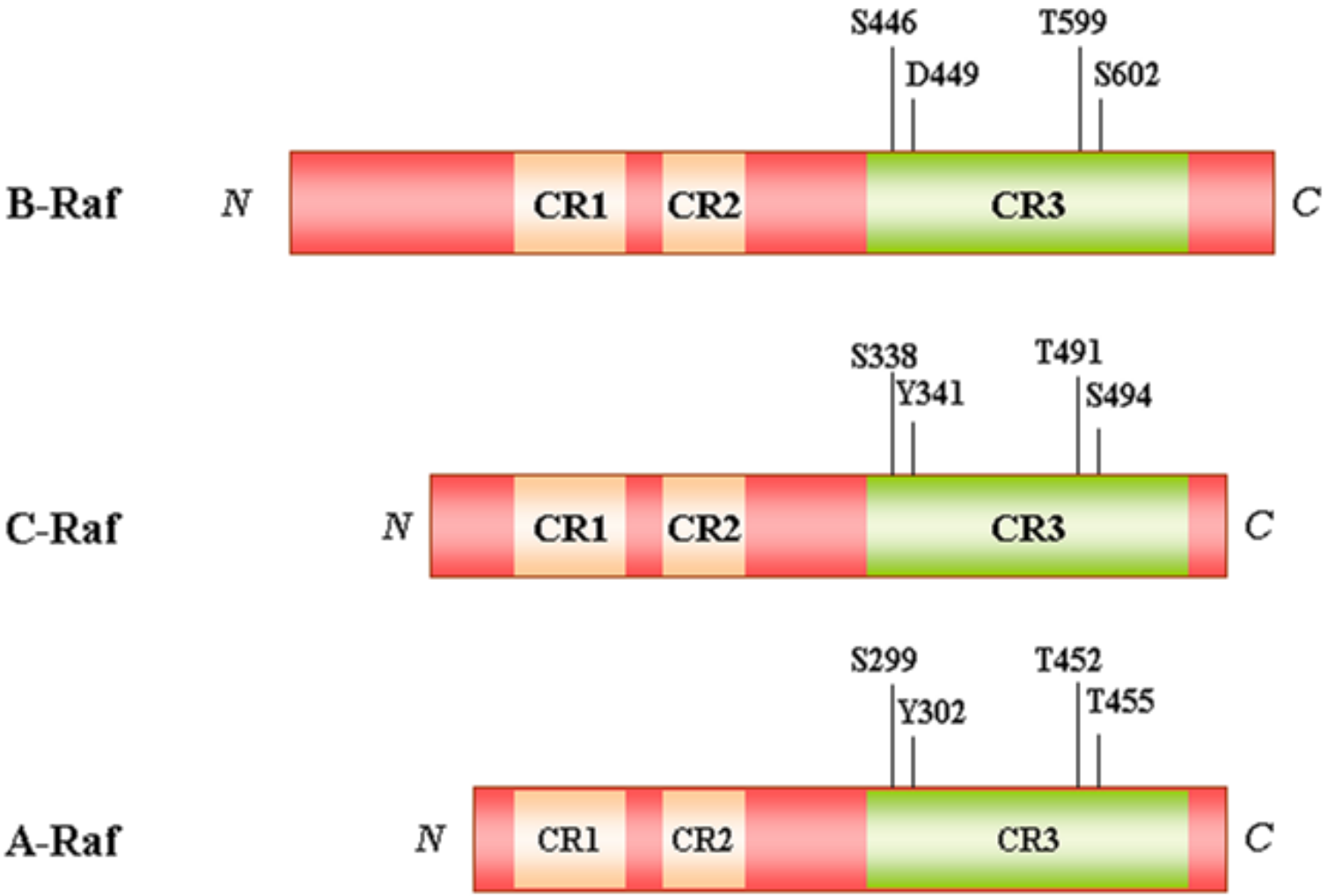


**Fig. 5 Raf family members**

B-Raf requires a lower "dose" of regulatory phosphorylation than does C-Raf for its activation. Following Ras-mediated stimulation, C-Raf requires two stages of phosphorylation events including Ras and SRC mediated phosphorylation of Ser-338 and Tyr-341 in the N-region [156-159] and Ras mediated phosphorylation of Thre-491 and Ser-494 in the activation loop [140]. B-Raf, however, does not require phosphorylation within the N-region due to the presence of a constitutive phosphorylation on Ser-335 and a phospho-mimicking aspartic acid at residue 448 [158]. Therefore, Ras mediated activation of B-Raf requires phosphorylation of Thr-599 and Ser-602 within the activation loop [160]. It has been proposed that the constitutive presence of negative charges in the N-region of B-Raf inhibits the interaction between the regulatory and catalytic domains, rendering an open conformation [161]. These differences account for a higher basal level activity in B-Raf than C-Raf.

Rafs are further regulated on the level of protein-protein interactions including direct interactions with Ras, Rap1 [162-167], MEK [149, 162-167] and C-Raf [168]. While C-Raf and B-Raf both interact with Rap1, Rap1 mediates activation of B-Raf while it inhibits C-Raf and downstream MAPK signaling [163, 167, 169]. As well, B-Raf and C-Raf both directly associate with MEK, however, B-Raf has a higher binding affinity to MEK than does C-Raf or A-Raf [170], which may account for the fact that B-Raf is a stronger activator of MEK than C-Raf or A-Raf [158, 160]. It has also been shown that B-Raf heterodimerizes with C-Raf, and is required for activation of C-Raf [171, 172]. While B-Raf/C-Raf heterodimers possess higher kinase activity than both respective monomers [168], B-Raf can be sufficiently activated by Ras alone [161].

**B-Raf Functions**

Analysis of Raf family members in knock-out mice has revealed that A-Raf, B-Raf and C-Raf all play essential roles in embryogenesis. Disruption of B-Raf causes embryonic lethality resulting from apoptotic death of differentiated endothelial cells [173]. Disruption of C-Raf leads to aberrations in lung development and A-Raf knock-out mice generate neurological and intestinal abnormalities [173, 174]. Knock-out studies also reveal that B-Raf and C-Raf alleles can partially compensate for one another and exhibit some functional redundancy [174].

Early studies revealed via northern blotting that B-Raf expression was restricted to tissues of the brain, testes and fetal membranes [175, 176]. However, the use of improved protein detection techniques demonstrated that B-Raf is ubiquitously expressed at low levels in most tissues with perhaps highest expression in the brain. Subcellular localization of B-Raf has exclusively been reported as cytoplasmic, however, a thorough analysis of B-Raf subcellular localization has yet to be published.

Analyses of B-Raf's specific cellular functions have been studied either in comparison with C-Raf and A-Raf, or relative to its oncogenic functions. It was shown that B-Raf and A-Raf, but not C-Raf exhibit sustained activation by neuronal growth factor (NGF) in PC12 cells [177], and epidermal growth factor (EGF) activated all three Raf isoforms. cAMP leads to activation of B-Raf in a Rap1/B-Raf dependent manner in neurons, whereas C-Raf is inhibited by cAMP [165, 178, 179]. It is widely presumed that B-Raf functions during S-phase in non-neuronal cells, however B-Raf's non-

neuronal functions have not been well studied nor distinguished from the functions of C-Raf.

**B-Raf as a Mitotic MEK Kinase**

It has been shown that ERK is activated during mitosis and contributes to normal mitotic functions. A recent report from our laboratory demonstrated that B-Raf is the MAP3K (MEK kinase) responsible for mitotic activation of the MAPK pathway in *Xenopus* egg extracts [180]. It was shown that B-Raf is activated in an M-phase specific manner and is required for the mitotic activation of the MEK/MAPK pathway. As well, the authors demonstrated that cyclinB-Cdk1 directly phosphorylates B-Raf and contributes to its activation during mitosis [181], suggesting that B-Raf activation at mitosis is mediated through mechanisms distinct from those that regulate MAPK signaling in response to mitogens. Further, it was shown that MAPK regulates B-Raf through negative feedback phosphorylation, which is presumed to ensure transient activity of B-Raf during mitosis in *Xenopus* egg extracts [180].

In summary, B-Raf is a member of the Raf family of kinases, but it stands out due to its unique structural and functional features. Cumulative evidence from the recent decade demonstrates that B-Raf is a major activator of the ERK 1/2 cascade. As well, novel functions have been ascribed to B-Raf. In particular, studies in *Xenopus* egg extracts have shown that B-Raf regulates the mitotic activation of MAPK.

## MAPK Pathway in Tumorigenesis

It has long been recognized that the MAPK cascade is a key regulator of cellular proliferation and survival. Thus, its continuous signaling could lead to cellular transformation. Indeed, the MAPK pathway is hyperactivated in approximately 30% of human tumors. Four well studied mechanisms of ERK activation in human tumors include mutations in the epidermal growth factor receptor (EGFR), Ras, the mitogen-activated protein kinase phosphatases (MKPs) and B-Raf.

### EGFR, Ras and MKPs in Human Cancers

The epidermal growth factor (EGF) and its receptor, EGFR [182, 183] signals through Ras activating the MAPK pathway [184]. It has become well recognized that EGFR is an oncogene [185-188] and is highly expressed in human cancers and correlated with poor prognosis [189]. EGFR is frequently overexpressed or mutationally activated [190] in breast, lung and head and neck cancers, glioblastomas, bladder, colorectal, ovarian and prostate cancers [191-195]. As well, transforming growth factor alpha (TGFα), an EGFR's ligand, is upregulated in a wide variety of transformed cells [196-198] thus causing persistent stimulation of EGFR.

Ras proteins are a family of small GTPases that are upstream activators of Rafs and therefore activators of the MAPK cascade [199]. In normal quiescent cells, Ras is in its GDP-bound inactive form. Following stimulation by EGF or other factors, Ras is transformed into its GPT-bound active form which then binds to and stimulates the activation of Rafs. Ras is converted to its oncogenic form by missense mutations that render the proteins to be constitutively GTP-bound and active [200]. Since oncogenic

Ras cannot be inactivated, it drives activation of the Raf-MEK-ERK cascade in a stimulus-independent manner. Oncogenic Ras occurs in 30% of human tumors including 90% of pancreatic cancers, 50% of colon and thyroid cancers, 30% of lung cancers and myeloid leukemias, and 15% of melanomas [200-202].

Recently it has come to light that several mitogen-activated protein kinase phosphatases (MKPs), negative regulators of the MAPK signaling, are involved in tumorigenesis [203]. MKPs are mutated in tumors of the breast, lung, prostate, ovaries, pancreas, liver and gastrointestinal tract. Overexpression of several MPKs is observed in tumors and correlates with poor outcome and progression [204-206], thus serving as a prognostic marker [207]. However, in several tumors, MKPs are down regulated or grossly underexpressed [208, 209]. Growth of tumors in nude mice from Ha-ras transformed cells was greatly delayed when MKP expression was induced, supporting a tumor suppressor role for MKPs [210]. While the mechanisms of MKP deregulation are not yet fully understood, it has been shown that hypermethylation leads to loss of MKP-3 expression in pancreatic cancers [211].

**B-Raf in Human Cancers**

Members of the Raf family were first identified as viral oncogenes causing tumors in mice and chickens [212-215]. C-Raf activity is increased in response to hyperactivated EGFR or Ras, however, to date B-Raf is the only Raf kinase that is known to be mutated in human cancers.

Two decades of testing human tumors for Raf mutations was largely unsuccessful until a fruitful, high-throughput screen of nearly 1000 human tumor samples identified B-

Raf missense mutations in many human cancers [216]. Activating B-Raf point mutations were discovered in nearly 70% of melanomas, 40% of papillary thyroid carcinomas [217-219]; 14% of ovarian cancers, 14% of liver cancers, 12% of colorectal tumors, 11% of gliomas, 9% of sarcomas a to a lesser extent in other lymphomas, leukemias, breast, lung and liver carcinomas, totaling 8% of all tumors sampled [216].

While more than 30 missense mutations were identified, all in the kinase domain of B-Raf, 80% of the mutations were accounted for by a single Valine to Glutamic acid substitution at residue 600, B-Raf$^{V600E}$ [216]. Melanomas by far accounted for the highest percentage of B-Raf mutations, in which over 90% of the mutations were represented with the V600E substitution. Ras mutations account for 15% of melanomas, however, Ras and B-Raf mutations are mutually exclusive in the vast majority of tumors, suggesting that Ras and B-Raf transform melanocytes through similar mechanisms. As well, it has been shown that 80% of benign nevi harbor a B-Raf$^{V600E}$ mutation [220], thereby implicating B-Raf in the early stages of transformation. Additional studies have shown that a paracentric inversion within chromosome 7 creates a fusion protein between a portion of the AKAP9 gene and the kinase domain of B-Raf rendering B-Raf constitutively active [221]. This rearrangement is found at a low frequency (1%) of sporadic thyroid papillary carcinomas, however its prevalence is 11% among thyroid papillary carcinomas that developed in children as a result of exposure to radiation from the Chernobyl explosion. Finally, less commonly noted are B-Raf copy number amplifications which occur most often in thyroid follicular adenomas (25%) and thyroid follicular carcinomas (35%) [222].

**B-Raf as an Oncogene**

The most common mutation in B-Raf, V600E, is flanked by a threonine at residue 599 and Serine at residue 602, both of which require phosphorylation for Ras mediated activation [160]. It is therefore conjectured that the negative charge acquired by substituting glutamic acid for valine suffices as a phospho-mimic capable of activating B-Raf [216]. Indeed, the vast majority of mutations in B-Raf were demonstrated to be activating mutations, with B-Raf$^{V600E}$ exhibiting a 10.7 fold increase in its kinase activity *in vitro* over wild-type B-Raf. The activating mutations increased endogenous ERK activation in cell culture, as tested by levels of ERK1/2 phosphorylation, whereas overexpression of wild-type B-Raf did not increase ERK1/2 phosphorylation [223]. Interestingly, four rare B-Raf mutations found in tumors [216] have reduced *in vitro* kinase activity [224] despite activating ERK in cells. It was shown that three of these exogenously expressed mutants, interact with and activate endogenous wild-type C-Raf, which then activates ERK [224].

Consistent with its elevated kinase activity, it was shown that B-Raf$^{V600E}$ is capable of inducing transformation in NIH3T3 cells [216] and immortalized mouse melanocytes [223] in an ERK dependent manner. Further, transformation of melanoma cells expressing B-Raf$^{V600E}$ was reversed upon downregulation of B-Raf [225, 226]. Additionally, it was shown that immortalized melanocytes expressing B-Raf$^{V600E}$ form tumors in nude mice. Consistent with the presence of B-Raf$^{V600E}$ mutations in 80% of benign nevi, transgenic zebrafish expressing B-Raf$^{V600E}$ formed benign nevi [227]. However, B-Raf$^{V600E}$ induced formation of invasive melanomas in zebrafish, only when expressed on a p53 deficient background. A conditional B-Raf$^{V600E}$ knock-in mouse

model produces hematopoietic displasia and skin polyps [228]. Transgenic mouse models targeting B-Raf$^{V600E}$ to melanocytes [229] or the lung [230] rapidly develop benign nevi or adenomas, respectively, but rarely develop melanomas or adenocarcinomas unless combined with the loss of tumor suppressors Pten, TP53 or Ink4a/Arf. However, targeted expression of B-Raf$^{V600E}$ to the thyroid serves as a tumor initiator and promoter, resulting in rapid accumulation of parathyroid carcinomas (PTC) that closely reflect human PTCs [231]. Therefore, B-Raf$^{V600E}$ is capable of transforming immortalized cells and causing benign tumor formation in several animal models. However, its role in tumor progression varies amongst tumor types, requiring additional mutations for full transformation to occur.

In summary, MAPK signaling has been implicated in a high percentage of human tumors. Hyperactivity of the Ras-Raf-MEK-ERK pathway is achieved by mutations on various levels including the upstream activator EGFR, its ligand, TGFα, activating mutations in Ras and deregulation of MPKs. Most notably, B-Raf is constitutively activated in a wide variety of cancers which depend on oncogenic B-Raf expression for proliferation and survival. 80% of benign nevi harbor oncogenic B-Raf, suggesting that it is an early transformation event.

## Mitosis and Cancer

It has long been recognized that human tumors are genetically unstable. Nucleotide-level genomic instability and gene mutations are well established causes of tumorigenesis. However, the form of genetic instability most frequently observed in

cancers is mitotically driven chromosomal aneuploidy. Mounting evidence supports a causal role for chromosomal aneuploidy in tumorigenesis, therefore, understanding how mitosis drives aneuploidy in human tumors has become a critical question of modern cancer biology.

**Types of Genomic Instability**

Human disease is largely attributed to genetic alterations [232]. Mutations in genes which repair or divide the genome cause cells to continuously acquire genomic changes over time rendering them genomically unstable. The two categories of genomic instability include nucleotide-level instabilities and mitotically driven aneuploidy [232].

The human genome contains thousands of microsatellites, short sequences of DNA that are tandemly repeated 10 to 100 times [233]. Microsatellites are highly susceptible to DNA replication errors, which are repaired by the highly conserved DNA mismatch repair (MMR). Mutations in MMR genes and occasionally mutations in the nucleotide excision repair (NER) genes [234] increase the rate of genomic mutations leading to microsatellite instability (MIN), the most common type of nucleotide-level genomic instability [232]. MIN occurs in approximately 13% of sporadic colorectal, endometrial and gastric cancers [235, 236]. It is widely accepted that MIN drives tumorigenesis [237].

Normal human cells contain 46 chromosomes. Deviation in chromosome number is referred to as aneuploidy. Gains and losses of whole chromosomes, gene amplifications and deletions and chromosomal rearrangements and are all forms of aneuploidy [232, 235, 237]. Embryogenic aneuploidy is typically lethal and when viable,

causes disease such as Down, Edward and Patau's syndromes [238]. However, nearly every tumor cell exhibits aneuploidy and the vast majority of tumor cells are genetically unstable [239].

Continual chromosomal gains and losses, a form of genomic instability termed chromosomal instability (CIN), is the most common form of aneuploidy in tumors [232, 237, 239]. Nearly all tumors that do not exhibit MIN are chromosomally unstable, often containing gross structural changes such as translocations, deletions and amplifications [237], as determined by classic and modern karyotype analyses. Structural rearrangements in the absence of whole-chromosomal instability are a well accepted cause of tumorigenesis, such as the BCR-ABL translocation that drives some cases of chronic myelogenous leukemias [240]. The role of CIN in tumorigenesis is less well defined. Some have argued that chromosomal aneuploidy is a side-effect of tumorigenesis. However, correlative evidence and direct experimental results have demonstrated that chromosomal aneuploidy contributes to cellular transformation and cancer development.

**Mitosis and Aneuploidy**

For well over a century it has been demonstrated that aneuploidy results from errors in cell division [241]. Some of the mitotic defects which cause aneuploidy include multipolar spindle formation, defects in chromosome cohesion, spindle-microtubule misattachments, and a weakened spindle assembly checkpoint [242].

Cells that form multi-polar spindles undergo chromosomal missegregation. It is believed that multi-polar spindles result from defects in the duplication, segregation and

maturation of centrosomes. Indeed, Aurora A amplification [243] or inactivation of p53 [244], BRCA1 and BRCA2 [245-248] or mitotic motor protein Eg5 cause errors in centrosomal duplication or segregation leading to spindle malformation and aneuploid daughter cells.

Defects in the cohesion of chromosomes have been shown to cause aneuploidy. Inactivation of securin or separase homologues in budding and fission yeast generates hypoploidy [249-251]. As well, deletion of securin from human cancer cells induces high levels of CIN [252].

Another potential mechanism for aneuploidy lies within faulty kinetochore-microtubule engagement. Merotelic attachments occur upon inhibition of the chromosomal passenger complex that corrects kinetochore-microtubule attachment errors [253]. As well, truncated forms of the adenomatous polyposis coli protein generate CIN by disrupting kinetochore-microtubule attachments [254-256].

An insufficiently performing spindle assembly checkpoint is also implicated in the production of aneuploidy [257]. Mice with reduced levels of Mad2 [258], BubR1 [259] or Bub3 [260] have a defective SAC and are prone to the acquisition of aneuploidy. While Mad2, BubR1 and Bub3 have roles throughout the cell cycle, CENP-E functions exclusively during mitosis [261]. Therefore, it is significant that reduction in CENP-E levels compromises the SAC and causes aneuploidy *in vitro* [262] and in mice [263].

**Causal Role for Aneuploidy in Tumorigenesis**

Aneuploidy is the most common feature found amongst tumors and is considered a hallmark of cancer [237]. Some of the earliest cancer biologists proposed that

aneuploidy causes tumorigenesis [264-266]. It is now widely accepted that changes in gene expression lead to tumorigenesis [267]. Despite arguments that aneuploidy is a benign consequence of transformation [268], modern biology suggests that mutations in genes that regulate cell division drive aneuploidy, which is ultimately the means for generating changes in gene expression that lead to tumorigenesis [232, 235, 269, 270].

Tumor development results from accumulated changes in gene expression. Some have argued that the accumulation of a few somatic mutations is sufficient to cause transformation [271]. However, mathematical modeling predicts that the acquisition of sufficient numbers of changes cannot be achieved solely by the acquisition of spontaneous mutations [272]. Mathematical models also predict that the onset of genomic instability is an early and necessary event in tumor development [235]. In fact, allelic loss occurs in extremely small polyps in early stage colorectal cancers [273], and aneuploidy is present in precancerous lesions of the cervix, head and neck, esophagus and bone marrow [274]. Human tumors gain and lose chromosomes at a rate of 10-100 times higher than normal cells [239]. Average tumors of the colon, prostate and breast have lost 25% of their alleles [232] and exhibit heterogeneity due to continual genomic changes [275].

It has been demonstrated that a large number of CIN colorectal tumors cannot adequately activate their spindle assembly checkpoint [276]. In fact, a large proportion of human tumors display misexpression of genes that regulate the SAC. BubR1 and Mad1 are frequently misregulated in a number of human cancers [261]. Mad2 was found to be transcriptionally overexpressed in several tumor types including hepatocellular, lung and intestinal carcinomas, B cell lymphomas and several others

[277]. Mutational inactivation of Bub1 or BubR1 have been observed in colon cancers [276]. Several tumor types, including pituitary adenomas and mammary and pulmonary adenocarcinomas, exhibit overexpression of securin [278-280]. Other genes that regulate mitosis such as Apc, BRCA1 and BRCA2 are misregulated in a number colorectal, duodenal, breast, ovarian, colon and pancreatic cancers [261].

Direct evidence has demonstrated that aneuploidy can drive tumorigenesis. In 2007, it was reported that cells from Mad2 transgenic mice become highly aneuploid and develop a wide variety of tumors including liver and lung carcinomas, sarcomas and lymphomas [277]. The mice developed whole chromosomal aneuploidy and structural chromosomal abnormalities, as shown by g-banding analysis. Immunofluorescence studies demonstrated that Mad2 cells exhibit lagging chromosomes and chromosome bridges during mitosis – a strong indication that mitotic errors were the driving factor behind the acquisition of aneuploidy. As well, it was shown that transient Mad2 expression is sufficient for long-term tumor development, suggesting that aneuploidy induced by Mad2, rather than Mad2 itself, was necessary for tumor maintenance.

Further direct evidence that aneuploidy is tumorigenic comes from studies in mice with reduced CENP-E levels [263]. These studies are particularly significant since the role of CENP-E is exclusively relegated to mitosis. Mice heterozygous for CENP-E exhibit whole chromosomal aneuploidy, in the absence of structural abnormalities, as shown by spectral karyotyping. Lagging and pole-associated chromosomes were detectable in 40% of cells isolated from CENP-E heterozygous mice, implicating mitotic errors as the cause of aneuploidy. After a long latency period, these mice develop splenic lymphomas and lung adenomas at a rate of 10%, comparable to the number of

smokers who develop lung cancer. The long latency period indicates that a small subset of the aneuploid cells have the potential to drive transformation. In the presence of other aneuploidy-inducing carcinogens, CENP-E heterozygous mice had a reduced incidence of tumorigenesis, indicating that a significantly high level of aneuploidy is incompatible with life [261].

In summary, mitosis must be accurately executed in order to preserve the genomic integrity of a cell. Mitotic proteins, whose misregulation drives aneuploidy *in vitro*, are frequently misexpressed in human tumors. Nearly all tumors are aneuploid and genomically unstable from an early stage in tumor development and the degree of aneuploidy is directly correlated with the stage of tumorigenesis. As well, direct studies of Mad2 and CENP-E confirm that mitotically induced aneuploidy is tumorigenic in mice. Together, these observations support the assertion that misexpression of spindle assembly proteins promote aneuploidy, which can contribute to tumorigenesis.

## Hypothesis and Dissertation Statement

Recently, it has come to light that B-Raf is a prominent oncogene, mutated in a wide spectrum of tumors including nearly 70% of melanomas. Oncogenic B-Raf is also expressed in 80% of benign nevi, indicating that it plays an early role in tumorigenesis. It is crucial to understand the molecular mechanism by which oncogenic B-Raf contributes to tumorigenesis. The cellular mechanisms through which oncogenic B-Raf may drive transformation are beginning to be appreciated. However, more work is needed in order to understand the full effects of oncogenic B-Raf.

It is well accepted that B-Raf is the most potent activator of MAPK signaling [158, 160]. The MAPK pathway is a critical signal transduction pathway necessary for cellular proliferation, cell survival, stress response and apoptosis [93]. MAPK signaling is also involved in the regulation of mitosis [108-110, 113, 114, 119, 134]. Interestingly, B-Raf has been reported to activate MAPK signaling during mitosis in *Xenopus* egg extracts [180], however, little is known about B-Raf functions in human cells. I hypothesize that **B-Raf regulates mitotic functions in human somatic cells and that oncogenic B-Raf disrupts mitosis, leading to aneuploidy**.

To address these hypotheses, I conducted loss-of-function experiments in cell cultures in order to evaluate the contribution of B-Raf to mitosis. Further, I introduced oncogenic B-Raf into cancer, immortalized, and primary cells, evaluating the cells mitoses and analyzing their karyotypes.

The results of my thesis work demonstrate that B-Raf regulates several critical mitotic functions and that oncogenic B-Raf perturbs mitosis, driving aneuploidy and chromosomal instability.

# CHAPTER 2

# SUBCELLULAR B-RAF LOCALIZATION

## Introduction

Regulatory functions of MAPK signaling are mediated in large part by the subcellular localization of MAPK pathway members. Active forms of MEK and ERK localize to the cytoplasmic compartment in order to phosphorylate substrates localized at the cytoskeleton structures and they translocate into the nucleus to regulate gene expression by phosphorylating transcriptional factors [281, 282]. During mitosis, active MEK and ERK colocalize to the mitotic spindle poles, the kinetochores, the midzone of the anaphase spindle and the telophase bridge during cytokinesis [112]. Little has been published on the subcellular localization of B-Raf with the exception of its localization throughout the cell body of post-mitotic neural cells [283].

B-Raf is itself regulated by phosphorylation events. Ras mediated activation of B-Raf requires phosphorylation on two key residues (Ser 599 and Thr 602) in B-Raf's kinase domain. Evaluating the localization of dually phosphorylated B-Raf can give clues to the cellular positioning of active B-Raf.

## Results

### B-Raf Localizes to Mitotic Structures

MEK and ERK, members of the MAPK signaling cascade, localize to mitotic structures when activated by phosphorylation. Work from our laboratory has revealed that B-Raf is critical for mitotic activation of the MAPK cascade and its activity is regulated in an M phase-dependent manner [180]. Therefore it stands to reason that B-Raf might also exhibit mitosis-specific localization.

#### *B-Raf is Detected at the Mitotic Spindle*

In order to test whether B-Raf localizes to the mitotic spindle apparatus, immunofluorescence studies were carried out in cycling NIH 3T3 cells (Fig. 6), MCF-7 cancer cells (data not shown) and human foreskin fibroblast (HFF) cells (Fig. 7) using a monoclonal alpha-tubulin antibody to stain the mitotic spindle, DAPI to visualize the chromosomes and a commercially available, polyclonal antibody against B-Raf. This antibody recognizes a single, 95 kD protein band in corresponding cellular lysates (data not shown). B-Raf was exclusively detected in the cytoplasmic compartment of interphase cells. Interestingly, as shown in HFF cells, at the onset of mitosis or prophase (as determined by chromosome condensation and aster formation), B-Raf localizes to the nuclear region. As cells enter metaphase, B-Raf becomes highly enriched in the region of the mitotic spindle and the spindle poles and to the spindle and midzone during anaphase. This was most evident upon utilizing a threshold analysis, which distinguishes the areas containing the highest relative levels of B-Raf staining. In late telophase and cytokinesis, the B-Raf staining pattern was mostly confined to the cytoplasmic compartment, as it was

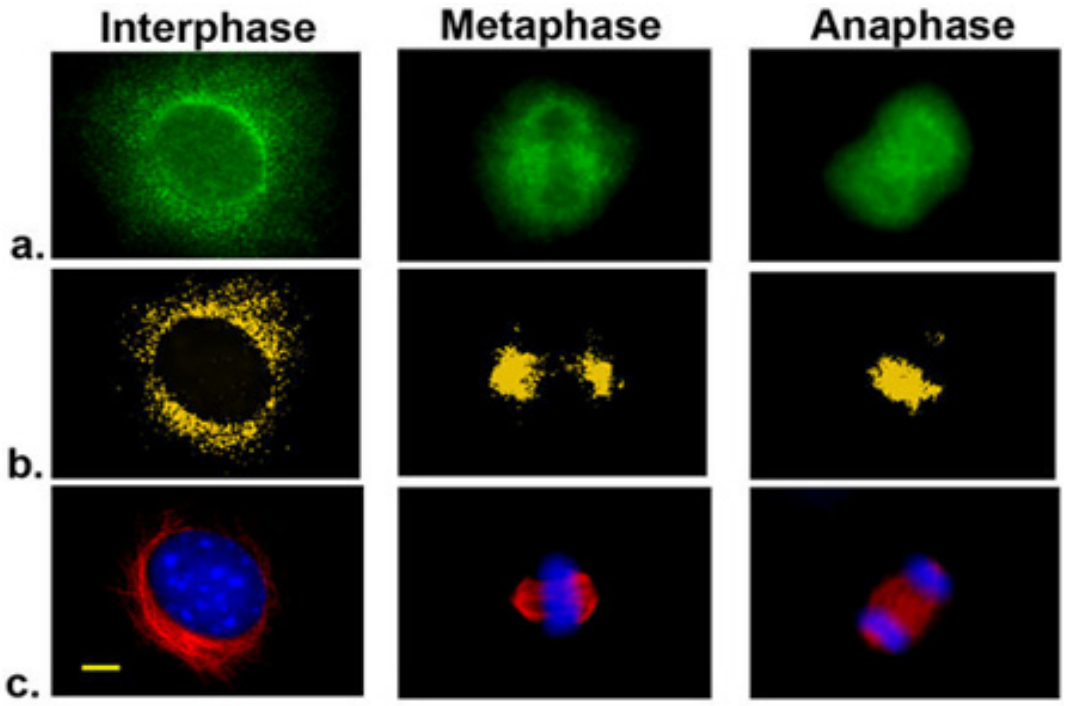


**Figure 6. B-Raf localizes to the mitotic spindle in NIH 3T3 cells**
a. Immunofluorescence staining of endogenous B-Raf protein. a. B-Raf; b threshold analysis depicting regions of strong B-Raf enrichment; c. overlay α-tubulin to visualize the spindle (red) and DNA (blue); Images were acquired at 100X magnification, scale bar represents 3μm, arrows depict mitotic cells.

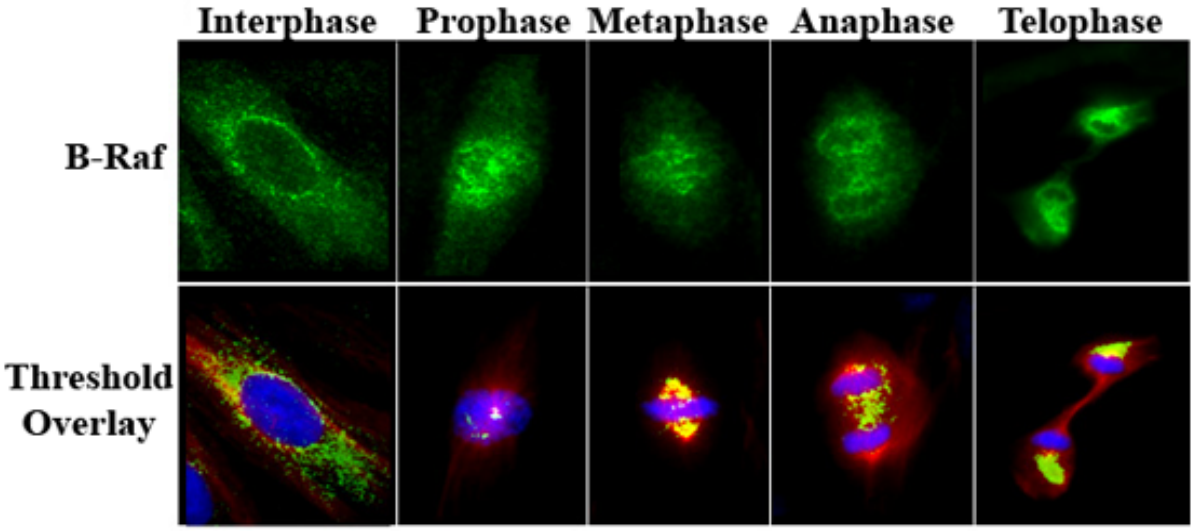


**Fig. 7 B-Raf localizes to the mitotic spindle in HFF cells**
Top Panel: Immunofluorescence in asynchronous HFF cells of endogenous B-Raf protein (green) Bottom Panel: Overlay of B-Raf threshold (green), α-tubulin (red) and DNA stained with DAPI (blue). Images were acquired at 100X magnification.

during interphase. The enrichment of B-Raf staining at the metaphase spindle region was also observed using a mouse monoclonal B-Raf antibody, indicating that the staining pattern from the two antibodies reflects the detection of B-Raf protein. Neither the isotype control for the polyclonal (Rabbit IgG) nor monoclonal (Mouse IgG2b) generated any appreciable staining pattern.

To further ascertain whether B-Raf's mitotic staining co-localizes to microtubule spindle structures, I used confocal microscopy to acquire 0.45 μm z-sections throughout HFF cells. The results demonstrate that B-Raf staining was restricted to the confocal sections containing spindle microtubules and condensed chromosomes (Fig.8). Strong B-Raf staining appears at the spindle poles and the spindle midzone in cells undergoing metaphase and anaphase, respectively. Viewing metaphase cells down the spindle pole axis permits us to visualize B-Raf along the radial microtubules and at the spindle poles. Thus, B-Raf localization is enriched at the spindle apparatus during mitosis in somatic tissue culture cells.

*B-Raf Interacts with Spindle Microtubules*

Immunofluorescence staining demonstrates that B-Raf is enriched at the region of the mitotic spindle, and therefore B-Raf may be directly associated with the microtubules of the spindle apparatus. In order to address this question, entire z-series of immunofluorescence images of B-Raf and the mitotic spindle were analyzed with Imaris Bitplane 3D blind deconvolution followed by processing with the ImarisColoc module to isolate, visualize and quantify region overlap. These analyses demonstrated that a portion

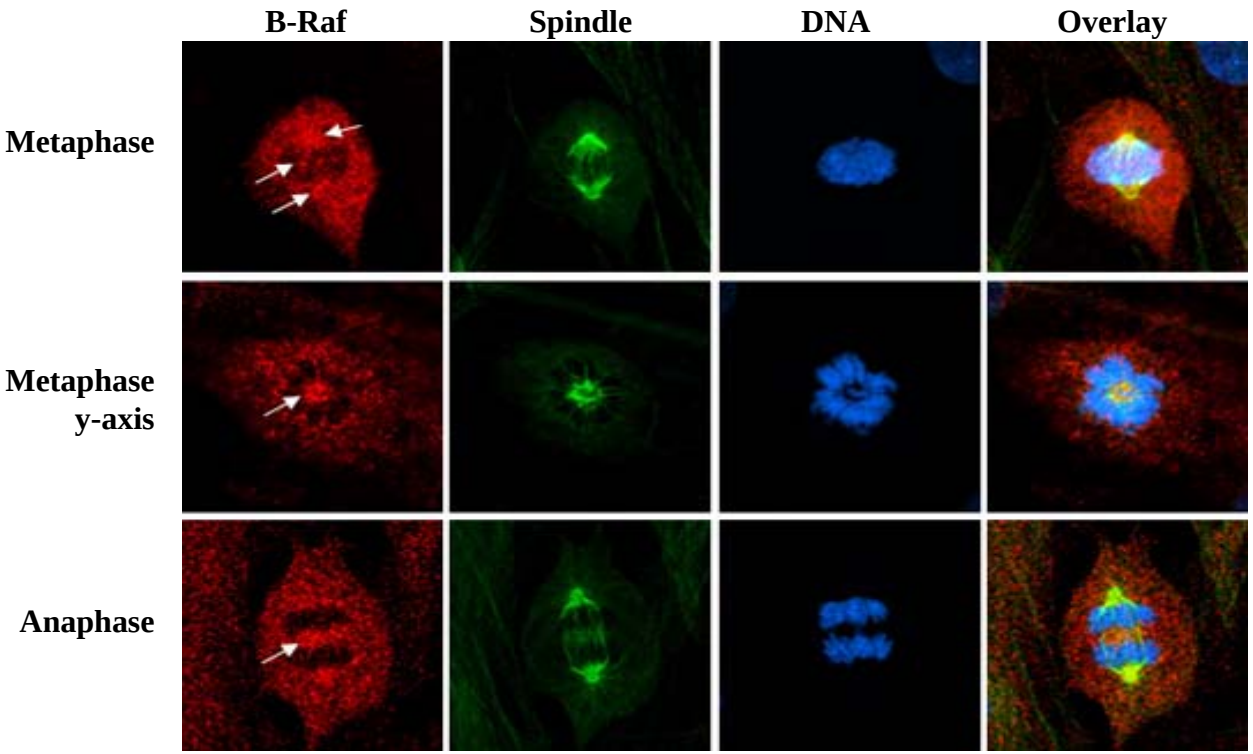


**Figure 8. B-Raf is detected at the spindle apparatus during mitosis in HFF cells**

Confocal microscopy of HFF cells stained with antibodies against endogenous B-Raf (red), α-tubulin to visualize the spindle (green) and DNA stained with DAPI (blue). Images represent 0.48μm along the z-axis from within a z-series.

of B-Raf directly colocalizes with the polymerized microtubules of the spindle (Fig. 9), suggesting that B-Raf directly interacts with the spindle microtubules.

In order to validate the Imaris data, HFF and HeLa cells were exposed to nocodazole in order to depolymerize the microtubules. Cells were stained with tubulin and B-Raf antibodies and the B-Raf staining pattern was assessed by fluorescence microscopy. As shown in Figure 10, the staining pattern of B-Raf corresponding to the metaphase spindle was radically altered upon nocodazole treatment indicating that B-Raf localization at metaphase reflects its association with the spindle microtubules.

Based on the same principals of nocodazole function, we performed a biochemical experiment in *Xenopus* egg extracts to determine if B-Raf interacts with polymerized microtubules during mitosis and if the interaction is disrupted when microtubules are depolymerized by nocodazole. As shown in Figure 11, B-Raf and polymerized microtubules are associated in a pelleted fraction of egg extracts and the association is decreased when microtubules are depolymerized with nocodazole.

*B-Raf Localizes to the Centrosomes*

Based on the immunofluorescence threshold analyses and confocal data demonstrating an abundance of B-Raf at the spindle poles during mitosis, I decided to analyze mitotic cells for B-Raf colocalization to the centrosome. The centrosome is comprised of an abundance of proteins concentrated into two centrioles. The centrosome and its associated proteins can be detected following a brief detergent extraction of soluble proteins. NIH 3T3 or HFF cells were briefly extracted with CHAPS

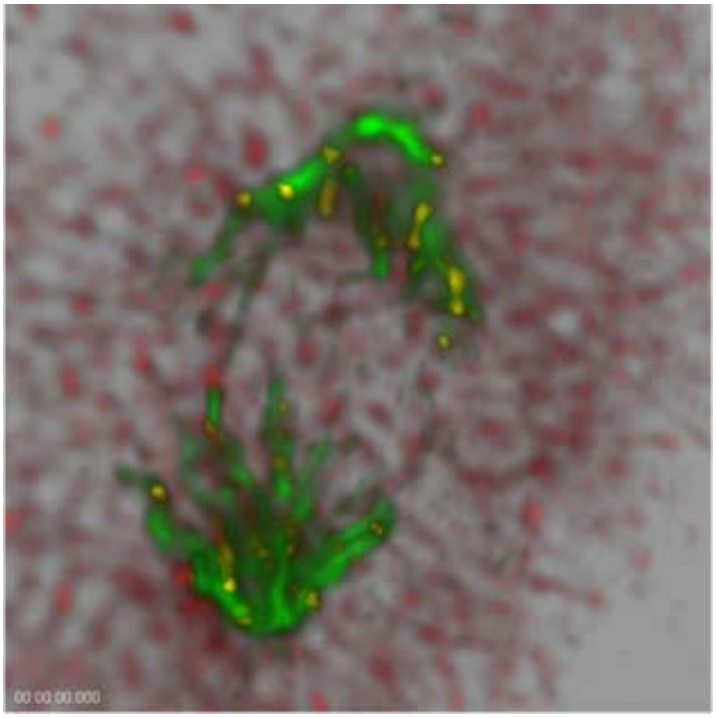

**Fig. 9 B-Raf interacts with the spindle microtubules in HFF cells**
Confocal images of B-Raf and the spindle were analyzed using Imaris Bitplane 3D blind deconvolution. Following deconvolution, resulting stack was processed with ImarisColoc module to isolate, visualize and quantify region overlap. Green represents α-tubulin, red is background B-Raf staining and yellow represents areas where B-Raf and microtubules interact.

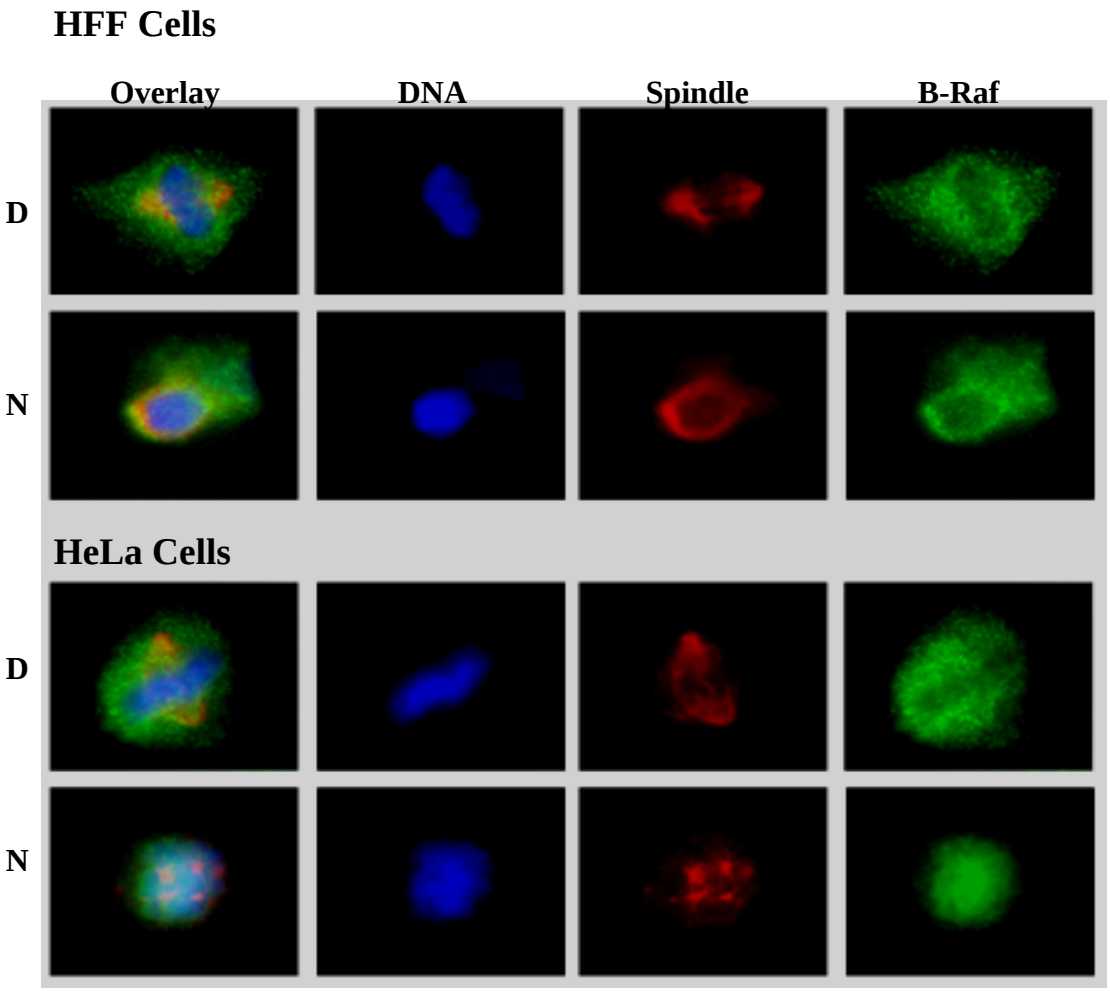


**Fig. 10 B-Raf spindle localization is disrupted when microtubules are depolymerized with nocodazole**
HFF and HeLa cells were treated for two hours with nocodazole to induce destabilization of microtubules. Cells were fixed with 4% paraformaldehyde and processed for immunostaining of B-Raf (green) and α-tubulin (red), and DAPI was used to detect DNA (blue). D=DMSO; N=Nocodazole.

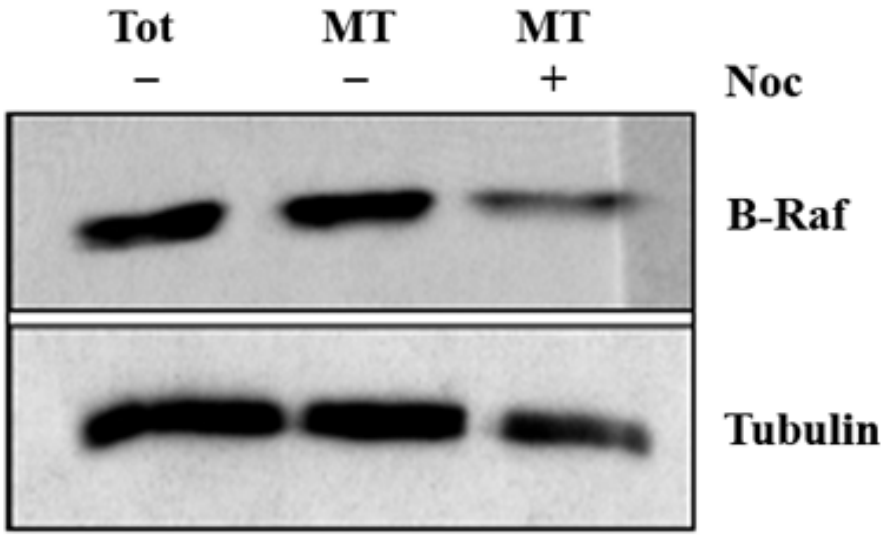


**Fig. 11 B-Raf co-pellets with microtubules isolated from M phase *Xenopus* egg extracts**
Spindle microtubules structures formed in mitotic *Xenopus* egg extracts, in the absence or presence of 10 ng/μl nocodazole, were pelleted through a 40% glycerol buffered cushion as previously described (Horne Guadagno, 2003). The microtubule pellet and its associated proteins were resuspended in SDS sample buffer, separated by 10% SDS-PAGE, and subjected to immunoblot analysis for α-tubulin and B-Raf.

detergent, fixed with 4% paraformaldehyde, stained for B-Raf, tubulin and DAPI to visualize the chromosomes. The results showed that throughout the cell cycle the majority of B-Raf was removed by CHAPS extraction with the exception of two discrete pairs of foci on opposite sides of the aligned chromosomes, a distinct centriolar staining pattern (Fig. 12). To confirm that B-Raf colocalizes directly with the centrioles, cells were costained with B-Raf and centrin, a centriole marker, followed by confocal analysis of 0.45 μm Z-sections. Both pairs of foci co-localized precisely with centrin in both NIH3T3 (Fig. 12) and HFF (Fig. 13) cells during mitosis. As shown in Fig. 14, B-Raf is present at the centrosome throughout the cell cycle. Hence, we conclude that a detergent-resistant pool of B-Raf is tightly associated with the centrioles in mammalian cells.

**B-Raf is Phosphorylated on Serine 599 and Threonine 602 at Mitotic Structures**

B-Raf is dually phosphorylated at conserved residues Thr599 and Ser602 during Ras-mediated activation (Zhang and Guan, 2000), therefore dual phosphorylation of B-Raf suggests that B-Raf is active and capable of phosphorylating downstream targets. To determine whether B-Raf is phosphorylated at these two residues during mitosis, HFF cells were subjected to immunostaining with a monoclonal alpha-tubulin antibody, a phospho-B-Raf (Thr599/Ser602) antibody and DAPI to visualize the DNA.

*Phosphorylated B-Raf Localizes to the Centrosomes*

During interphase, phospho-B-Raf (Thr599/Ser602) staining was weakly visible at the centrosome and the remainder of the cells is devoid of phospho-B-Raf staining, however, a notable staining pattern of phospho-B-Raf (Thr599/Ser602) was detectable

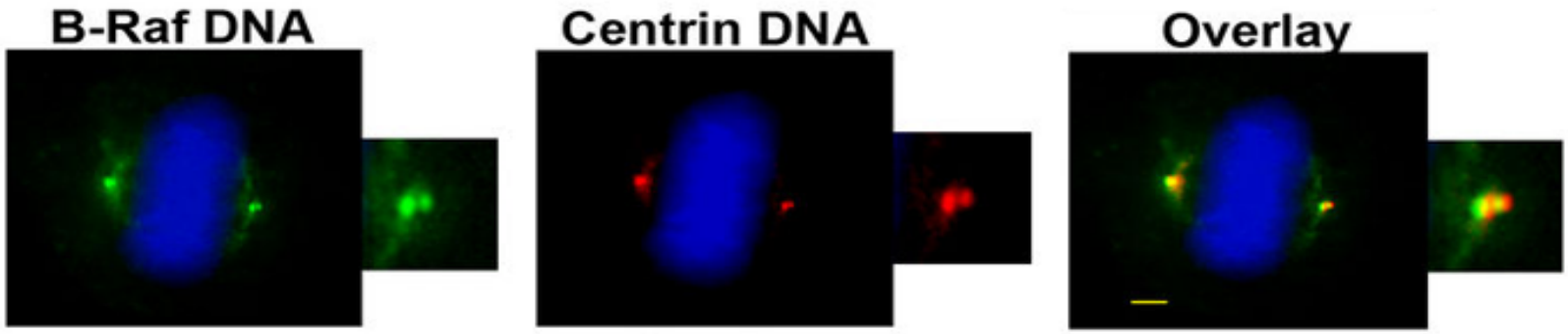


**Figure 12 B-Raf localizes to the centrosomes in NIH 3T3 cells**
Immunofluorescence of endogenous B-Raf protein. Cells were incubated with 1% CHAPS containing buffer, prior to fixation, in order to wash away soluble proteins and retain insoluble proteins and proteins tightly associated with insoluble structures. Cells were stained with antibodies against endogenous B-Raf (green), centrin to visualize the centrosome (red) and DNA (blue). Images were acquired at 100X magnification, scale bar represents 3µm. Centrioles are magnified 4X in the outset panel.

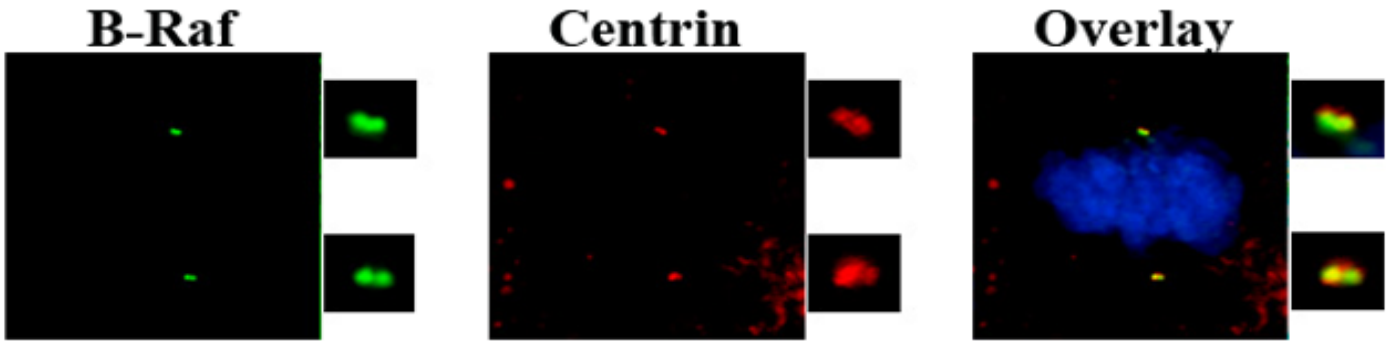


**Figure 13 B-Raf localizes to the centrosomes in HFF cells**
Immunofluorescence of endogenous B-Raf protein. Cells were incubated with 1% CHAPS containing buffer, prior to fixation, in order to wash away soluble proteins and retain insoluble proteins and proteins tightly associated with insoluble structures. Cells were stained with antibodies against endogenous B-Raf (green), centrin to visualize the centrosome (red) and DNA (blue). Images were acquired at 100X magnification. Centrioles are magnified 5X in the outset panel.

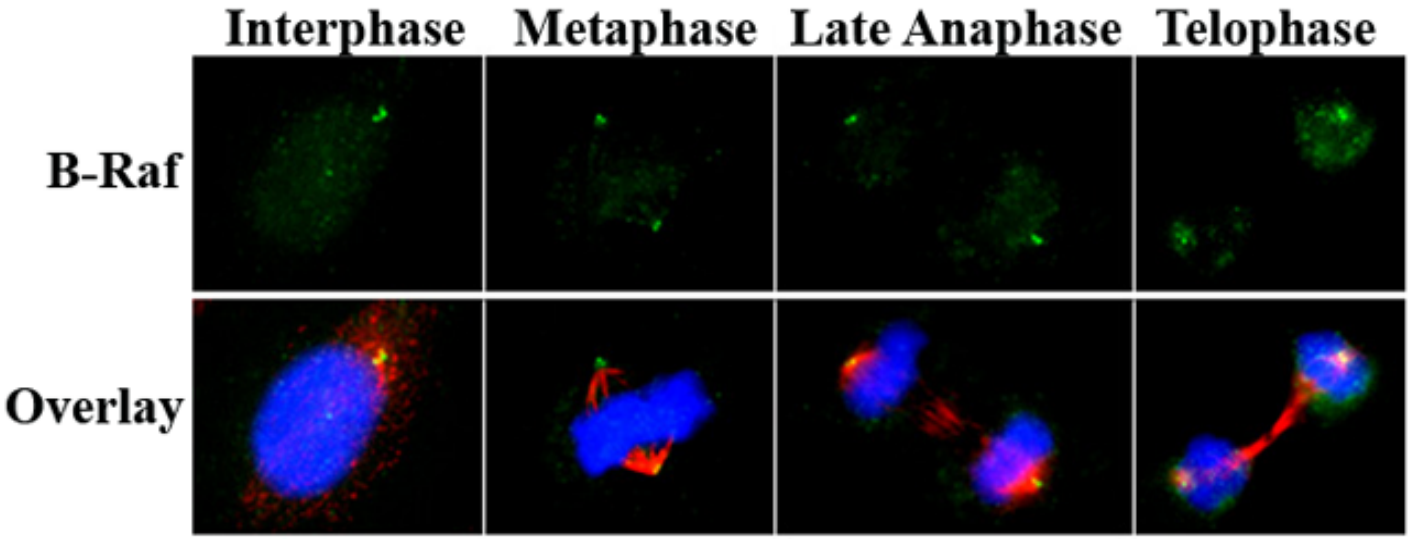


**Figure 14 B-Raf localizes to the centrosomes throughout the cell cycle**
Immunofluorescence of endogenous B-Raf protein. Cells were incubated with 1% CHAPS containing buffer, prior to fixation, in order to wash away soluble proteins and retain insoluble proteins and proteins tightly associated with insoluble structures. Cells were stained with antibodies against endogenous B-Raf (green), α-tubulin to visualize the spindle (red) and DNA (blue). Images were acquired at 100X magnification.

during all stages of mitosis (Fig. 15). At prophase, the onset of mitosis, strong phospho-B-Raf staining was detectable at the centrosomes and remained at the spindle poles throughout metaphase and anaphase. This staining pattern was nearly identical to the non-phosphorylated B-Raf centrosomal staining. Additionally, phospho-B-Raf (Thr599/Ser602) staining was detected at the spindle midzone in cells undergoing anaphase and, at the midbody in late telophase cells undergoing cytokinesis. Collectively, these results indicate that pools of active B-Raf localize to specific spindle structures including the centrosomes during cell division.

*Phosphorylated B-Raf Localizes to Condensed Chromatin*

While phospho-B-Raf (Thr599/Ser602) staining was exclusively detected at the centrosome during interphase, staining became prominent at the nuclear region containing condensed chromosomes during prophase, in agreement with the staining pattern for total B-Raf protein (Fig. 7). During metaphase, phospho-B-Raf (Thr599/Ser602) staining was concentrated at regions surrounding the aligned chromosomes (Fig. 15). The perichromosomal space is the region that directly encircles each condensed chromosome. Many proteins localize to the perichromosomal space during mitosis and the functions of these proteins and the perichromosomal region have not been fully defined. However, it has been shown that several components that localize to the perichromosomal space are involved in mitotic functions such as chromosome condensation, decondensation, mitotic progression, cytokinesis and nuclear envelope reformation following exit from mitosis. In order to directly address whether B-Raf is phosphorylated in a perichromosomal fashion, chromosomes were isolated from

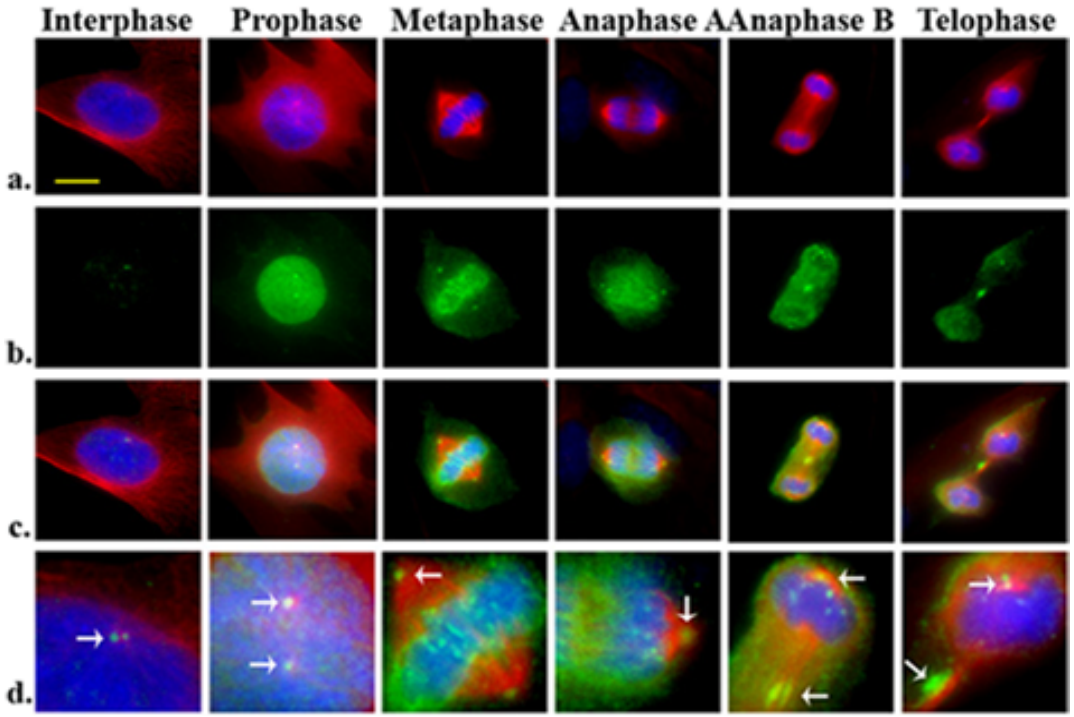


**Figure 15 B-Raf is phosphorylated at key mitotic structures**
HFF cells were immunostained for phospho-B-Raf using a phospho-B-Raf (Thr599/Ser602) antibody (b.). Microtubules and DNA (a.) were detected with anti-α-tubulin antibody and DAPI. Images were captured at 100X magnification. Overlay is shown in c and d - d is magnified 4X. Scale bar represents 10 μm. Arrows point to the centrosomes and the midbody.

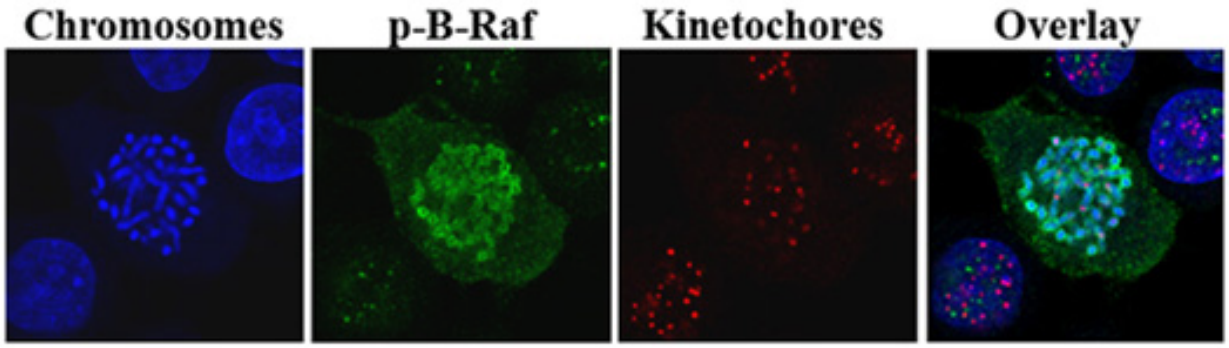


**Figure 16 Phosphorylated B-Raf localizes to the condensed chromosomes**
Phospho-B-Raf (Thr599/Ser602) localizes to the perichromosomal space during metaphase, but not interphase. Chromosomes were isolated from HeLa cells treated with nocodazole for 2 hrs and subjected to immunostaining and visualized with confocal microscopy. Kinetochores were visualized with CREST antiserum (red); green foci represent phospho-B-Raf staining. Shown are single 0.45 μM sections from within a z-series of a metaphase cell. A metaphase cell is shown in the center of each panel surrounded by three interphase cells, in which no colocalization is observed.

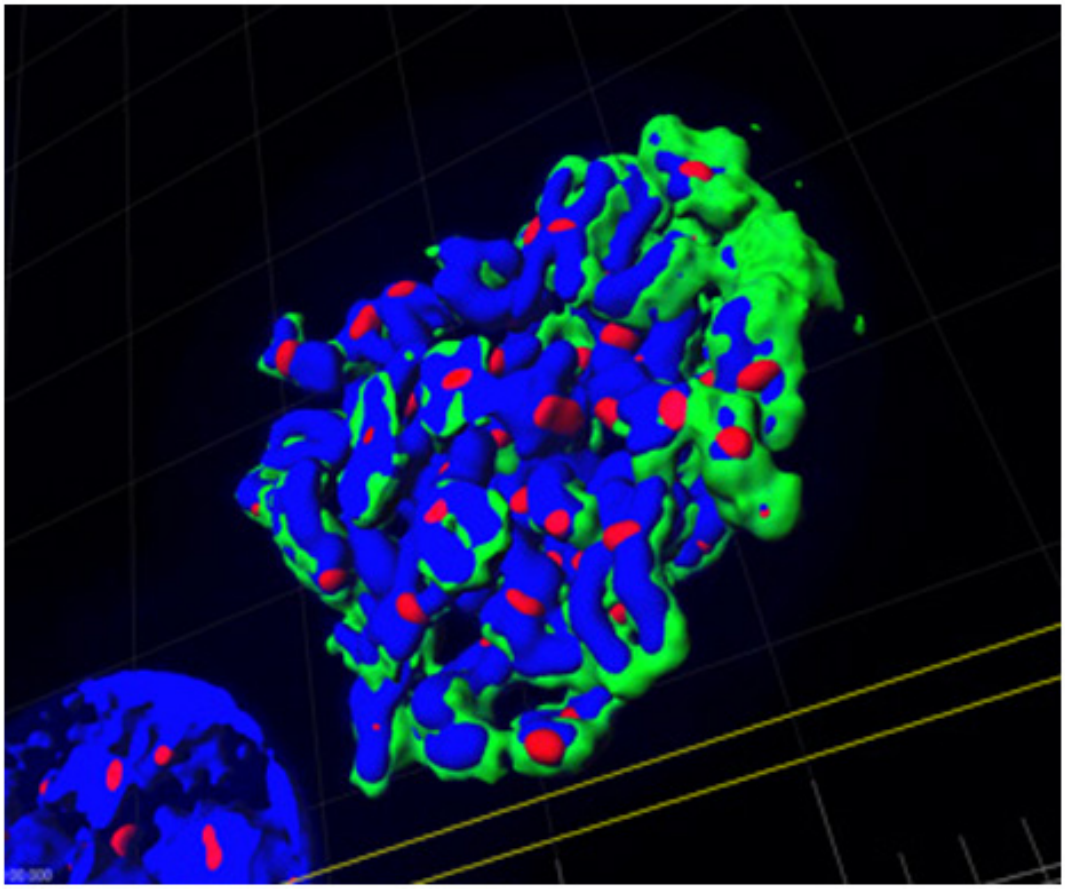

**Figure 17 Phosphorylated B-Raf localizes to the perichromosomal sheath**
Phospho-B-Raf (Thr599/Ser602) localizes to the perichromosomal sheath during metaphase, but not interphase. Images from figure 18 were analyzed using Imaris doconvolution software and a 3D isosurface model was rendered. Kinetochores were visualized with CREST antiserum (red); green foci represent phospho-B-Raf and chromosomes are shown in blue (DAPI). A metaphase cell is shown in the center and an interphase cells, in which no colocalization is observed, to the bottom left of the panel. Joseph Johnson created this image.

interphase and metaphase cells, spun onto coverslips and stained with DAPI and the phospho-B-Raf antibody. Confocal microscopy revealed that phospho-B-Raf (Thr599/Ser602) encircles each individual chromosome during metaphase, whereas no chromatin associated staining was detected in interphase cells (Fig. 16). The perichromosomal staining is further supported by rendering a three-dimensional isosurfacing model of the chromosomes (Fig. 17).

*Phosphorylated B-Raf localizes to the Kinetochores*

Confocal imaging of B-Raf staining in HFF cells revealed discrete foci detectable along the metaphase plate of aligned chromosomes (Fig. 8, metaphase) reminiscent of kinetochores. A view along the spindle pole axis (Fig. 8, metaphase y-axis) showed these foci appeared as a ring-like structure that co-localized at the juncture where spindle microtubules meet the aligned chromosomes, typically the site of the kinetochores. Close inspection phospho-B-Raf (Thr599/Ser602) staining revealed the appearance of foci overlapping with chromosomes during metaphase and anaphase (Fig. 15, row d). To determine whether these foci were localized at kinetochores, metaphase chromosomes were isolated from nocodazole-treated HFF cells, fixed and adhered to coverslips. Chromosomes were subjected to immunofluorescence analysis. Co-staining with the kinetochore marker CREST antiserum and phospho-B-Raf showed that phospho-B-Raf foci overlap directly with every pair of kinetochores of metaphase chromosomes (Fig. 18, metaphase). In contrast, interphase nuclei demonstrated no kinetochore colocalization of phospho-B-Raf (Fig. 18, interphase). These results demonstrate that phospho-B-Raf (Thr599/Ser602) co-localizes with the kinetochores during metaphase.

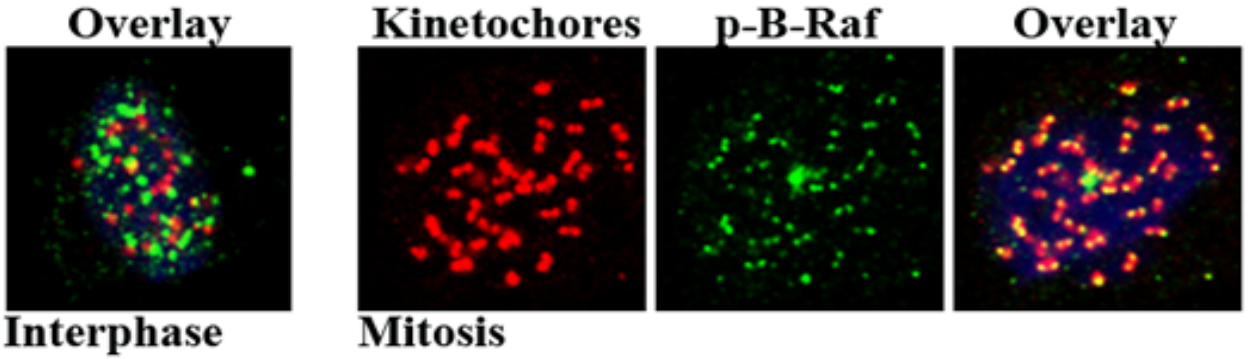


**Figure 18 Phosphorylated B-Raf localizes to the kinetochores during mitosis**
Phospho-B-Raf (Thr599/Ser602) stained foci co-localize to kinetochores at metaphase, but not interphase, chromosomes. Chromosomes were isolated from HeLa cells treated with nocodazole for 2 hrs and subjected to immunostaining and visualized with confocal microscopy. Kinetochores were visualized with CREST antiserum (red); green foci represent phospho-B-Raf staining. Shown are single 0.45 μM sections from within a z-series of a metaphase cell.

## Conclusions

Prior to my studies, reports on the subcellular localization of B-Raf were limited strictly to the cytoplasm of interphase neurons. My results demonstrate that B-Raf localization and phosphorylation is cell-cycle specific. Specifically, B-Raf localizes to and is phosphorylated at mitotic structures, many of which are known to play a critical role in the accuracy and timing of mitosis.

# CHAPTER 3

# B-RAF PERFORMS CRITICAL MITOTIC FUNCTIONS

## Introduction

Previous studies from our laboratory show a role for MAPK in promoting the formation and stability of the mitotic spindle [115]. Specifically, blocking MEK activity or depleting p42 MAPK from *Xenopus* egg extracts inhibits spindle assembly and leads to the generation of aberrant half spindles, a portion with unfocused poles, and microtubule (MT) asters. Moreover, when mammalian cells are treated during late G2 and M phases with the pharmacological MEK inhibitor U1026, a high frequency of spindle abnormalities and misaligned chromosomes is observed indicating that MEK signaling is also important for spindle functions in somatic cells. A role for B-Raf in activating the MAPK cascade during mitosis has been suggested from studies in *Xenopus* egg extracts that mimic the early embryonic cell cycles of S and M phases [180]. As well, it has been reported that peaks of B-Raf activity are detected at M phase and early $G_1$ phase during the cell cycle of HeLa cells [134], but hard evidence for B-Raf having a role in regulating mitosis in somatic cells had not been described. The studies described in this chapter show evidence for mitotic functions of B-Raf at mitosis in human somatic cells.

## Results

### B-Raf Contributes to Mitotic Spindle Assembly in *Xenopus* Egg Extracts

Work from our laboratory has shown that proper mitotic spindle assembly in *Xenopus* egg extracts requires ERK phosphorylation. In the same system, we have shown that B-Raf is the MEK kinase which activates ERK signaling during mitosis. B-Raf and ERK activities do not regulate S-phase functions in *Xenopus* egg extracts, as they are strictly relegated to mitosis. These data suggests that B-Raf may regulate spindle assembly in *Xenopus* egg extracts through direct effects on mitosis.

#### *Spindle Assembly is Compromised in the Absence of B-Raf in Xenopus Egg Extracts*

*Xenopus* egg extracts are a powerful biochemical system for studying the regulation of spindle assembly. Antibodies can be used to efficiently immunodeplete endogenous proteins and spindle assembly can be monitored. As shown in figure 19, B-Raf protein in *Xenopus* CSF-arrested egg extracts is immunodepleted using B-Raf antibodies but not rabbit IgG mock control. Metaphase spindle formation was monitored by the addition of rhodamine labeled tubulin in both mock- and B-Raf-depleted extracts. Formation of spindles in mock-depleted egg extracts occurred properly, as shown, exhibiting bipolar spindles with focused poles and well-organized microtubules (Fig. 20). In contrast, the depletion of B-Raf from egg extracts disrupted spindle assembly, resulted in unfocused spindle poles and splayed spindle structures. Several monopolar, half spindle structures were also formed as well as structures lacking organized microtubules and containing misaligned chromosomes. These results indicate that B-Raf is required for mediating proper spindle assembly in *Xenopus* egg extracts.

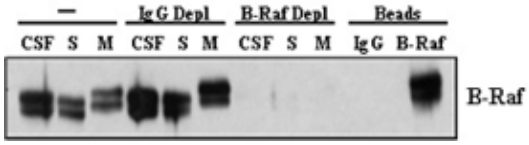


**Figure 19 Immunodepletion of B-Raf from *Xenopus* egg extracts**
CSF-arrested *Xenopus* egg extracts were depleted of endogenous B-Raf protein with B-Raf specific antibodies. Extracts were activated into S phase (S) with 0.4 μM $Ca^{+2}$ addition and cycled into M phase (M) with nondegradable cyclin B.

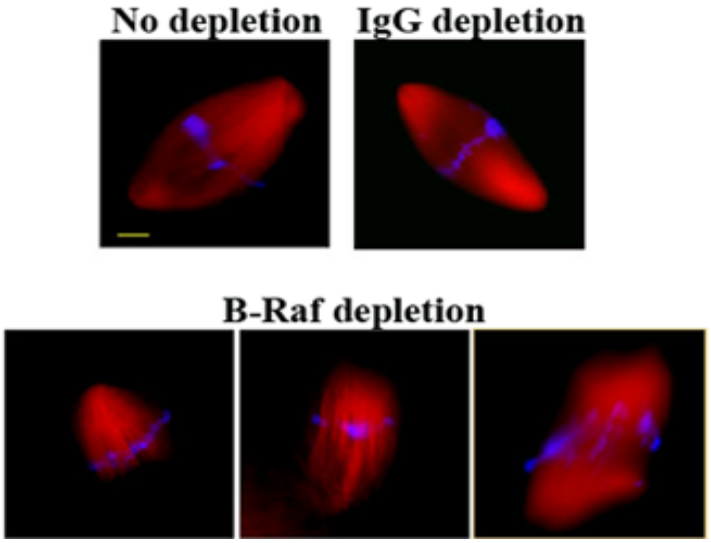


**Figure 20 B-Raf contributes to spindle assembly in *Xenopus* egg extracts**
Extracts were prepared as in figure 20. Rhodamine labeled α-tubulin was added to visualize spindle assembly and DNA was stained with Hoechst buffer. Images were taken on 100X magnification.

## B-Raf is Necessary for Spindle Formation and Chromosome Congression in Human Somatic Cells

Our preliminary studies in *Xenopus* egg extracts suggest a role for B-Raf in the regulation of mitotic spindle assembly. Immunofluorescence data suggests that active forms of B-Raf reside at mitotic structures in human somatic cells. Therefore I investigated whether B-Raf regulates the assembly of the mitotic spindle in human somatic cells.

### *Knockdown of B-Raf by siRNA Inhibits Proper Spindle Formation and Chromosome Congression*

To determine if B-Raf regulates spindle assembly in human somatic cells, two independent 21-base pair RNA duplexes corresponding to conserved B-Raf sequences in exon 11 (BE11), and exon 3 (BE3) were utilized to downregulate B-Raf . Spindles of mitotic cells were subsequently analyzed via immunofluorescence microscopy. siRNAs were transfected individually into human foreskin fibroblast (HFF) cells and HeLa cells (data not shown). A 21-base pair scrambled sequence was used as a control. Transfection of the BE11 or BE3 siRNAs led to an 80-95% reduction of B-Raf protein levels in HFF cells within 72 hours as assessed by immunoblot (Fig. 21). The scrambled control siRNA had no apparent effects on spindle morphology (Fig. 22). However, knockdown of B-Raf with the BE11 or BE3 siRNA resulted in pleiotropic spindle abnormalities in 80-90% of the mitotic cells analyzed from at least eight independent experiments. Three general groups of abnormal spindle phenotypes were observed: 49% with abnormal spindle morphology, including unfocused poles, 29% with shortened

spindle structures, and 22% with microtubule bundles. In the scrambled control cells, chromosome congressed in an organized, linear fashion at the metaphase plate in nearly 90% of cells. In contrast, chromosome alignment at the metaphase plate was perturbed in the vast majority of B-Raf depleted cells. Cells exhibited chromosomes throughout the region of the metaphase plate, along the perimeter of the mitotic spindle structures, at the spindle poles, and encircling entire spindle structures. Thus, our data suggest that B-Raf is critical for proper spindle formation and chromosome congression in human somatic cells.

*C-Raf is Dispensable for Normal Spindle Assembly*

Previous studies suggested that C-Raf (Raf-1) might play a cell cycle role at the G2/M transition [118, 284, 285]. Therefore, we also examined the consequences of reducing C-Raf protein levels in HFF cells. We transfected a 21-base pair RNA duplex (siRNA) specifically targeting C-Raf into human foreskin fibroblast (HFF) cells. A 21-base pair scrambled sequence was used as a control. Transfection of HFF cells with the C-Raf specific siRNA led to an 85% or greater reduction of C-Raf, but not B-Raf, after 48-72 hr (Fig. 23, A). In contrast to the phenotypic abnormalities generated in B-Raf knockdown cells, spindle morphology and chromosome alignment appeared completely normal in C-Raf depleted HFF cells as evaluated by immunofluorescence microscopy (Fig. 23, B). Thus, we conclude that C-Raf is not required for proper spindle formation or chromosome congression in somatic tissue culture cells.

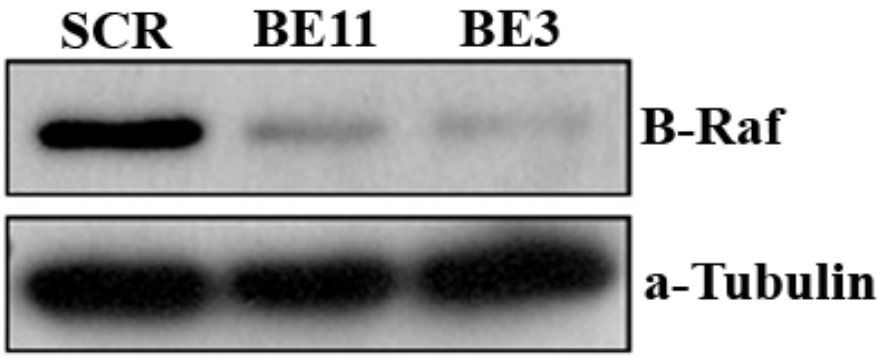


**Figure 21 Downregulation of B-Raf by siRNAs**
HFF cells were transfected with scrambled siRNA (SCR) or siRNAs targeting sequences within exons 11 or 3 of B-Raf (BE11 or BE3, respectively) and analyzed 48-72 hours post-transfection. Western analysis probing for B-Raf or α-tubulin (loading control).

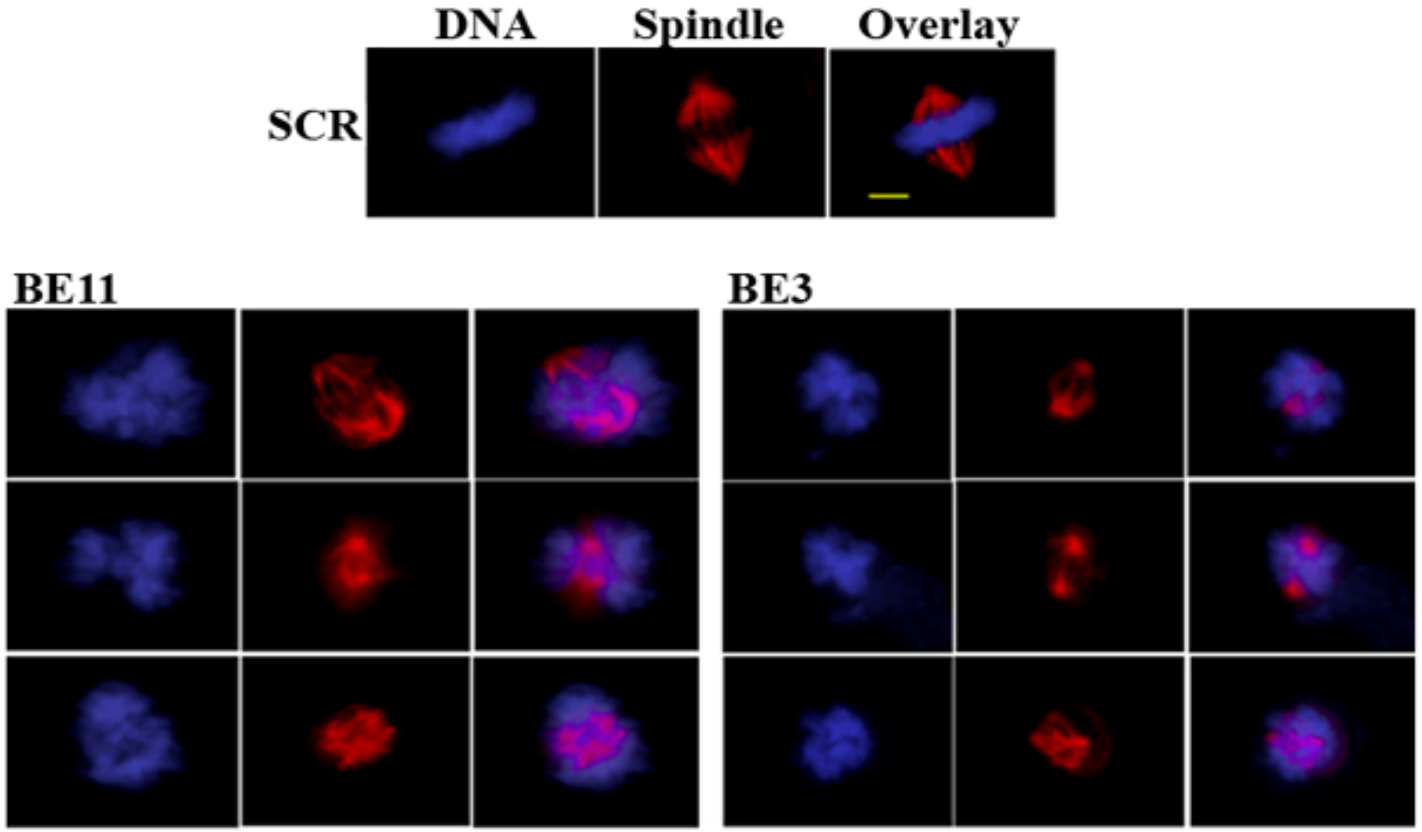


**Figure 22 B-Raf contributes to proper spindle assembly in human somatic cells**
HFF cells were transfected with scrambled siRNA (SCR) or siRNAs targeting B-Raf (BE11 or BE3) and analyzed 72 hours post-transfection. Photos are representative of typical abnormalities observed in spindle (red) morphology and chromosome (blue) congression. 50-100 spindle structures were analyzed in each of 8 experiments for each siRNA. Images were acquired at 60X magnification; scale bar represents 5 μM.

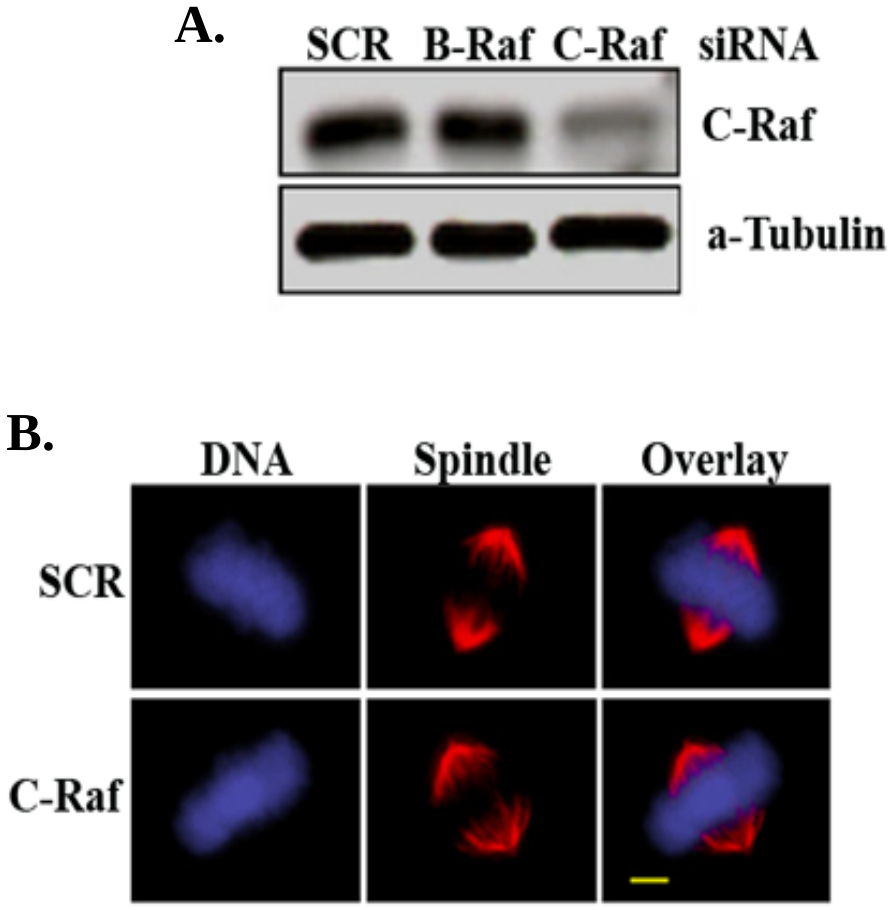


**Figure 23 C-Raf is not necessary for assembly of the mitotic spindle**
Knockdown of C-Raf by siRNA has no effect on spindle assembly or DNA alignment. HFF cells were transfected with a scrambled control siRNA (SCR), B-Raf specific siRNA, or C-Raf specific siRNA and analyzed 72 hours post-transfection. (A) Western analysis probing for C-Raf or α-tubulin (loading control). (B) Mitotic spindle and DNA alignment appear normal in C-Raf-depleted cells transfected with siRNA. Results are representative of at least three independent experiments. Images were acquired at 60X magnification; scale bar represents 5 μM.

## B-Raf Regulates Microtubule-Kinetochore Engagement

Metaphase is the stage of mitosis during which chromosomes align in the metaphase plate, equidistant from each centrosome, a process termed chromosome congression. Chromosome congression is preceded by and dependent upon the bipolar attachment of spindle microtubules to the kinetochores of each chromosome, otherwise known as "microtubule-kinetochore engagement" or "microtubule capture". Microtubule capture depends on the coordination of proteins which localize to the kinetochores. Following the downregulation of B-Raf, cells exhibit aberrancies in both spindle assembly and chromosome congression. One explanation for the lack of chromosome congression could be that microtubule-kinetochore engagement is impaired in the absence of B-Raf. The localization data demonstrates that B-Raf localizes to and is phosphorylated at the kinetochores, suggesting that B-Raf may indeed play a role in kinetochore mediated functions.

### *CENP-E Levels are Elevated at the Kinetochores in the Absence of B-Raf*

In order to determine whether the microtubules and kinetochores are engaged following siRNA downregulation of B-Raf, cells were analyzed for the presence of an engagement marker. The CENP-E motor protein is essential for microtubule capture by kinetochores and for regulating subsequent microtubule-kinetochore dynamics [286]. It has also been established that the levels of CENP-E bound to the kinetochores during early mitotic stages is increased three to five fold when microtubules are unattached to kinetochores [286]. While the significance of this increase is not fully understood,

kinetochore associated CENP-E levels serve as a marker of microtubule-kinetochore engagement.

HeLa and HFF cells were transfected with B-Raf or scramble control siRNAs as previously described. 72 hours post-transfection, it was determined that the B-Raf knock-down cells exhibited the aforementioned phenotypic abnormalities. A corresponding set of scrambled control and B-Raf knock-down cells were subjected to immunostaining for CENP-E and the kinetochore marker, CREST. Cells were imaged via confocal microscopy and 3-dimentional z-series projections were used to quantify the CENP-E colocalized with the kinetochores. While CENP-E was present at the kinetochores in the scrambled control cells, levels of kinetochore bound CENP-E increased by an average of 3.8 fold in cells transfected with the B-Raf siRNA (Fig. 24). The B-Raf knock-down cells that were analyzed exhibited chromosomal misalignment.

*Microtubules are not Cold Stable in the Absence of B-Raf*

Cells transfected with B-Raf siRNA display misaligned chromosomes and have elevated CENP-E, a marker for impaired microtubule capture. Microtubule polymerization from tubulin dimers is a dynamic and reversible process. Polymerized spindle microtubules are cold-stable when the microtubule's plus ends are attached to kinetochores and conversely they are cold-labile when unengaged. The classic experiment to directly assess whether spindle microtubules are engaged with kinetochores is to perform a cold-microtubule depolymerization assay.

To do this, I downregulated B-Raf using siRNA as described above and cells subsequently were plated on coverslips in tissue dishes. 72 hours post- transfection,

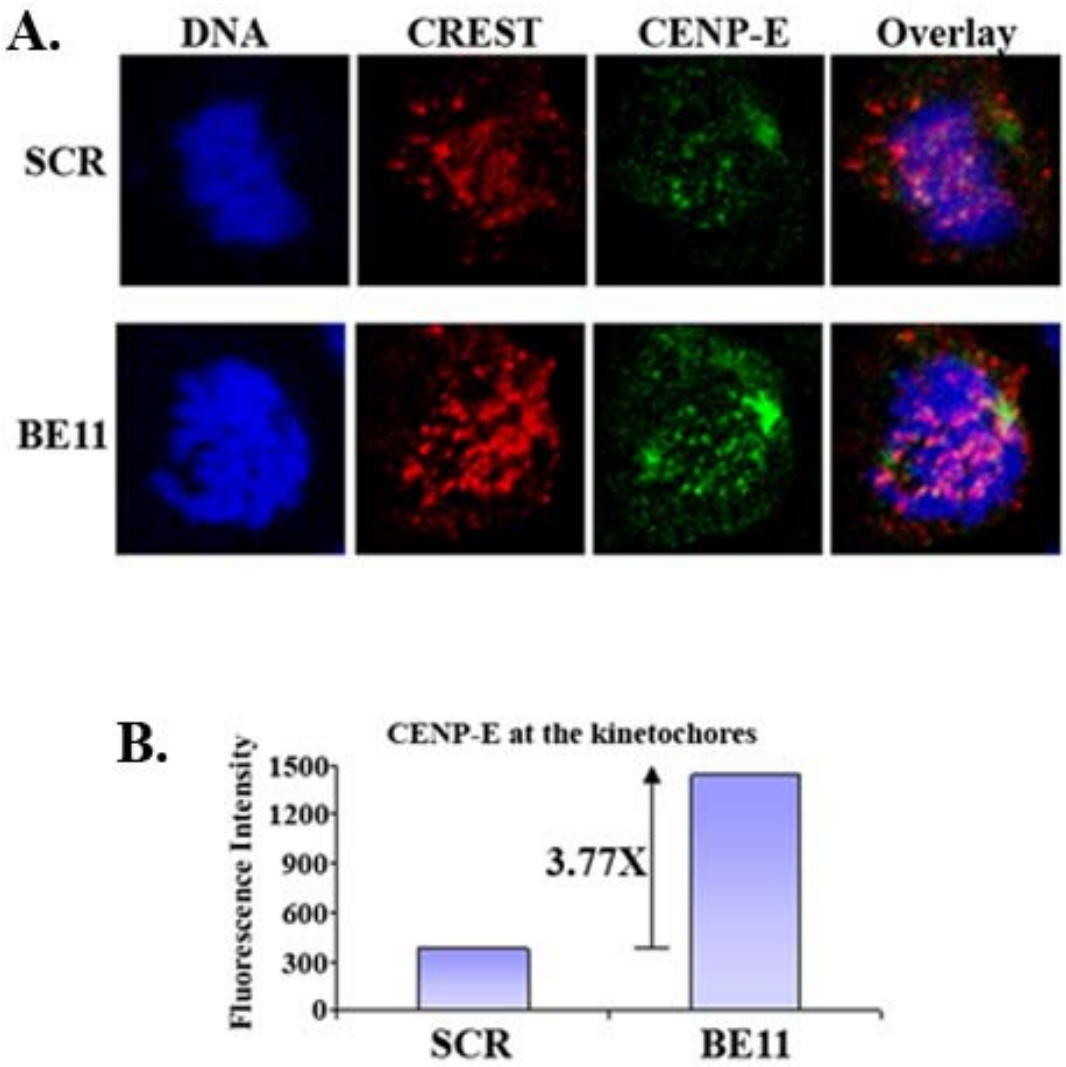


**Figure 24 Kinetochore bound CENP-E levels following downregulation of B-Raf**

Quantitation of CENP-E bound to the kinetochores. (A) HeLa cells were transfected with a SCR control siRNA or siRNA targeting B-Raf (BE11) and 72 hours post-transfection cells were stained for DNA (blue), kinetochore (red), CENP-E (green). (B) CENP-E that localizes directly with kinetochores was quantified.

the tissue culture dishes on which the cells were plated were subjected to cold by incubation on ice for several minutes. Cells were then fixed, stained for alpha-tubulin and DNA, and their microtubules were analyzed by immunofluorescence microscopy. The scrambled control cells exhibited normal chromosome congression spindle assembly (Fig. 25). Following cold treatment, the microtubules of the control cells remained polymerized. (The cells exhibited the anticipated morphological changes associated with cold). The cells in which B-Raf was transfected exhibited misaligned chromosomes and abnormal spindles. When subjected to cold treatment nearly 100% of these microtubules underwent complete and rapid depolymerization, thus demonstrating an absence of kinetochore-microtubule engagement in these cells.

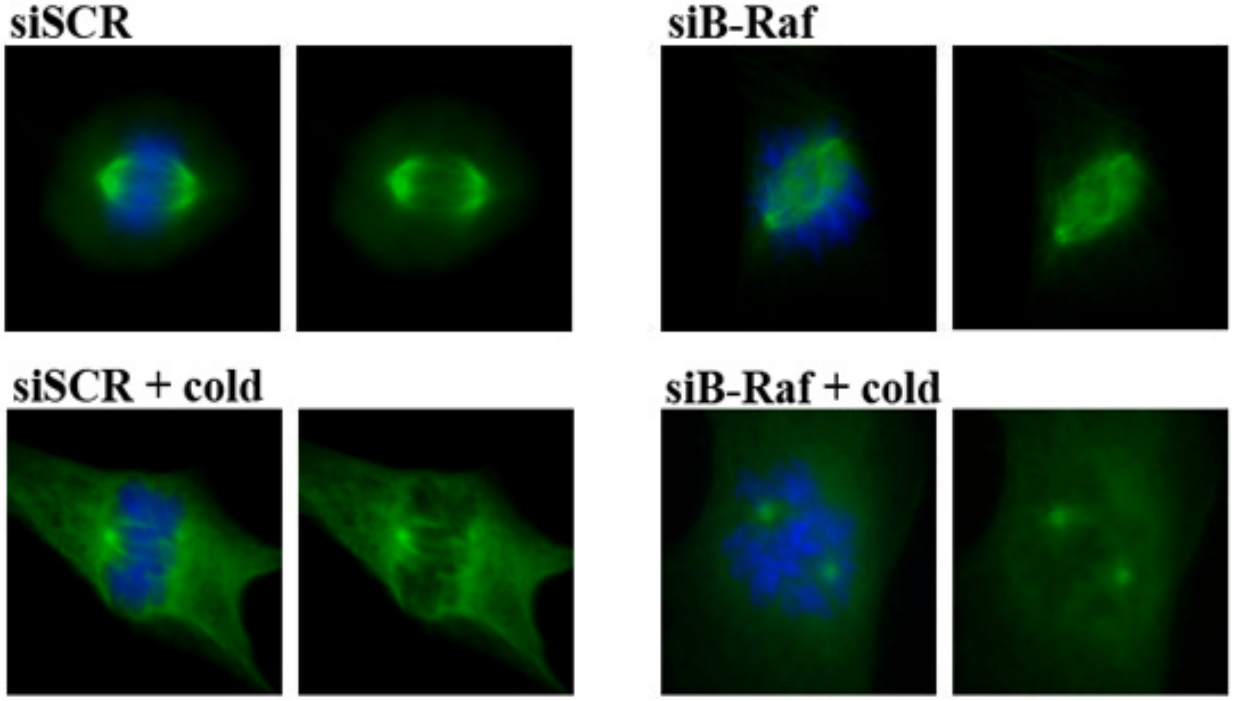


**Figure 25 Microtubules are not cold-stable in the absence of B-Raf**
HFF cells were transfected with a scrambled siRNA (siSCR) or a B-Raf targeting siRNA (siB-Raf). 72 hours post-transfection cells were exposed to ice for 10 minutes to depolymerize unengaged microtubules. Cells were then fixed with 4% paraformaldehyd and stained for DNA (blue) and α-tubulin (green). B-Raf depleted cells retained few to no polymerized microtubules, demonstrating that those cells had few to no microtubules engaged with kinetochores.

## B-Raf Regulates the Spindle Assembly Checkpoint

The spindle assembly checkpoint (SAC) arrests cells in mitosis prior to anaphase until all sister chromatid pairs are attached at the mitotic spindle. Activation of the SAC is dependent upon the activities of proteins which localize to the kinetochores. B-Raf itself localizes to and is dually phosphorylated at the kinetochores exclusively during mitosis. B-Raf depleted cells generate abnormal spindle structures and misaligned chromosomes and have deficiencies in microtubule-kinetochore engagement. Regardless of such dramatic mitotic defects, B-Raf depleted cells continue to proliferate over a 3-4 day period similar to control cells treated with scrambled siRNA. Therefore, we asked whether the spindle assembly checkpoint is functional in cells that are lacking B-Raf.

### *Cells Cycle through Mitosis in the Absence of B-Raf*

It is anticipated that cells will arrest in mitosis if they have defects in spindle assembly. To address whether B-Raf depleted cells arrest at the spindle assembly checkpoint, control and B-Raf depleted cells were counted and scored as being in interphase or mitosis based on their flattened or rounded morphology, respectively. The percentage of rounded cells following B-Raf downregulation was not significantly increased over cells in the control group (Fig. 26, A).

Cyclin B levels peak during metaphase and drop off rapidly to initiate anaphase, therefore Cyclin B levels serve as a biochemical marker of mitosis, specifically of metaphase. We analyzed Cyclin B levels, via western blot analysis, in cells transfected with the scrambled control siRNA or a B-Raf specific siRNA 72 hours post-transfection.

Levels of cyclin B were not increased in the B-Raf depleted cells relative to SCR control cells (Fig. 26, B).

Together, these data indicate that 72 hours of downregulation of B-Raf does not lead to a spindle assembly checkpoint arrest despite the notable induction of spindle abnormalities and the impairment of microtubule-kinetochore engagement.

*Induced Spindle Assembly Checkpoint is Compromised in the Absence of B-Raf*

Downregulation of B-Raf drives significant mitotic abnormalities that persist without induction of a SAC, suggesting that B-Raf may be necessary for SAC function. In order to determine whether B-Raf is required for activation of the SAC, scrambled control or B-Raf downregulated cells were subjected to a classic SAC challenge with microtubule poisons.

HFF and HeLa cells were challenged with nocodazole or taxol in order to induce a SAC 48 hours after transfection with scrambled control or B-Raf siRNAs. After 24 hours of challenge cells were analyzed for their capacity to arrest in mitosis. Cells were lysed and subjected to western blot analysis to evaluate Cyclin B levels as a biochemical marker of a spindle assembly arrest. Cyclin B level are reduced to nearly undetectable levels in cells depleted of B-Raf upon challenge nocodazole or taxol (Fig. 27) confirming that an artificially induced SAC is not fully functional in the absence of B-Raf. Live imaging microscopy of taxol treated cells confirmed that scrambled control cells entered and remained in a rounded morphological state consistent with the expected induction of metaphase arrest, whereas B-Raf depleted cells acquired a flattened morphology following a brief rounded state induced by taxol, indicative of a breached arrest (Fig. 28).

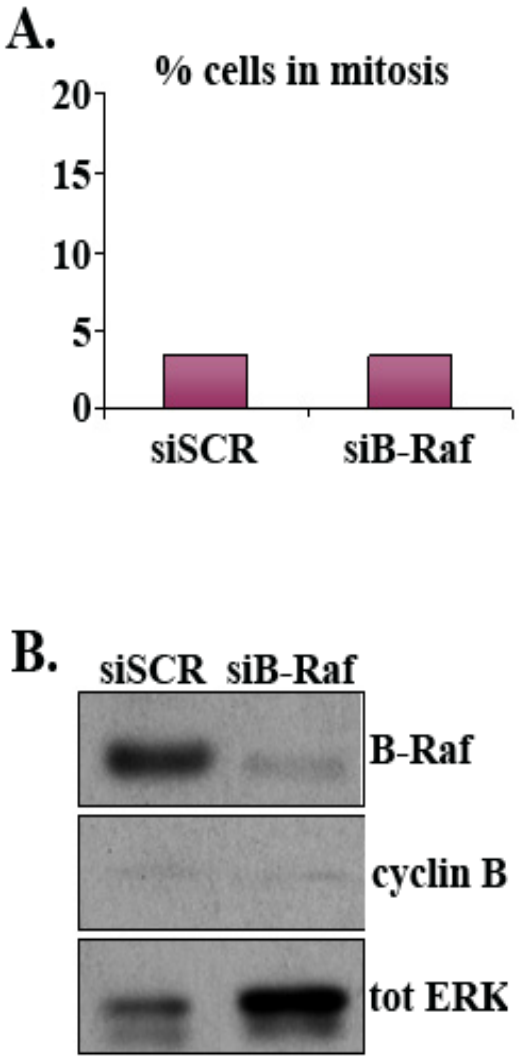


**Figure 26 Cells do not enter mitotic arrest in the absence of B-Raf**
HFF cells were transfected with a scrambled or B-Raf targeting siRNA. (A) Mitotic cells were scored based on round morphology. (B) Cells were lysed and probed for B-Raf, the mitotic marker, cyclin B and total ERK for a reference.

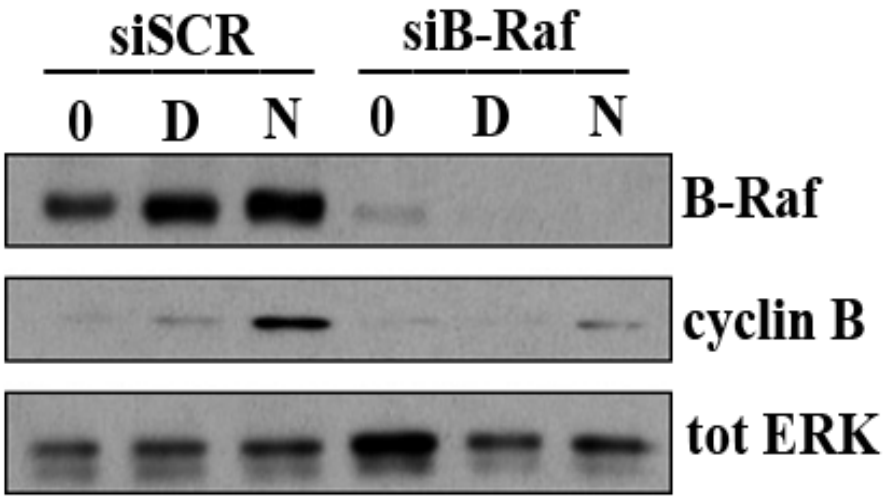


**Figure 27 Cells do not maintain a spindle checkpoint arrest in the absence of B-Raf**
HFF cells were transfected with scrambled or B-Raf targeting siRNAs for 48 hours followed by a nocodazole challenge for 24 hours. Cells were lysed and probed for B-Raf, the mitotic marker, cyclin B and total ERK.

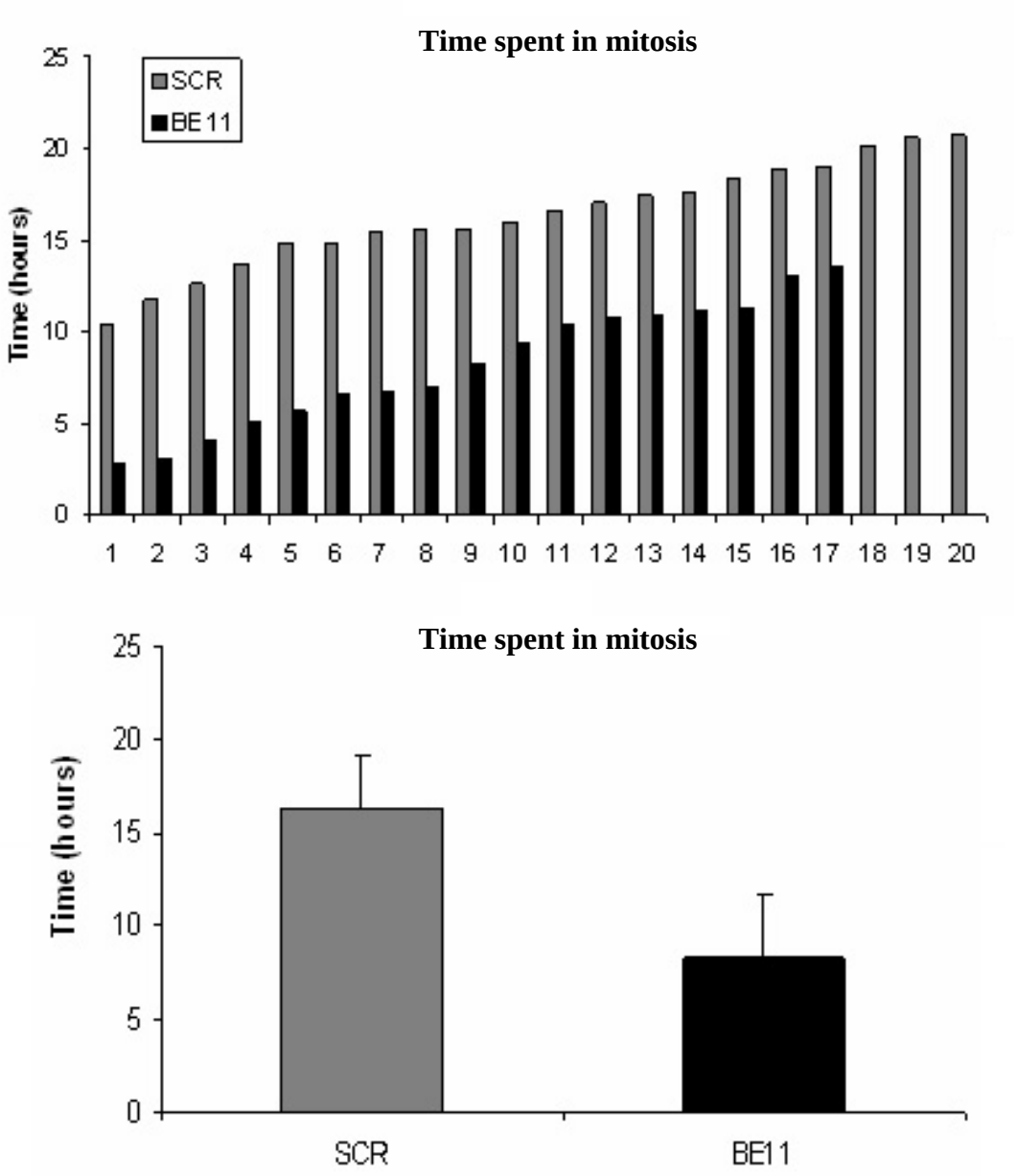


**Figure 28 B-Raf depleted cells exit mitotic arrest in the presence of taxol**

HeLa cells were transfected with scrambled control or B-Raf targeting siRNAs for 48 hours and then treated with 50nM taxol in 0.1% DMSO for 24 hours during which time cells were imaged using live imaging phase contrast microscopy. (A) 20 (SCR) or 17 (BE11) individual cells were analyzed for their time spent in mitosis. (B) On average, B-Raf depleted (BE11) cells spent significantly less time in mitosis relative control cells.

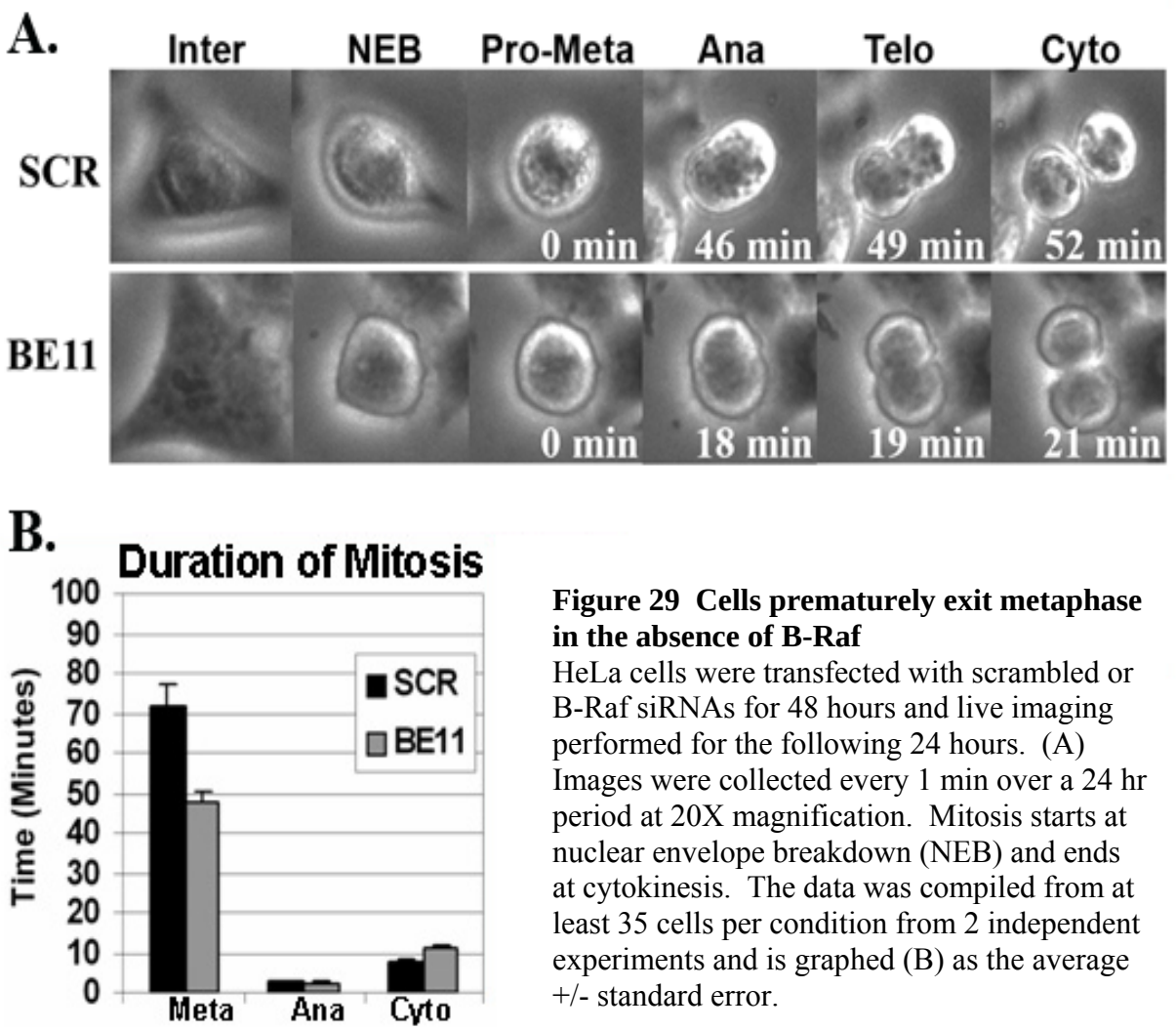


**Figure 29 Cells prematurely exit metaphase in the absence of B-Raf**

HeLa cells were transfected with scrambled or B-Raf siRNAs for 48 hours and live imaging performed for the following 24 hours. (A) Images were collected every 1 min over a 24 hr period at 20X magnification. Mitosis starts at nuclear envelope breakdown (NEB) and ends at cytokinesis. The data was compiled from at least 35 cells per condition from 2 independent experiments and is graphed (B) as the average +/- standard error.

*B-Raf Depleted Cells Exit Metaphase Prematurely*

To directly test whether the SAC is compromised in B-Raf depleted cells, scrambled control or B-Raf depleted HeLa cells were subject to live imaging phase-contrast microscopy for 24 hours. The total duration of mitosis was scored from nuclear envelope breakdown (NEB) through cytokinesis. HeLa cells treated with B-Raf siRNA accelerated faster through mitosis than SCR control cells, averaging 66 vs. 83 min, respectively (Representative photo Fig. 29, A). Closer inspection revealed that B-Raf-depleted cells remained in metaphase on average 24 minutes less than non-depleted cells (Fig. 29, B). In contrast, timing through anaphase-telophase was not significantly affected in B-Raf siRNA-treated HeLa cells, although a modest delay in cytokinesis was consistently observed. These results, imply that the spindle checkpoint is suppressed in HeLa cells depleted of B-Raf.

*Kinetochore Localization of Mad2 and Bub1 is Inhibited in the Absence of B-Raf*

Published data in *Xenopus* egg extracts has indicated ERK signaling regulates the requisite kinetochore localization of key spindle assembly checkpoint proteins. Since B-Raf's only known functions are regulated via ERK, we postulated that B-Raf regulates localization of SAC proteins to the kinetochores. To test this possibility, kinetochore localization of spindle checkpoint proteins Bub1 and Mad2 was analyzed in control and B-Raf depleted cells. To do this, metaphase chromosomes were isolated from colcemid-treated HeLa cells, immunostained for the kinetochore marker, CREST, and Bub1 or Mad2. In chromosomes isolated from scrambled siRNA transfected cells, localization of Bub1 and Mad2 at CREST-stained kinetochores was readily detectable (Fig. 30). In

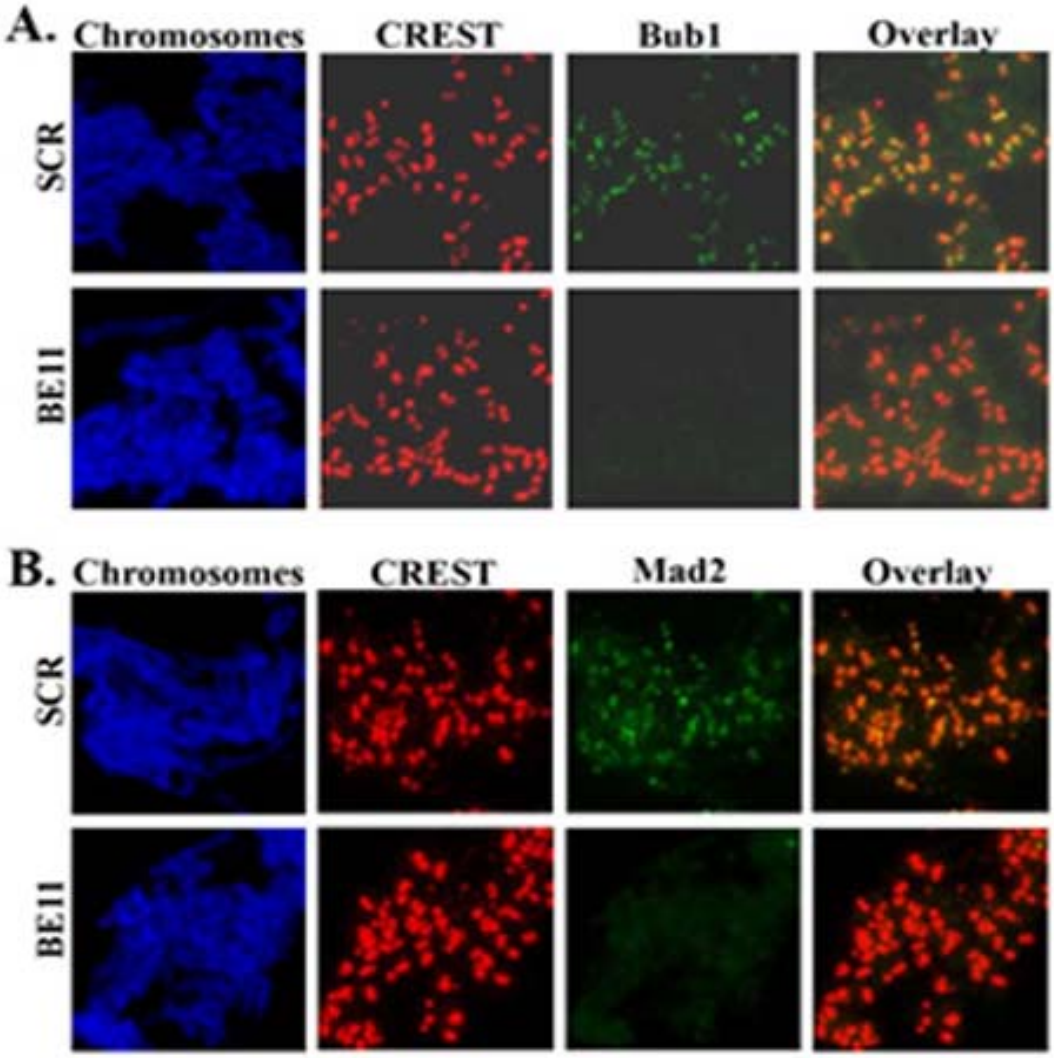


**Figure 30 Mad2 and Bub1 kinetochore localization is inhibited in the absence of B-Raf**

HeLa cells were transfected with a scrambled (SCR) or B-Raf specific (BE11) siRNA for 72 hours prior to chromosomal isolation. Kinetochore localization of Bub1 (B) and Mad2 (C) was analyzed using immunofluorescence on isolated chromosomes. DNA is stained with DAPI (blue), kinetochores are stained with CREST (red), Bub1 and Mad2 are shown in green.

contrast, Bub1 and Mad2 immunostaining was greatly diminished or undetectable at the kinetochores of HeLa cells treated with the B-Raf siRNA, demonstrating that B-Raf is necessary for proper localization of critical spindle assembly checkpoint proteins, Bub1 and Mad2. Since kinetochore localization of spindle checkpoint proteins is an indication of SAC activation, we conclude that B-Raf is critical for SAC activation.

## Conclusions

Our lab previously demonstrated that B-Raf regulates MAPK signaling during mitosis in *Xenopus* egg extracts. However, B-Raf had no known functional role in mitosis in *Xenopus* egg extracts or in mammalian cells. The work described in this chapter demonstrates that B-Raf is necessary for proper spindle assembly in *Xenopus* egg extracts and in human somatic cells. Chromatin congression is severely impaired upon B-Raf downregulation in human cells and we show evidence suggesting that microtubules are not fully engaged with the kinetochores in the absence of B-Raf. While such grave mitotic errors ought to elicit a spindle assembly checkpoint arrest, I have demonstrated B-Raf depleted cells accelerate faster through mitosis and bypass the spindle assembly checkpoint. We conclude that B-Raf contributes to several critical mitotic functions including spindle assembly, chromatin congression, microtubule capture and activation of spindle assembly checkpoint.

# CHAPTER 4

# ONCOGENIC B-RAF DISRUPTS MITOSIS AND CAUSES CHROMOSOMAL INSTABILITY

## Introduction

Mutationally activated B-Raf is detected in ~8% of human cancers with a particularly high frequency in melanoma (60-70%), colorectal (15-20%), papillary thyroid (35-50%), and ovarian (30%) cancers [216, 217, 287-291]. The B-Raf$^{V600E}$ mutant accounts for at least 90% of all B-Raf mutations detected to date which renders B-Raf into a constitutively active state [216, 224]. As such, B-Raf$^{V600E}$ sustains 10-fold higher levels of ERK activity in melanoma cells [292]. Ectopic B-Raf$^{V600E}$ expression transforms immortalized NIH 3T3 fibroblasts and mouse melanocytes in culture [216, 223, 226, 293, 294] and is required for melanoma cell proliferation, survival, and melanoma tumor growth and vascular development *in vivo* [226, 295, 296]. Together, these finding underscore crucial roles for B-Raf in tumorigenesis. How oncogenic B-Raf is required for tumorigenesis remains poorly understood. Part of the transforming activities of B-Raf$^{V600E}$ may occur through subverting adhesion-dependent G1 phase controls for cyclin D1 expression and p27 down-regulation [297, 298] and suppressing anoikis in melanoma cells [299, 300].

Aneuploidy is a widely recognized trait of many human cancers and is associated with tumor progression and poor prognosis [301, 302]. Aneuploidy results from mitotic errors in chromosome segregation due to defects in the spindle assembly checkpoint (SAC) and centrosome amplification [242, 303]. It is widely believed that aneuploidy itself can be a transforming event through the generation and selection of chromosomal profiles that favor cell growth, resistance to cell death and metastatic potential. Human melanomas are highly aneuploidy. In fact, changes in DNA copy number are detected in greater than 95% of human primary melanomas [304, 305] suggesting that early oncogenic events contribute to the onset of aneuploidy.

We have demonstrated that B-Raf regulates mitotic functions that are required to ensure proper chromosomal segregation and the genomic fidelity of the cell. In this chapter, we explore the possibility that the most common oncogenic mutation in B-Raf, V600E, contributes to mitotic defects leading to the acquisition of aneuploidy.

## Results

### B-Raf$^{V600E}$ Expression Promotes Mitotic Abnormalities in Melanoma Cells

B-Raf plays a critical role in the regulation of spindle formation, microtubule-kinetochore engagement and activation of the spindle assembly checkpoint in human somatic cells. This prompted us to ask whether the constitutively active oncogenic form of B-Raf, carrying a V600E mutation, might have adverse effects at mitosis.

### *B-Raf$^{V600E}$ Status in Melanoma Cells is Associated Mitotic Abnormalities*

To address the possibility that B-Raf$^{V600E}$ may have adverse effects on mitosis, mitotic events in A375 and SK-MEL28 melanoma cells, that are known to harbor B-Raf$^{V600E}$ mutations, were analyzed by immunofluorescence microscopy. In parallel, we examined mitoses in WM35, SbCl2, and SK-MEL5 melanoma cell lines expressing wild type B-Raf. Normal mitotic spindles were detected in at least 90% of the mitotic figures examined in melanoma cells with wild type B-Raf (Fig. 31). In contrast, abnormal spindles with misaligned chromosomes were observed at a high frequency (70-85%) in both A375 and SK-MEL28 cells (Fig. 31). These results indicate that melanoma cells carrying B-Raf$^{V600E}$ mutations are more prone to forming aberrant mitotic spindle structures during cell division.

### *B-Raf$^{V600E}$ Promotes Spindle Abnormalities and Centrosome Amplification in Human Melanoma Cells*

Based on the correlative findings between oncogenic B-Raf expression and mitotic abnormalities, we hypothesized that the constitutively active B-Raf$^{V600E}$ mutant was responsible for causing the abnormal mitoses observed in the mutant B-Raf melanoma cells. In experiments carried out in the Guadagno lab, by Yongping Cui, B-Raf$^{V600E}$ was introduced into SK-MEL-5 human melanoma cells with a wild type B-Raf background. Cells were infected via a retrovirus using a pBabe-puro-B-Raf$^{V600E}$ vector or the corresponding empty vector control. Expression of the recombinant B-Raf$^{V600E}$ mutant was confirmed by western analysis (Fig. 32, A) and led to elevated phospho-ERK levels as previously reported [306]. Strikingly, SK-MEK-5 melanoma cells transduced

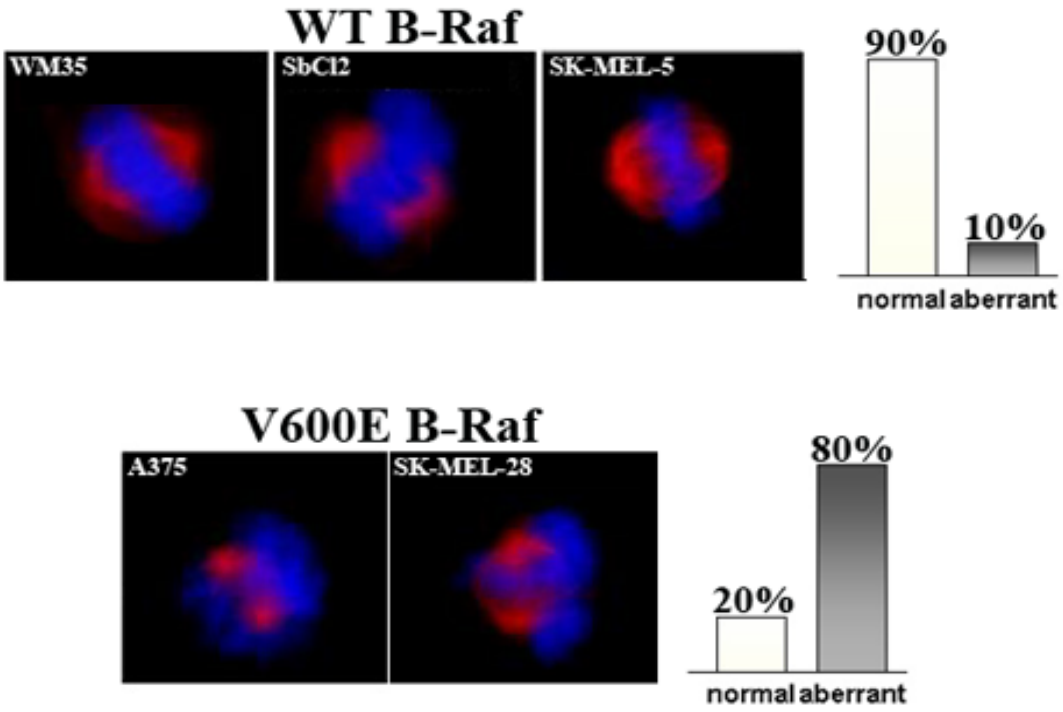


**Figure 31 Aberrant chromatin congression in B-Raf$^{V600E}$ positive melanoma cells**

Panel of human melanoma cell lines during mitosis containing wild type (WT) or mutant (V600E) B-Raf. Microtubule spindles and DNA were detected by staining with a α-tubulin antibody and DAPI, respectively. Magnification is 63X. (B) Graphs show the percent of normal versus abnormal spindles in human melanoma cells at mitosis (n=200).

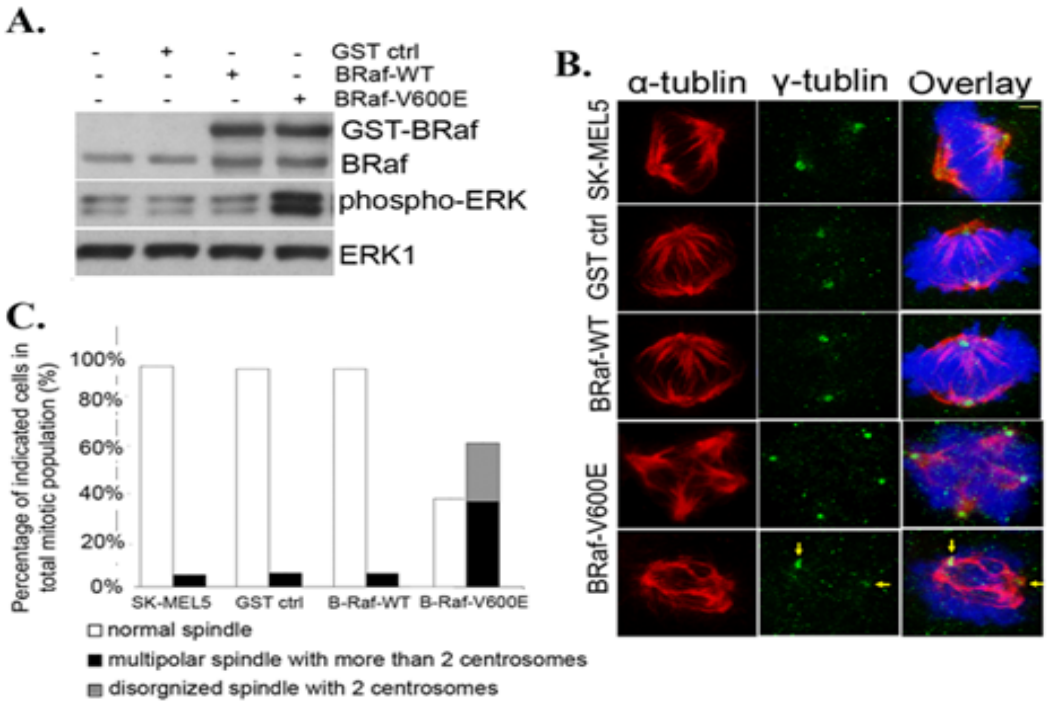


**Figure 32 Aberrant mitotic spindle formation and chromatin congression in melanoma cells ectopically expressing B-Raf$^{V600E}$**
SK-MEL5 melanoma cells were transfected with pGST, pGST-B-Raf, or pGST-B-Raf$^{V600E}$ plasmid DNAs. (A) Western blot analysis and (B) immunofluorescence staining of mitotic spindles and centrosomes. DNA was detected by DAPI staining. (C) Graph of data from Sbcl2 and SK-MEL5 cells. 200 mitotic figures were analyzed for each condition per experiment. Scale bar, 5 μM.

*This figure was contributed by Yongping Cui, Ph.D.*

with pBabe-B-Raf$^{V600E}$, but not with pBabe alone (empty vector), displayed pleiotropic spindle abnormalities in ~76% of mitotic figures examined by fluorescence microscopy (Fig. 32, B & C). These abnormalities include abnormal spindle morphology, multi-polar spindles and misaligned chromosomes. Similar results were obtained in SbCl2 melanoma cells transfected with pGST-B-Raf$^{V600E}$ constructs but not pGST empty vector (data not shown). The abnormal spindle phenotypes were not due to over-expression of B-Raf protein *per se* as ectopic expression of wild type B-Raf in SK-MEL5 cells had little effect on spindle formation. Hence, expression of constitutively active B-Raf$^{V600E}$ promotes spindle abnormalities in melanoma cells.

Abnormal numbers of centrosomes often arise in tumor cells resulting in multi-polar aberrant spindle structures [303]. A portion of mitotic spindles displayed multiple poles in melanoma cells transfected with B-Raf$^{V600E}$ (Fig. 32, B). To confirm whether this reflects the presence of extra centrosomes, parental and B-Raf$^{V600E}$-modified melanoma cells were subjected to immunostaining with an anti-γ-tubulin antibody. Depending on the phase of the cell cycle, G1 (unduplicated) or G2 (duplicated) centrosomes were typically detected in either parental or vector control SK-MEL-5 cells with fewer than 5% containing greater than 2 centrosomes (Fig. 32, C). In contrast, supernumerary centrosomes (as indicated by γ-tubulin stained foci) were detected in ~30% of interphase cells for both SbCl2 and SK-MEL5 cell lines containing the B-Raf$^{V600E}$ mutant. Co-staining of microtubules with a α-tubulin antibody revealed multipolar spindles at mitosis in cells containing supernumerary centrosomes. This represented about half of the abnormal spindles. The remaining abnormal spindles

contained two centrosomes suggesting that B-Raf$^{V600E}$ also perturbs spindle formation independent of centrosome amplification.

## B-Raf$^{V600E}$ Drives Aneuploidy and Chromosome Instability in SbCl2 Melanoma Cells

The results shown here demonstrate that exogenous B-Raf$^{V600E}$ expression promotes spindle abnormalities and centrosomal amplification in human melanoma cells. While a large number of these cells die, some of these cells are retained in the population despite the severity of mitotic abnormalities. It stands to reason that errors in chromosome segregation errors may have occurred in these cells, leading to aneuploidy. Since these experiments demonstrate that B-Raf$^{V600E}$ drives mitotic abnormalities in cells, which continue to divide, I decided to determine if the chromosomal composition of these cells is changing over time. Such insights are significant since chromosomal instability gives rise to a karyotypically varied population of cells thereby providing a pool for selection of cells that have tumorigenic and metastatic potential.

### *B-Raf$^{V600E}$ Induces Aneuploidy in SbCl2 Melanoma Cells*

Most tumor cells and cell lines exhibit aneuploidy, therefore I screened several melanoma cell lines for their chromosomal number via metaphase spread analysis. SbCl2 cells isolated from an early primary tumor are genomically stable with a mode of 46 chromosomes (Fig. 33). In order to test whether B-Raf$^{V600E}$ can induce aneuploidy in this genomically stable cancer cell line, cells were retrovirally infected with a pBabe-B-Raf$^{V600E}$ vector or the corresponding empty vector control and positively expressing cells

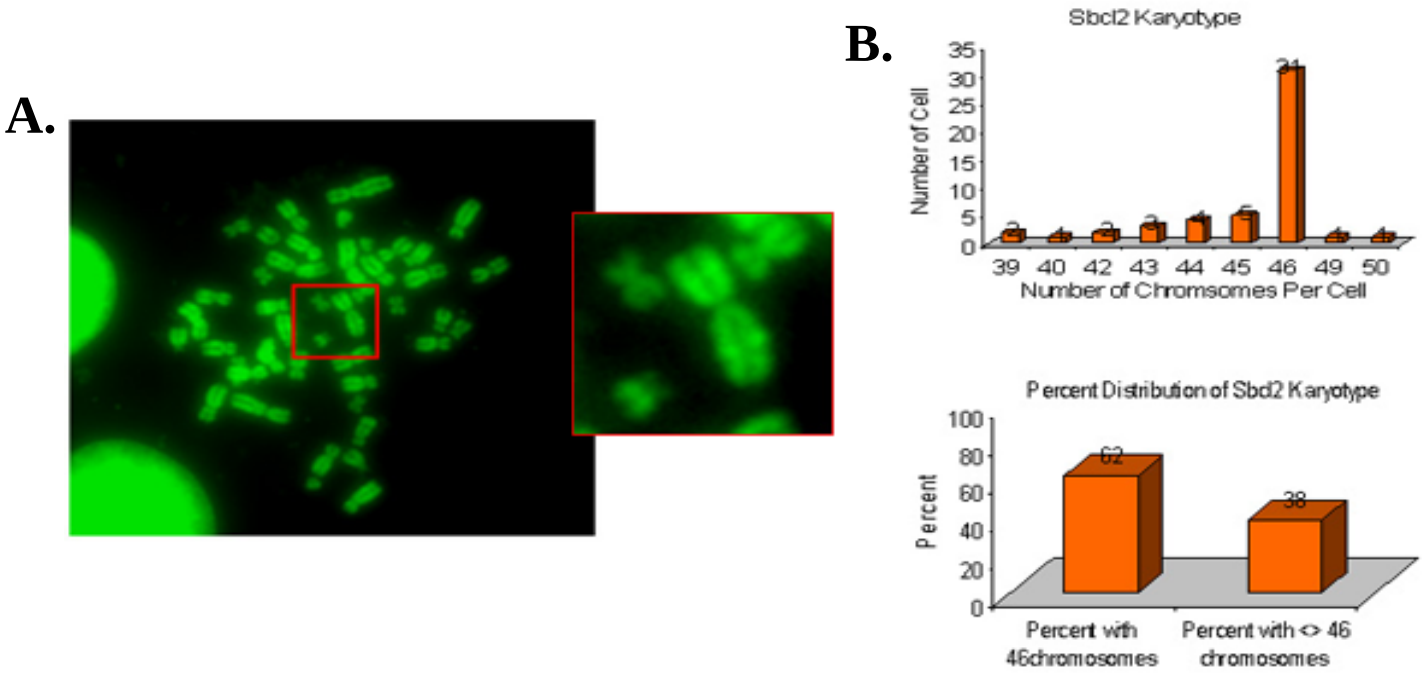


**Figure 33 SbCl2 melanoma cells are near diploid**
(A) Metaphase spreads were performed on SbCl2 cells and the chromosomes were stained with DAPI and pseudocolored green for contrast. (B) 50 metaphase spreads were counted and the chromosomal distribution s are shown. The upper panel indicated the number of chromosomes each cell contains and the lower panel shows the percentage of cells containing 46 chromosomes or <>46 chromosomes.

were selected for two weeks in puromycin containing media. Immunofluorescence and western blot analysis was performed to confirm exogenous B-Raf expression and activation of ERK (Fig. 34, A & B). Fluorescence in situ hybridization (FISH) was performed on the cells to evaluate their ploidy. In the empty vector control cells, 5.5% and 9.5% of interphase nuclei displayed less than or greater than two signals for centromere probes to chromosomes 2 or 8, respectively (Fig. 35, A), which is consistent with SbCl2 having a mode of 46 chromosomes. In contrast, B-Raf$^{V600E}$ expressing SbCl2 cells exhibited aneuploidy at a frequency of 16.5% in chromosome 2 and 20.5% in chromosome 8 in (Fig. 35, A). This data demonstrates a role for constitutively active B-Raf$^{V600E}$ in promoting aneuploidy in tumor cells.

*B-Raf$^{V600E}$ Drives Chromosome Instability in SbCl2 Melanoma Cells*

B-Raf$^{V600E}$ expression causes significant levels of aneuploidy in SbCl2 melanoma cells as demonstrated via FISH analysis. It is anticipated that the persistence of spindle abnormalities in these cells would continue to generate segregation errors and perpetually change the chromosomal content of the cells. Therefore, SbCl2 cells were used to test whether B-Raf$^{V600E}$ expression can induce chromosomal instability. SbCl2 cells were retrovirally infected and selected for expression of B-Raf$^{V600E}$ or an empty vector control as described above. The karyotypes of individual cells were evaluated to assess the precise number of chromosomes per cell. To evaluate the karyotype, metaphase spreads were prepared, chromosomes were stained with DAPI and counts were performed on 100 cells per sample. A mode of 46 chromosomes was observed in the vector control SbCl2 cells two weeks post-infection (Fig. 35, B). As expected in cell culture 50% of the

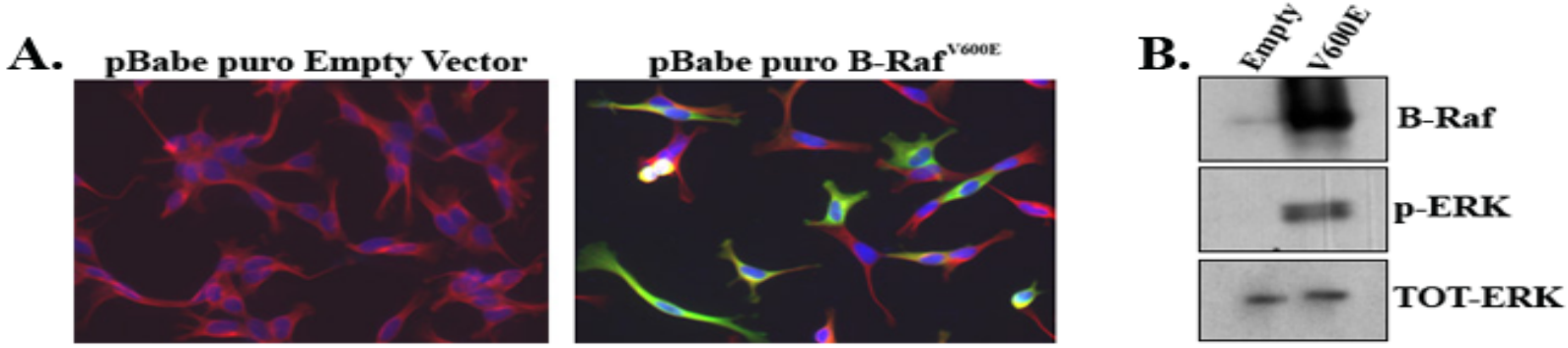


**Figure 34 Exogenous expression of B-Raf$^{V600E}$ in SbCl2 cells**
Retroviral expression of B-RafV600E or empty vector control in SbCl2 melanoma cells that endogenously express WT B-Raf. (A) Immunofluorescence staining of DNA (blue), tubulin (red) and B-Raf (green). Threshold is lowered until endogenous B-Raf is undetectable in empty vector control. (B)Western analysis of cell lysates prepared from control (empty vector) or B-Raf$^{V600E}$ overexpressing Sbcl2 cells.

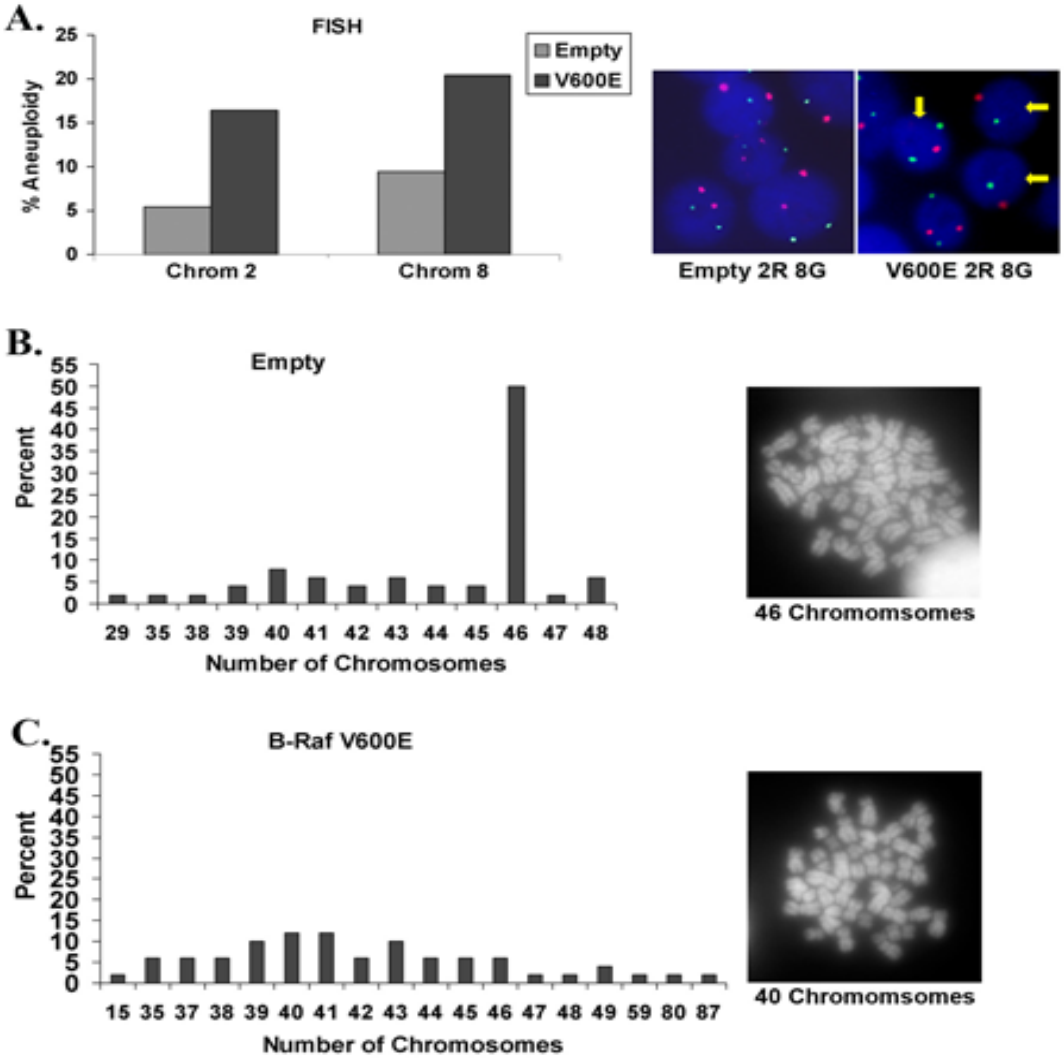


**Figure 35 Aneuploidy induced by B-Raf$^{V600E}$ in SbCl2 cells**
SbCl2 melanoma cells that endogenously express WT B-Raf were retrovirally infected to expression of B-RafV600E or empty vector control. (A) Percentage of 200 nuclei per condition, that scored positive for aneuploidy by FISH analysis with probes to either chromosome 2 or 8. * p-values for chromosomes 2 and 8 are <0.001 and <0.005, respectively. Photos of FISH analysis using centromere probes specific to chromosomes 2 (red, 2R) and 8 (green, 8G). Yellow arrows point to nuclei positive for aneuploidy. (B and C) Percent distribution and representative examples of chromosome numbers obtained from at least 50 metaphase spreads. Chromosomes were detected by staining with DAPI and imaged at 100X magnification.

control cells had some degree of aneuploidy, ranging from 29 to 48 chromosomes per cell. In contrast, expression of B-Raf$^{V600E}$ resulted in the complete absence of a chromosomal mode, with aneuploidy in 94% of the cells (Fig. 35, C). B-Raf$^{V600E}$ expressing cells exhibited a large distribution of chromosomes ranging from 15-87 chromosomes per cell. These results demonstrate that SbCl2 cells became aneuploid due to expression of B-Raf$^{V600E}$.

In order to determine if the population of B-Raf$^{V600E}$ cells are chromosomally unstable, cells were allowed to continue proliferating and their karyotypes were re-evaluated at later time point. 52% and 48% of the control cells maintained 46 chromosomes at week four (Fig. 36, A) and week six (Fig. 36, B), respectively, and the chromosomal variability ranged from 30 to 51 chromosomes per cell. Thus the mode and the chromosomal variability in the control cells did not change significantly over time. B-Raf$^{V600E}$ cells continued to be highly aneuploid with only ~5% having 46 chromosomes. However, the chromosomal distribution was sharply reduced from 15-87 chromosomes per cell at two weeks post-infection to 18-52 at four weeks (Fig. 36, C) and 15-49 at 6 weeks (Fig. 36, D). This demonstrates that the population of B-Raf$^{V600E}$ cells is chromosomally unstable with an increase in the percentage of hypoploidy cells over time.

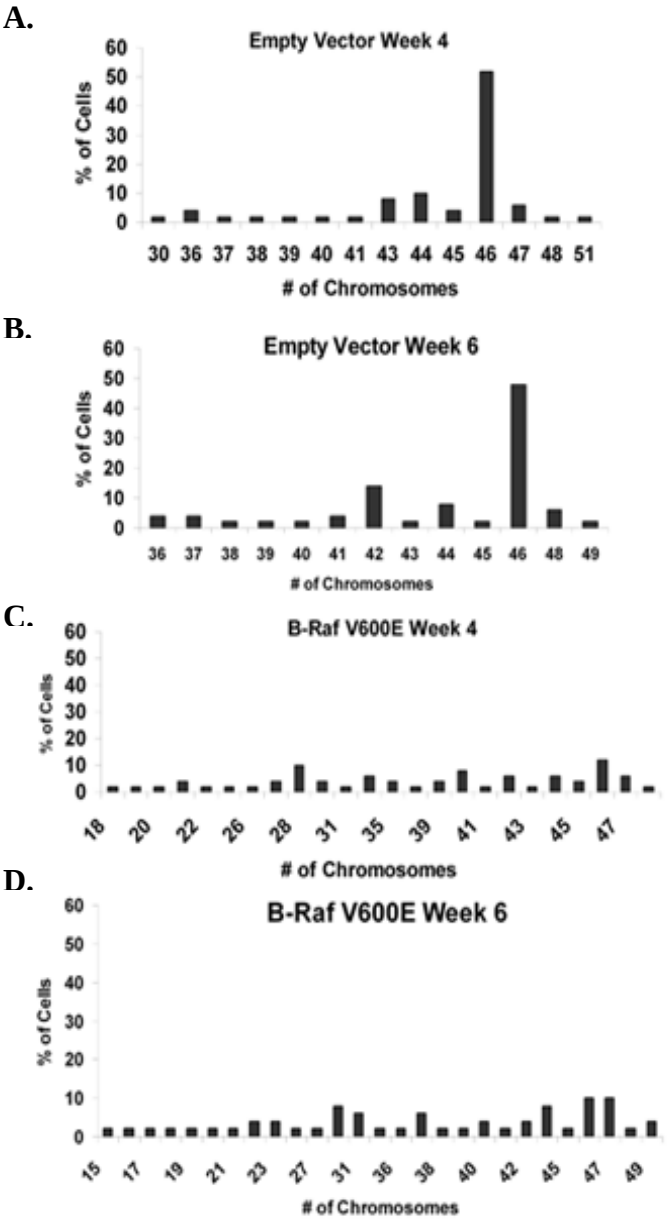


**Figure 36 Change in chromosome number generated by 4 and 6 weeks of B-Raf$^{V600E}$ expression**
SbCl2 melanoma cells endogenously expressing WT B-Raf were retrovirally infected to expression of B-Raf$^{V600E}$ or empty vector control. (A) Karyotype of cells cultured for 4 weeks in the presence of the pBabe puro empty vector. (B) Karyotype of cells cultured for 6 weeks in the presence of the pBabe puro empty vector. (C) Karyotype of cells cultured for 4 weeks in the presence of the pBabe puro B-Raf$^{V600E}$ vector. (D) Karyotype of cells cultured for 6 weeks in the presence of the pBabe puro B-Raf$^{V600E}$ vector. 50 cells per condition were analyzed.

## B-Raf$^{V600E}$ Induces Rapid Aneuploidy in Primary Human Cells

We have demonstrated the emergence of aneuploidy in SbCl2 melanoma cells. While this is significant, it raises two important mechanistic questions. First, B-Raf$^{V600E}$ positive SbCl2 cells were selected for over a minimum of 2 weeks time. This could be sufficient time for the cells to generate changes which could indirectly be driving aneuploidy. Secondly, SbCl2 cells are already transformed prior to the introduction of oncogenic B-Raf, and could therefore possess alterations that allow for the generation and survival of aneuploid cells. Therefore it is important to test whether B-Raf$^{V600E}$ can induce aneuploidy rapidly in cells of a primary nature.

### *B-Raf$^{V600E}$ Rapidly Induces Aneuploidy in Primary Human Melanocytes*

In order to determine if B-Raf$^{V600E}$ is capable of inducing aneuploidy in non-transformed cells, we evaluated the potential for oncogenic B-Raf to initiate aneuploidy in primary human melanocytes (HEM cells). Melanocytes are the cell of origin in melanoma development. This is a particularly relevant model considering that B-Raf is mutated into its oncogenic form in nearly 70% of melanomas and is mutated 80% of benign nevi of melanocytic origin.

To examine whether B-Raf$^{V600E}$ expression can cause aneuploidy in HEM cells, I transiently transfected the cells with the p-Babe-B-Raf$^{V600E}$ vector, or the corresponding empty vector control, using a high-efficiency, high-viability electroporation transfection method. Transfection efficiency was monitored by visualizing GFP fluorescence of a co-transfected GFP-containing plasmid and was found to be approximately 90%. Cells were permitted to divide for 96 hours after transfection, the equivalent two cell division cycles,

and then subjected to FISH analysis using centromeric probes against chromosomes 3 and 10. A low background of 4.5 and 5.5% aneuploidy was observed in non-transfected or empty vector (control) transfected cell, respectively (Fig. 37). Strikingly, 44% of nuclei from primary human melanocytes exhibited aneuploidy in either chromosome 3 or 10 following exogenous expression of B-Raf$^{V600E}$ (Fig. 37). Therefore, we conclude that oncogenic B-Raf$^{V600E}$ is sufficient to rapidly induce aneuploidy in primary human melanocytes.

### *B-Raf$^{V600E}$ Rapidly Induces Aneuploidy in hTERT Immortalized Mammary Epithelial Cells*

While B-Raf is mutated in the vast majority of melanomas, it is as well mutated and expressed in its oncogenic form in several other tumor types including colorectal and liver cancers, sarcomas and gliomas. In order to confirm that the induction of aneuploidy by B-Raf$^{V600E}$ was not specific to HEM cells, I tested the effects of B-Raf$^{V600E}$ expression in human mammary epithelial cells immortalized with human telomerase (hTERT HME1s). hTERT HME1 cells were transfected and evaluated as described above for HEM cells. As scored via FISH analysis, 7.0 and 6.5% of non-transfected or empty vector (control) transfected cells (Fig. 38) are aneuploidy in chromosomes 3 or 10. However, hTERT HME1 cells transfected with B-Raf$^{V600E}$ exhibited aneuploidy in 39.5% of the nuclei, results nearly identical to the results in HEM cells (Fig. 39). Therefore, we conclude that oncogenic B-Raf$^{V600E}$ is sufficient to rapidly induce aneuploidy in multiple, non-transformed human cell lines.

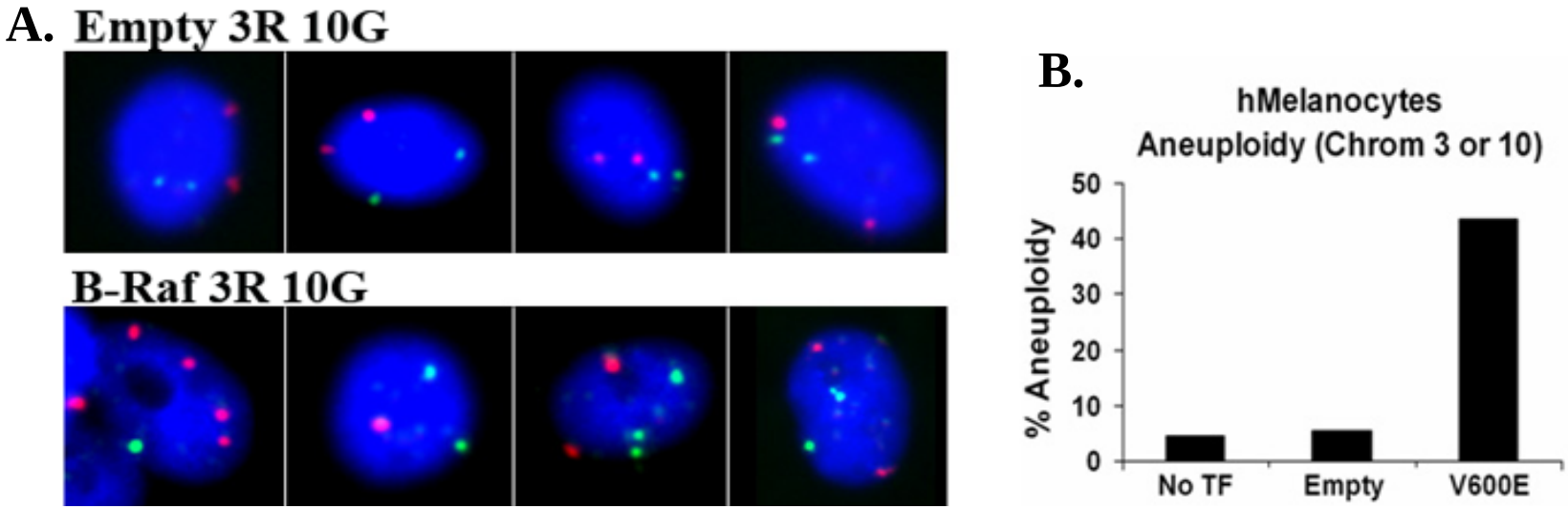


**Figure 37 Aneuploidy induced by B-Raf$^{V600E}$ in primary human melanocytes**
B-Raf$^{V600E}$ or empty vector plasmids were transfected into early passage hTERT-HME1s 96 hours post-transfection, interphase FISH analysis was performed using probes to chromosomes 3 (red) and 10 (green), (A) representative pictures are shown. (B) Percent aneuploidy detected in non-transfected (no TF), vector alone (Empty), and B-Raf$^{V600E}$. Percent aneuploidy by FISH analysis was calculated from 200 nuclei.

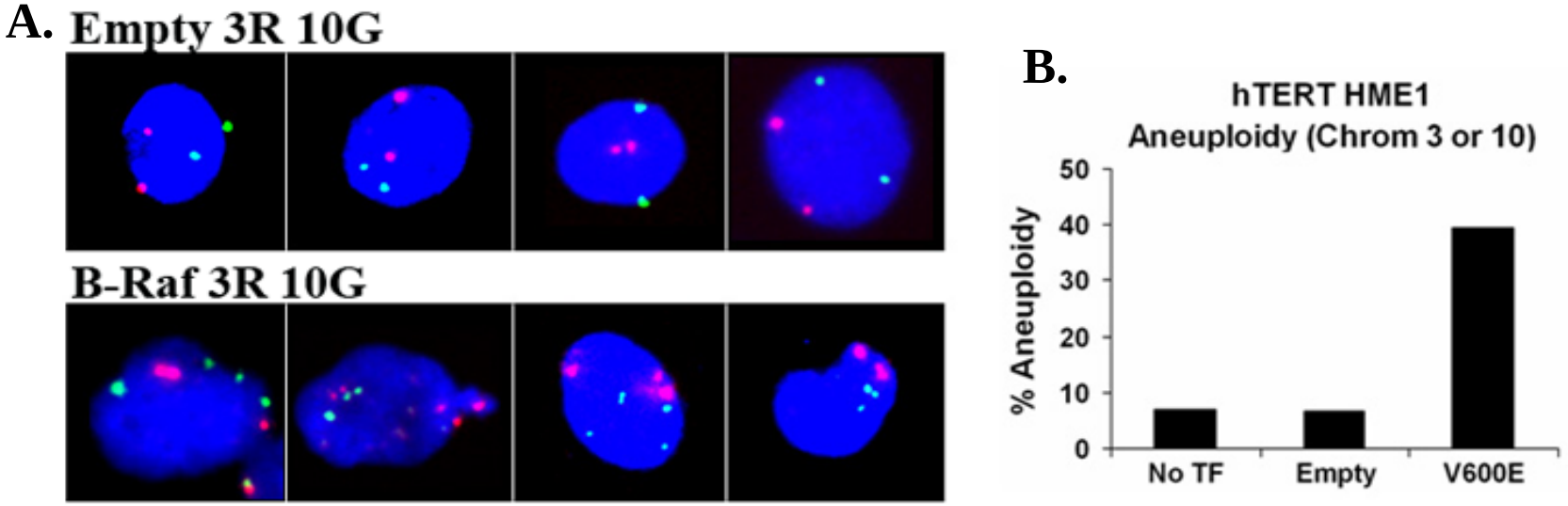


**Figure 38 Aneuploidy induced by B-Raf$^{V600E}$ in immortalized primary human epithelial cells**
B-Raf$^{V600E}$ or empty vector plasmids were transfected into early passage hTERT-HME1s 96 hours post-transfection, interphase FISH analysis was performed using probes to chromosomes 3 (red) and 10 (green), (A) representative pictures are shown. (B) Percent aneuploidy detected in non-transfected (no TF), vector alone (Empty), and B-Raf$^{V600E}$. Percent aneuploidy by FISH analysis was calculated from 200 nuclei.

## Conclusions

B-Raf is mutated into a constitutively active oncogenic form in an extraordinarily high percentage of melanomas and other cancers. Therefore, understanding the mechanisms by which B-Raf elicits its oncogenic effects is of great significance. Prior to my work the transforming activities of oncogenic B-Raf have been exclusively limited to interphase related roles including cell cycle entry, adhesion controls and resistance to anoikis. The results from this chapter demonstrate for the first time that expression of oncogenic B-Raf, V600E, causes mitotic abnormalities when expressed in melanoma cells. B-Raf$^{V600E}$ subsequently causes melanoma cells to become aneuploid, and destabilizes their genome. As well, expression of B-Raf$^{V600E}$ generates rapid aneuploidy in primary human melanocytes and primary immortalized mammary epithelial cells. From this data, we conclude that oncogenic B-Raf, V600E, drives mitotic abnormalities, aneuploidy and chromosomal instability.

# CHAPTER 5

# DISCUSSION

The key discoveries of this dissertation are the novel findings that B-Raf regulates critical functions in mammalian cell mitosis, and that oncogenic B-Raf perturbs mitosis and directly causes aneuploidy. Together, the results of my thesis research expand our understanding of mitotic regulation and highlight the significance of B-Raf overactivation in tumorigenesis.

## B-Raf Performs Critical Functions during Mitosis

In the studies described herein, a combination of immunocytochemistry and RNA interference was used to assess potential functions for B-Raf at mitosis in human somatic cells. Immunofluorescence studies demonstrate that B-Raf localizes to key mitotic structures. Consistently, functional studies demonstrate that B-Raf expression is critical for allowing proper spindle formation, chromosome congression, microtubule-kinetochore engagement and spindle checkpoint function. These are the first studies that link B-Raf to mitotic functions in human somatic cells.

### MAPK Mitotic Functions

It has long been known that MAPK signaling regulates several functions in mammalian cell mitosis including mitotic entry [111, 117, 118] and exit [130, 131],

spindle assembly [115] and Golgi apparatus fragmentation [135, 136, 307]. Studies in *Xenopus* egg extracts have suggested that MAPK regulates the spindle assembly checkpoint [73, 129]. However, beyond mitotic entry, a role for the MAPK cascade in mammalian cell mitosis had not been firmly established. Work from our lab demonstrated that B-Raf is the MEK kinase that activates the MAPK cascade during mitosis in *Xenopus* egg extracts [180], however, prior to my studies it was not known whether B-Raf had functional roles in mitosis.

**B-Raf Localizes to the Cytoplasm during Interphase in Human Somatic Cells**

It has long been thought that B-Raf is a cytoplasmic protein that gets transiently recruited to the plasma membrane for Ras mediated activation upon stimulation by mitogens. Using epifluorescence, we confirm that during interphase B-Raf exhibits cytoplasmic localization, and nuclear exclusion, (Fig. 7). While cytoplasmic B-Raf staining appears to be diffuse, upon close inspection, it appears that B-Raf is most highly concentrated in the perinuclear area. Further, I have found that B-Raf distinctly colocalizes with the early endosome during interphase (data not shown). While we did not investigate the significance of these localization patterns, they are consistent with a study demonstrating that endosome associated Rap1 activates prolonged MAPK signaling through B-Raf in response to neural growth factor (NGF) [308]. It is tempting to speculate that within endosomes B-Raf undergoes Rap1 mediated activation. Further analyses would be required in order to make any substantial claims regarding B-Raf's perinuclear and endosomal localization.

**B-Raf Localizes to Mitotic Structures in Human Somatic Cells**

Prior to the study presented here, B-Raf was thought to reside exclusively in the cytoplasm. Using epifluorescence and confocal microscopy, I show that a portion of B-Raf becomes associated with distinct mitotic structures in human foreskin fibroblast (HFF) cells (Fig. 7, 8). During prophase, B-Raf undergoes a dramatic relocation to the nuclear region, a portion of B-Raf is detected at the spindle apparatus and B-Raf is tightly associated with the centrosomes (Figs. 7, 8, 14). B-Raf's presence at the spindle is most prominent during metaphase at which time it can be detected at the spindle poles, spindle microtubules, and kinetochores. This mitotic staining pattern of B-Raf is not cell line specific as we detected similar staining at the mitotic spindle in several other cell lines including mouse NIH 3T3 fibroblasts (Fig. 6, 13). We propose that a portion of B-Raf is directly associated with the microtubules during interphase, as seen by the reticular perinuclear staining pattern (Fig. 7), and during mitosis as suggested by several experiments in human cells and *Xenopus* egg extracts (Fig. 9, 10, 11). This would account for B-Raf's re-localization to the prophase nuclear region, where the microtubule organizing centers reside, and its enrichment at the metaphase spindle. B-Raf is enriched at the spindle and spindle midzone during metaphase and anaphase, respectively. Colocalization of B-Raf to these key mitotic structures suggests that it has a role in spindle formation and spindle dynamics during mitosis. This data indicates that a portion of B-Raf is temporally and spatially regulated at the spindle apparatus throughout the phases of mitosis.

Phosphorylation of Thr599 and Ser602 is critical for Ras-mediated B-Raf activation [160]. During interphase phospho-B-Raf (Thr599 Ser602) is largely undetectable with the exception of weak centrosomal staining. At the onset of mitosis, however, phospho-B-Raf (Thr599/Ser602) is prominently localized to the nuclear region of condensing chromosomes (Fig. 15), which overlaps with the temporary localization of active Cyclin B-Cdk1 [309]. Thus, this localization pattern is consistent with the idea that mitotic B-Raf is activated in a Cyclin B –Cdk1 dependent manner [181]. Phospho-B-Raf (Thr599 Ser602) is readily detectable at the centrosomes throughout mitosis. This corresponds to the localization of active forms of MEK and ERK [112, 114]. As well, phospho-B-Raf (Thr599 Ser602) is detectable in the region of condensing chromatin throughout mitosis and is distinctly localized to the perichromosomal space (Fig. 16, 17). B-Raf is also phosphorylated at the midbody during telophase/cytokinesis, likewise, active MEK and ERK localize to the midbody during telophase [112, 114]. Activated forms of MEK and ERK have also been shown to localize to mitotic kinetochores. Upon inspection of the isolated chromosomes, it is shown that phospho-B-Raf colocalizes precisely at the kinetochores of metaphase cells, whereas kinetochore localization is absent during interphase (Fig. 18). These results indicate that pools of B-Raf are active at the spindle apparatus during mitosis. These pools colocalize with active forms of MEK and ERK, indicating that B-Raf activates MAPK signaling at discrete mitotic sites. Further research is necessary to determine whether different mitotic B-Raf is activated in one location and transported to various destinations or if the pools are independently activated.

The kinase that phosphorylates B-Raf at the Thr599 Ser602 residues is unknown. It would be interesting to determine whether phosphorylation of B-Raf is executed by the same kinase throughout interphase and mitosis. Interestingly, work performed in the cell-free system of *Xenopus* egg extracts showed that Cyclin B-Cdk1 directly associates with and phosphorylates *Xenopus* B-Raf at a Ser144 [181], a site conserved in human B-Raf. This phosphorylation event is necessary, but not sufficient for its activation at mitosis. Development of phospho-Ser144 specific antibodies will help to elucidate whether this phosphorylation occurs in somatic cells and whether B-Raf phosphorylated at Ser144 associates with mitotic structures.

Our results showing that pools of active B-Raf on mitotic structures are in agreement with a previous study detecting a small peak of B-Raf activity at mitosis of synchronized HeLa cells [134]. Taken together, these data suggest that B-Raf may function during mitosis in human somatic cells. Specifically, these data imply that during mitosis B-Raf may be involved in regulating spindle assembly and spindle, chromosome condensation, microtubule-kinetochore attachment, the spindle assembly checkpoint, anaphase and cytokinesis. Although it was not addressed in my thesis studies, I observed a pronounced distribution of B-Raf in the region around the mitotic spindle, which may overlap with the localization of the fragmented Golgi and endoplasmic reticulum during mitosis. Therefore, it is possible that B-Raf as well activates ERK signaling necessary for mitotic fragmentation of Golgi network.

**B-Raf Regulates Mitotic Functions in Human Somatic Cells**

B-Raf's mitotic localization is strongly suggestive of a functional role during mitosis. In my thesis studies, I tested whether B-Raf functions at mitosis in human cells by using siRNA to selectively deplete B-Raf from cells. Knockdown of B-Raf, but not Raf-1, had pleiotropic effects on spindle formation and chromatin congression in human somatic cells (Fig. 22, 23).

A minimum of 80% of the mitotic figures examined from B-Raf-depleted cells display various spindle abnormalities including unfocused spindle poles and alterations in spindle morphology (Fig. 22). Corroborating these results is immunofluorescence detection of B-Raf at various structures of the spindle apparatus during mitosis. A portion of B-Raf appears to interact directly with the spindle microtubules and a pool of B-Raf is detectable specifically at the centrioles after pre-extraction with CHAPS detergent (Fig. 14). However, reduction of B-Raf did not appear to have an effect on centrosome duplication or separation (unpublished observations). Instead, a high frequency (40-50%) of aberrant spindles with unfocused poles was observed. Similarly, *Xenopus* egg extracts treated with the MEK inhibitor, U0126 exhibited several phenotypically abnormal spindle structures including monastral structures lacking condensed chromatin [115]. Together, these findings support a possible role for the B-Raf/MEK/ERK pathway in mediating spindle pole focusing. This might occur through regulation *via* ERK-mediated phosphorylation of one of the various regulators implicated in spindle pole functions including dynein, NuMA, Aurora A, and Xklp2. Alternatively, B-Raf signaling may target structural components of the centrosome that are necessary for the maturation or focusing of spindle poles.

Chromosome alignment at the metaphase plate was dramatically altered in the majority of B-Raf-depleted cells (Fig. 22). As well, NIH3T3 cells treated with the U0126 inhibitor exhibited abnormal spindles including those with unattached chromosomes [115]. Chromosome alignment is dependent upon microtubule capture and the subsequent countering forces that pull chromosomes poleward. Thus, the observation that chromosomes are misaligned in the absence of B-Raf could be due to direct defects in microtubule-kinetochore engagement. Alternatively or additionally, chromosomal misalignment could manifest as a result from a precipitous exit from metaphase, in other words, a defective SAC that gives insufficient time for proper chromosome congression. In accordance with both of these options, phospho-B-Raf (Thr599/Ser602) is readily detectable at mitotic kinetochores (Fig. 18), the site of microtubule engagement and the SAC.

Through analysis of a marker for impaired microtubule-kinetochore engagement, my data indicates that microtubules are not engaged with kinetochores in the absence of B-Raf (Fig. 24) and this is confirmed through direct analysis of the microtubule-kinetochore attachments (Fig. 25). CENP-E is the only protein identified to date that directly facilitates microtubule-kinetochore engagement. Thus, it can be proposed that B-Raf signaling governs CENP-E's mitotic functions. Indeed, it is known that mitotic phosphorylated MAPK interacts with CENP-E and that MAPK can phosphorylate CENP-E on sites that regulate CENP-E's interaction with microtubules [114].

Another possible mechanism by which B-Raf affects chromosome congression is that B-Raf regulates the duration of metaphase, necessary for permitting proper chromosomal alignment. Indeed, results from imaging mitotic progression in live cells depleted of B-Raf support this possibility. On average, B-Raf siRNA treated cells entered anaphase 24 min earlier than control SCR-treated cells, displaying a 33% reduction in the duration of the prometaphase/metaphase period (Fig. 29).

Despite the absence of microtubule-kinetochore attachments and chromosome misalignment, B-Raf depleted cells continue to divide for at least 120 hours with no indication of widespread mitotic arrest (Fig. 26). These observations suggest that the SAC is defective in the absence of B-Raf. Bub1 and Mad2 are critical spindle checkpoint proteins, whose kinetochore localization is a strong indicator of spindle checkpoint activation [286]. As shown in figure 31, kinetochore localization of Bub1 and Mad2 is blocked upon B-Raf depletion. Furthermore, B-Raf depleted cells do not maintain an SAC when challenged with taxol (Fig. 28) and live-cell imaging showed that the depletion of B-Raf leads to a shortening of the period from prometaphase to anaphase, which is consistent with having a defective spindle checkpoint (Fig. 29). These results strongly implicate B-Raf as a regulator of the SAC.

Mps1 is an essential component of the SAC network [310, 311] and functions to localize spindle-checkpoint proteins Bub1, Mad1, and Mad2 to unattached kinetochores [70, 73, 310]. Interestingly, it was shown that the *Xenopus* homologue of Mps1 is phosphorylated by MAPK in *Xenopus* egg extracts at Serine-844, and this phosphorylation is necessary for kinetochore localization of Mps1 and other spindle

checkpoint proteins [73]. Importantly, recent data from our laboratory demonstrates that Mps1 is indeed a target of B-Raf signaling [312]. Specifically, it was shown that B-Raf associates with Mps1 *in vivo* and directs its MAPK-dependent phosphorylation and kinetochore localization during mitosis. Therefore, we speculate that B-Raf mediated phosphorylation of Mps1 is important for spindle checkpoint functions. While beyond the scope of this study, it will be important to dissect the contributions of phosphorylation events that regulate mitotic functions of Mps1. Finally, MAP kinase has been reported to phosphorylate other critical regulators of the spindle checkpoint, Bub1 [313] and Cdc20 [129], indicating that B-Raf signaling at mitosis may target multiple components of the spindle checkpoint network *via* MAPK.

We propose that B-Raf elicits its mitotic effects through MAPK signaling. This is supported by the colocalization of B-Raf, MEK and ERK to the spindle poles and kinetochores. However, we cannot preclude the possibility that B-Raf may have MAPK independent mitotic functions. This could be addressed by analyzing B-Raf's mitotic functions in cells with compromised MEK1/2, the only identified down-stream target of B-Raf which directly activates ERK 1/2.

B-Raf signals through MAPK to regulate gene transcription during interphase. Therefore, it can be proposed that B-Raf indirectly affects spindle assembly and chromosome congression rather than having a direct effect on mitosis. To address this question, we utilized *Xenopus* egg extracts where B-Raf and MAPK activities are strictly limited to mitosis. Indeed, B-Raf depletion from *Xenopus* egg extracts results in dramatic effects on spindle assembly and DNA alignment (Fig. 20), suggesting that B-Raf directly

regulates mitosis in this system. Together with the localization of B-Raf to mitotic structures cell culture, we propose that B-Raf directly regulates mitosis in mammalian cells.

Besides its kinase activity, B-Raf may also function as a scaffold protein. Based on results shown here, we cannot exclude that some or all of B-Raf's mitotic functions are executed via scaffolding capacity. To address this concern directly, one would need to compare WT and kinase dead B-Raf-driven mitotic phenotypes in cells depleted of endogenous B-Raf.

In summary, our results reveal several mitotic roles for B-Raf including proper spindle formation, chromatin congression, microtubule capture, and the spindle assembly checkpoint. It is feasible to propose that these functions are all independent or interdependent. In the most interdependent example, one could suggest that B-Raf is necessary for proper functioning of the SAC, in the absence of which, microtubule capture is mitigated, thereby inhibiting chromosome congression and perturbing the arrangement of spindle microtubules. However, since B-Raf localizes to several key mitotic structures including the kinetochores, centrosomes and microtubules, I would propose that mitotic B-Raf signaling is important for regulating several mitotic functions through independent mechanisms. For instance, B-Raf signaling may regulate the SAC through Mps1 and microtubule-kinetochore attachment through CENP-E. A thorough analysis of MAPK substrates at mitosis would potentially reveal other effectors of B-Raf signaling that regulate its mitotic functions.

Spindle assembly, chromatin congression and the SAC are all critical mitotic elements necessary for proper chromosome segregation. While I did not perform karyotype analysis on B-Raf depleted cells, it is likely that these cells become aneuploid and chromosomally unstable. The demonstration that B-Raf regulates critical mitotic functions opens a new avenue in addressing how oncogenic B-Raf contributes to tumorigenesis.

## Oncogenic B-Raf Deregulates Mitosis Causing Aneuploidy and Chromosomal Instability

Aneuploidy is a hallmark of cancer and it is associated with tumor progression and poor clinical prognosis [301, 302] and has a causal role in tumorigenesis [263, 277, 314]. As described previously, B-Raf is overactivated in the majority of human melanomas [216]. My studies presented in this section, demonstrate that the main activating B-Raf mutation deregulates mitosis and provokes aneuploidy.

### Cellular Effects of Oncogenic B-Raf

The vast majority of oncogenic B-Raf mutations cause constitutive activation of the MAPK cascade. Prior to and during my thesis studies, a variety of experiments have revealed several cellular roles through which B-Raf$^{V600E}$ may elicit its oncogenic effects including cell survival, anchorage independent cell cycle progression, and invasion. However, the question of how B-Raf contributes to tumorigenesis is not fully understood.

Soon after the 2002 discovery that B-Raf is mutated in a wide variety of tumors, it was demonstrated that oncogenic B-Raf, specifically B-Raf$^{V600E}$, is necessary for cell

survival in B-Raf$^{V600E}$ expressing cells. siRNA and shRNA-mediated downregulation of B-Raf$^{V600E}$ causes inhibition of ERK signaling and induces cell cycle arrest and apoptosis in cultured cancer cells [225, 226, 315].

Normal cells require adhesion for signaling and survival [316]. Loss of adhesion causes normal cells to undergo anoikis, whereas tumor cells develop the capacity to resist anoikis [317]. B-Raf$^{V600E}$ expression is necessary for anoikis resistance in melanoma cells [299] and this is dependent on B-Raf$^{V600E}$'s negative regulation of pro-apoptotic proteins Bad and Bim [300].

In addition to anoikis, normal cells die when they are subjected to a low-oxygen environment. In contrast, the central tumor zone is hypoxic and tumor cells must evolve mechanisms for survival under such conditions [318]. It has been shown that B-Raf$^{V600E}$ induces expression of hypoxia inducible factor-1α (HIF-1α) and its expression is essential for melanoma cell survival in a hypoxic tumor-like environment [319]. Together, these data demonstrate that B-Raf$^{V600E}$ mediates survival in melanoma cells.

In addition to cell survival, B-Raf$^{V600E}$ appears to regulate cell cycle progression in an anchorage independent manner. In normal human melanocytes, anchorage to an extracellular matrix is necessary for growth factor activation of ERK1/2, which leads to induction of cyclin D1 and downregulation of p27$^{Kip1}$, both key events in G1 to S phase progression [298, 320]. B-Raf$^{V600E}$ expression in melanoma cells causes constitutive expression of cyclin D1 and down regulation of p27$^{Kip1}$, in the absence of cellular adhesion and growth factors [297]. Growth arrest concurrent with a decrease in expression of cyclins D1 and D3 was observed following downregulation of B-Raf$^{V600E}$ in human melanoma cells [226, 298]. Brn-2, a transcription factor involved in the

proliferation of melanoma cells [321], was also downregulated following siRNA mediated reduction of B-Raf$^{V600E}$ [322].

Besides its role in progression from G1 to S phase, recent evidence suggests that B-Raf$^{V600E}$ regulates the G2 to M phase progression. Required for melanoma growth is Skp2 [297], an E3 ubiquitin ligase that targets multiple proteins for degradation, thus promoting the G2-M phase transition [323-328]. In melanoma cells B-Raf$^{V600E}$ induces expression of Skp2, suggesting that B-Raf$^{V600E}$ mediates entry into mitosis [329].

A hallmark feature of tumor cells is the acquired ability to invade nearby tissues [330]. It has been shown that B-Raf$^{V600E}$ upregulates expression of several matrix metalloproteinases (MMPs) [331, 332], which are known to mediate invasion through cleavage of extracellular matrix components [333]. Using a matrigel assay, it was shown that downregulation of B-Raf$^{V600E}$ decreases the invasive potential of PTCs. Additionally, it has been demonstrated that the actin cytoskeleton and focal adhesion in melanoma cells is disrupted by B-Raf$^{V600E}$ expression through MAPK activation of Rnd3 [334]. Such results implicate B-Raf$^{V600E}$ in the promotion of tumor invasion.

These studies demonstrate several mechanisms through which B-Raf$^{V600E}$ drives cell cycle progression and survival under tumorigenic conditions. However, B-Raf$^{V600E}$ expression and its downstream effectors are not sufficient for transformation to occur. It is widely speculated that loss of tumor suppressors, such as p16$^{INK4a}$, must accompany B-Raf$^{V600E}$ for tumorigenesis to occur. My thesis studies demonstrate that B-Raf$^{V600E}$ causes widespread genomic changes through disregulation of mitosis. Such a mechanism could provide the heterogeneity through which other necessary genomic changes could arise.

## B-Raf$^{V600E}$ Expression Drives Mitotic Abnormalities

B-Raf$^{V600E}$ can transform immortalized melanocytes and mouse fibroblasts *in vitro* [216, 223, 225] but how it exerts its oncogenic effects has been an important area of study. Our studies investigated the mitotic effects of oncogenic B-Raf$^{V600E}$ in cultured human melanoma cells. Data from these studies show for the first time that B-Raf$^{V600E}$ induces pleiotropic spindle abnormalities, chromosome misalignment and supernumerary centrosomes (Fig. 32). A high incidence of spindle abnormalities, similar to those observed from ectopic expression of the B-Raf$^{V600E}$ mutant, were also found in melanoma cells carrying endogenous B-Raf$^{V600E}$ mutations but not in wild type B-Raf melanoma cells (Fig. 31) [335]. Thus, we conclude that oncogenic B-Raf$^{V600E}$ abrogates mitosis in human melanoma cells.

The spindle abnormalities induced by B-Raf$^{V600E}$ include a high percent of multipolar spindles due to cells having 3 or more centrosomes. As well, B-Raf$^{V600E}$ causes abnormalities in spindle assembly and chromosome alignment independent of centrosomal amplification in approximately 50% of abnormal mitoses. The mechanisms that generate these abnormalities have yet to be defined. One possibility is that B-Raf$^{V600E}$ deregulates the proteins involved in microtubule capture, thereby leading to the observed abnormalities. Analyzing the mitotic localization and substrates of B-Raf$^{V600E}$ would shed light on these mechanisms. Like B-Raf$^{V600E}$, expression of oncogenic Ha-ras induces mitotic abnormalities in mouse NIH3T3 cells, including multipolar spindles and misaligned chromosomes, and it has been proposed that oncogenic Ras deregulates

spindle assembly [131]. It is exceedingly rare for Ras and B-Raf mutations to coincide in human tumors, therefore suggesting that they elicit overlapping effects.

In the absence of B-Raf the SAC is not full activated, thus causing early mitotic exit and most likely errors in the chromosome segregation. Consistent with this, recent studies from the Guadagno laboratory demonstrated that B-Raf$^{V600E}$ signaling promotes hyper-activation of the spindle checkpoint causing a delay in mitotic progression [306]. This is mediated, at least in part, through Mps1, a known target of MAPK signaling. Depleting cells of Mps1 by siRNA alleviates the checkpoint effects induced by B-Raf$^{V600E}$ [306]. It is also possible that, due to B-Raf's uncontrollable high activity, it targets unusual substrates, yet to be identified. Interestingly, published evidence indicates that both an under-activated and over-activated SAC compromises the timing and quality of chromosome segregation during anaphase leading to generation of aneuploid cells [263, 276, 277, 314]. We propose that by over-activating the SAC, oncogenic B-Raf$^{V600E}$ induces aneuploidy. In contrast to our studies, oncogenic Ras has been shown to shorten a nocodazole-induced SAC in rat thyroid cells, and it does this in a MAPK independent manner [231]. These data suggest that oncogenic Ras may regulate the SAC through different mechanisms than B-Raf$^{V600E}$.

### B-Raf$^{V600E}$ Expression Causes Chromosomal Instability

It is well understood that mitotic errors drive aneuploidy. Therefore, it was not surprising that aneuploidy resulted from the mitotic abnormalities generated by introducing the B-Raf$^{V600E}$ mutant into SbCl2 melanoma cells (data not shown) and SK-MEL5 melanoma cells (Figure 32). Many of the B-Raf$^{V600E}$-expressing cells died,

probably due to losses of vital chromosomes. However, experiments in SbCl2 cells showed that many cells continued to survive and proliferate for 4-6 weeks of extended culturing. These cells continued to exhibit abnormal chromosomes numbers that changed over time and failed to establish a stable karyotype, as evident by the absence of a chromosomal mode (Fig. 35, 36). Indeed this data is supported by previously published findings that induced B-Raf$^{V600E}$ expression in rat thyroid cells increases micronuclei formation 2-fold, indicating that chromosomes or chromosome fragments are lost during mitosis [336]. Interestingly, the vast majority of B-Raf$^{V600E}$-expressing SbCl2 cells were hypoploid, the significance of which remains to be addressed. Hypoploidy is thought to arise from loss of chromosomes to micronuclei [337], a result of mitotic abnormalities that generate lagging chromosomes. Oncogenic Ras expression causes lagging chromosomes and micronuclei formation in NIH3T3 cells harboring mutant p53 [338] and in rat thyroid cells [339], in a MAPK dependent manner. This suggests that B-Raf$^{V600E}$ and oncogenic Ras generate mitotic abnormalities that lead to aneuploidy. However, a role for Ras in mitosis has not been confirmed in human cells.

The mechanisms by which B-Raf$^{V600E}$ drives chromosomal instability have yet to be elucidated. One possibility involves Mps1, a spindle checkpoint kinase identified as a potential target downstream of the B-Raf/MEK/ERK signaling pathway [73, 306, 312]. Mps1 levels are elevated by constitutive B-Raf$^{V600E}$ signaling in melanoma cells, which allows for hyper-activation of the spindle checkpoint [306]. A hyper-activated spindle checkpoint could, in turn, contribute to chromosome segregation errors that lead to aneuploidy. Consistent with this proposal, elevated levels of Mad2 expression are

observed in various tumors defective in the Rb pathway [340] and are sufficient to induce chromosome instability, aneuploidy, and tumorigenesis in mice [277].

It was shown that immortalization itself can indirectly cause aneuploidy [270]. It was therefore proposed that aneuploidy-causing agents must induce aneuploidy in pre-immortalized cells in order to fully meet the criteria as an aneuploidogen [232]. My results have shown that B-Raf$^{V600E}$ induced aneuploidy in hTERT-immortalized epithelial cells (Fig. 38), thereby confirming B-Raf$^{V600E}$ as a direct mediator of CIN. The results described here further show that oncogenic B-Raf$^{V600E}$ is sufficient to rapidly induce aneuploidy in primary human melanocytes (Fig. 37). Together, these results indicate that B-Raf$^{V600E}$-induced CIN could be a mechanism for induction of aneuploidy in both melanomas and other human cancers carry activating B-Raf mutations.

A large proportion (~82%) of benign nevi harbor activating B-Raf mutations [220] lending to the idea that B-Raf activation is an early and critical step in the development of melanocytic neoplasia. While genetic evidence supports an early role for B-Raf$^{V600E}$ in nevi formation [227], sustained B-Raf$^{V600E}$ activity is also associated with oncogene-induced senescence [341, 342], explaining why most nevi never develop into invasive melanomas and remain dormant over long periods of time. We speculate that induction of aneuploidy in proliferating melanocytes creates additional genetic changes, which, if tolerated, contribute to melanoma initiation. This would be in line with several reports showing that additional mutations in melanoma susceptibility genes (i.e. p16$^{INK4a}$, ARF, PTEN) are needed to cooperate with oncogenic B-Raf (or Ras) to allow for melanoma initiation [341].

Several studies would further help confirm a role for B-Raf$^{V600E}$ induced aneuploidy in tumorigenesis. First, karyotypic evaluation of benign nevi harboring the B-Raf$^{V600E}$ mutation would reveal whether the oncogene induces aneuploidy early in tumorigenesis. Since my studies in primary melanocytes and immortalized primary epithelial cells demonstrated that B-Raf$^{V600E}$ induces rampant aneuploidy after only 2 cell divisions, I would predict that some benign nevi are aneuploid. However, this study would have to be conservatively analyzed, since only a minority of benign nevi ever proceed to melanomas. It is perhaps feasible that B-Raf$^{V600E}$ induces senescence in the majority of nevi, prior to the selection of a large number of aneuploid cells.

It would also be of interest to determine whether the initial aneuploidy induced by B-Raf$^{V600E}$, in human primary melanocytes or immortalized epithelial cells, is sufficient for transformation. These experiments could be conducted utilizing an inducible B-Raf$^{V600E}$ vector, such as an estrogen receptor B-Raf$^{V600E}$-fusion. Once B-Raf$^{V600E}$ induces aneuploidy in cells, expression of B-Raf$^{V600E}$ could be turned off and surviving cells would be selected and grown in soft agar. It would be predicted that the majority of cells would depend to B-Raf$^{V600E}$ expression for survival. However, a minority of cells could acquire the proper combination of aneuploidy to become capable of survival and colony formation. Mathematical modeling, such as is available through Moffitt Cancer Center's Integrated Mathematical Oncology group, would be a useful tool in determining how well these experiments reflect a clinical model for melanoma progression.

Aneuploidy induced by mitotic errors leads to CIN in nearly all cases reported [232]. The effects of CIN cannot be understated as it gives rise to a continuously

changing gene expression pattern. Frequent changes in the genomic profile of cells within a population allow for rapid Darwinian adaptation to the intra- and extracellular environment. Thus, selection of the appropriate combinations of CIN can not only drive tumorigenesis, but may provide a mechanism for generating cells capable of invasion, metastasis and drug resistance.

## Relevance for Therapeutics

The most common treatment modality for melanomas is tumor resection alone or in combination with immunotherapy, chemotherapy or radiation for advanced stage disease. Therapies targeted against B-Raf or B-Raf$^{V600E}$, its oncogenic form, have recently been tested in clinical trials, however, most have not shown strong efficacy as single agents [343]. Rational efforts have turned toward combination therapies, targeting multiple signal transduction pathways or combining B-Raf inhibitors with chemotherapeutic agents. In fact, unpublished data from our lab (not reviewed in this thesis) demonstrates that sequential use of placitaxol and a B-Raf$^{V600E}$ inhibitor synergize to induce caspase-dependent cell death. Another rational therapeutic strategy employs the use of geldanamycin derivatives, since it has been shown that B-Raf$^{V600E}$ stability is Hsp90 dependent, while WT B-Raf stability is independent of Hsp90 [344]. As with other efforts, this appears to be most beneficial in combination with other agents [345].

It is interesting to speculate on how our findings might contribute to the development of cancer therapeutics for use against B-Raf$^{V600E}$ positive tumors. Classic chemotherapeutic agents and some modern rationally developed drugs target mitosis as an effective means of killing cancer cells. In elegant and elaborate live-imaging studies,

it was recently shown that these agents induce mitotic cell death via caspase-dependent mechanisms, which are dependent upon a prolonged, cyclin B-induced mitotic arrest [346]. Therefore, I would propose that development of agents that stabilize cyclin B combined with a caspase activator would synergize with existing drugs in many tumor types, including B-Raf$^{V600E}$-positive tumors. My work and the work of others from the Guadagno lab [306, 312] have demonstrated that B-Raf regulates the SAC and that B-Raf$^{V600E}$ generates an extended SAC. While we have not directly demonstrated that B-Raf$^{V600E}$ stabilizes cyclin B, such stability could enhance the efficacy of chemotherapeutic agents, thus arguing against the use of B-Raf$^{V600E}$ inhibitors.

Aneuploidy is another interesting feature of tumor cells that may be useful to consider in the treatment of cancers. Aneuploidy exists in nearly all solid tumors and is directly driven in primary cells through B-Raf$^{V600E}$, an early mutation in many tumors. It is reasonable to speculate that aneuploidy-driven intratumoral heterogeneity would frequently lead to drug resistance even with the most appropriately targeted therapies. It has recently been proposed that aneuploidy not only drives tumorigenesis, but can be protective [263] when aneuploidy drives specific combinations of gene expression. While 96 hours of B-Raf$^{V600E}$ expression generates viable aneuploid cells, the majority of cells are not viable after prolonged expression of B-Raf$^{V600E}$, thus supporting the idea that some or most aneuploidy is not tolerated long-term. Therefore, it may be feasible to utilize known aneuploidogens to induce a wide-spread intolerable aneuploidy load in an effort to kill tumor cells.

## Summary

Mitosis is a complex and critical stage of the cell cycle. While mitosis has been studied for well over a century, the players and the consequences are still being elucidated and debated. Likewise, the cancer biology field has generated volumes of data; however, we still have much to learn about tumorigenesis. B-Raf has been identified as an oncogene in a strikingly high number of tumors and it has therefore become fundamental to understand how it contributes to cancer. Through the work in this thesis, I have demonstrated that B-Raf is necessary for regulating mitosis, the cell cycle stage that maintains the cell's genomic integrity. Genomic changes provide cells with the capacity to acquire new features and new functions. It is quite feasible that advantageous changes are selected to promote tumor initiation, progression, metastasis and drug resistance. Therefore, our findings that oncogenic B-Raf disregulates mitosis and drives genomic instability open a new path for understanding how B-Raf contributes to tumorigenesis (Fig. 39).

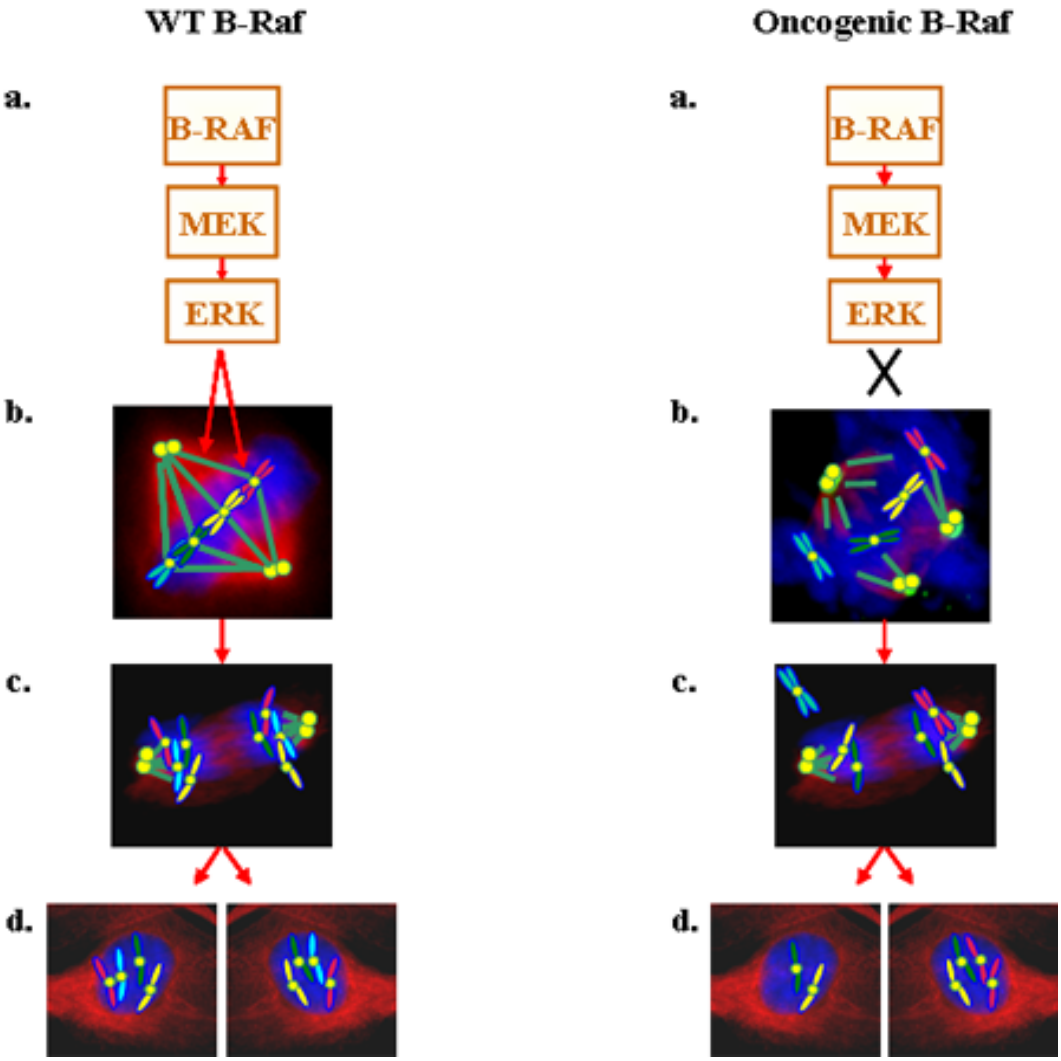


**Figure. 39 Model for B-Raf mediated mitosis**
B-Raf regulates critical mitotic functions which lead to proper chromosomal segregation thus maintaining the diploid nature of the daughter cells. Contitutively active B-Raf$^{V600E}$ disregulates mitosis thereby causing missegregation of chromosomes and producing aneuploid daughter cells. a. B-Raf regulates the MAPK pathway; B-Raf$^{V600E}$ overactives the MAPK pathway; b. B-Raf signaling regulates spindle assembly and kinetochore functions including microtubule-kinetochore engagement and the spindle assembly checkpoint; B-Raf$^{V600E}$ disregulates these functions; c. Proper mitosis leads to proper anaphase onset and accurate chromosome segregation; disregulated mitosis causes premature anaphase onset and lost and missegregated chromosomes; d. Proper chromosomes segregation generates diploid daughter cells whereas missesgregation caused by B-Raf$^{V600E}$ renders the daughter cells aneuploid.

# CHAPTER 6

# MATERIALS AND METHODS

## Cell Culture and Cell Synchronization

Human foreskin fibroblasts (HFF), HeLa and NIH3T3 cells were cultured in DMEM (Gibco) containing 10% newborn calf serum (Gibco) and 46μg/ml gentamycin. Cells were synchronized at G2/M with 50nM taxol in 0.1% DMSO for 30 hours and treated with 30μM U0126 or 0.1% DMSO for 6 hours prior to cell collection. SK-MEL5, SK-MEL28, and A375 human melanoma cell lines were obtained from American Type Culture Collection (ATCC, Manassas, VA) and maintained in Dulbecco's modified Eagle's medium supplemented with 10% fetal bovine serum (FBS). SK-MEL5 cells are wild type for B-Raf, while SK-MEL28 and A375 cells carry B-Raf$^{V600E}$ mutations [216, 292]. Sbcl2 and WM35 melanoma cells, originally derived from early radial growth phase primary melanomas, were obtained previously from M. Herlyn (Wistar Institute, Philadelphia, PA). Sbcl2 and WM35 cells are wild type for B-Raf and were grown in 2% tumor media (4:1 mix of MCDB153/L15 media, 2% FBS, 5 μg/ml insulin, 1 mM $CaCl_2$). To further confirm the absence of an activating mutation in B-Raf, phospho-ERK levels were assessed for SK-MEL5, Sbcl2, and WM35 melanoma cells switched to 0.5% FBS for 24 hr. All three melanoma cell lines exhibited minimal ERK activity whereas SK-MEL28 and A375 (both containing B-Raf$^{V600E}$ mutations) cells showed robust levels of

phospho-ERK (data not shown). Human Mammary Epithelial cells immortalized with human telomerase (hTertHME1 cells), were gifted to us by Huntington Potter at the Johnnie B. Byrd Alzheimer's Center and Research Institute at the University of South Florida (Tampa, FL). Cells were cultured in MEGM media from Lonza. Primary Human Epidermal Melanocytes (HEM) were purchased from ScienCell Research Laboratories and cultured in Melanocyte Medium from ScienCell. Primary cells were transfected using the Nucleofector system from Amaxa, now part of Lonza, using kits V and NHEM for hTertHME1 and HEM, respectively. Cells were co-transfected with GFP for assessment of transfection efficiency.

**Transfections and Retroviral infections**

Cells were grown to approximately 70% density in 12-well plates and transfected with 21-mer double stranded oligo short interfering RNAs (siRNAs) to human B-Raf specific sequences at exon 11 (BE11) [AAAGAATTGGATCTGGATCAT] or exon 3 (BE3) [AAGCTAGATGCACTCCAACAA] or, to C-Raf specific sequence [AATAGTTCAGCAGTTTGGCTA] obtained from Qiagen. A scrambled siRNA for B-Raf or C-Raf sequences was used in parallel as a control. siRNAs were used at 110 nM. 488λ-conjugated scrambled oligo was used to verify transfection efficiency. By 48-72 hours, protein levels for B-Raf or C-Raf decreased 85-95% as confirmed by Western blotting.

pBabe-puro and pBabe-puro-B-Raf$^{V600E}$ retroviral vectors were a generous gift from Dr. Daniel Peeper (The Netherlands Cancer Institute). Retroviral vectors were transfected into HEK 293T replication-defective packaging cells for retrovirus

production. Melanoma cells were infected with pBabe-puro or pBabe-B-Raf$^{V600E}$ retroviruses as described and selected in puromycin (0.8 μg/ml) for up to 10 days. Puromycin-resistant colonies were pooled and checked for ectopic B-Raf$^{V600E}$ expression by immunoblot analysis.

Human melanocytes or hTERT-HME cells were transfected using the Nucleofector system from Amaxa. Transfection efficiencies were monitored by evaluating green fluorescent cells following co-transfection with pMaxGFP vector from Amaxa.

**Immunoblot Analysis**

Cells grown in 12-well or 6-well dishes were washed with PBS and scrape-lysed in ice-cold TNES buffer containing protease and phosphatase inhibitors (50mM Tris·Cl pH 7.4, 1% NP40, 2mM EDTA, 100mM NaCl, 20μg/ml aprotenin, 20μg/ml leupeptin, 500μM PMSF, 40mM β-glycerophosphate, 500μM $Na_3VO_4$, 20mM NaF), incubated on ice for 30 minutes and centrifuged for 30 minutes at 14Xg at 4º. Supernatants were analyzed for protein concentrations were determined by a BCA protein assay (Pierce) and analyzed by a spectrophotometer (BioRad). Cell lysates were separated by SDS-PAGE, and electrotransferred onto PVDF, 0.45μm membranes. Membranes were blocked in 5% milk/0.15% Tween 20 for 1h at room temperature, incubated with primary antibodies against B-Raf and α-tubulin (detailed above), total ERK, C-Raf (BD Transduction labs), CAS (BD Transduction Labs), Cyclin B (Santa Cruz) and Beta-actin (Abcam) diluted in 5% milk/0.15% Tween 20 for 1h at room temperature and washed 3X in 0.15% Tween 20/PBS. Membranes were incubated for 1h at room temperature with goat anti-mouse

(Jackson ImmunoResearch Laboratories) or goat anti-rabbit (Sigma) alkaline phosphatase-conjugated secondary antibodies diluted in 5% milk/0.15% Tween 20, washed 4X in 0.15% Tween 20/PBS, incubated for 5 minutes in alkaline phosphatase buffer pH 9.5, 5 minutes in CDP-Star chemiluminescence substrate (Roche Diagnostic) and exposed to blue sensitive autoradiography X-Ray film (Molecular Technologies). Band densitometry data was performed using Image Quant analysis.

## Microtubule Depolymerization by Cold Treatment

For cold-induced microtubule depolymerization, cells transfected with B-Raf or control (scrambled) siRNA were grown on coverslips in 35 mm dishes. Media was removed, replaced with ice-cold media, and dishes were subsequently incubated on ice for 10 minutes to induce depolymerization of unattached kinetochore-microtubules. Cells were then fixed in 4% paraformaldehyde and processed for immunocytochemistry as described above.

## Nocodazole-Induced Microtubule Depolymerization

HFF and HeLa cells were grown overnight on coverslips. Nocodazole was added at 125ng/mL (HFF) or 25ng/mL (HeLa) for 2 hours at 37º to depolymerize microtubules. Immunofluorescence was performed as described above.

CSF extracts were generated from unfertilized *Xenopus* oocytes as described below and activated into S-phase using 0.4mM $CaCl_2$ and cycled into a stable mitotic state with addition of equal volume of CSF extract. Reactions were incubated in the

presence of 200/µl sperm DNA for 75 minutes at 24ºC to allow for spindle formation alone, with DMSO or with 10ng/µl nocodazole. Microtubules were fixed and spun down as previously described [115]. The pellet was resuspended in SDS sample buffer, separated by 10% SDSPAGE, and immunoblotted for α-tubulin and B-Raf.

## Immunocytochemistry

Cells grown on glass coverslips were fixed at 4º in 4% paraformaldehyde, permeabilized with 0.5% triton-X-100 and blocked in 2% BSA. Alternatively, cytoplasmic proteins were solubilized using 1% CHAPS in PHEM buffer containing protease and phosphatase inhibitors (60mM Pipes, 25mM Hepes pH 6.9, 10mM EGTA, 4mM $MgSO_4$, 1µg/ml aprotenin, 1µg/ml leupeptin, 1µM pepstatin, 50mM β-glycerophosphate, 200µM $Na_3VO_4$) for 60 seconds at room temperature, fixed at 4º in 4% paraformaldehyde and blocked in 2% BSA. Cells were incubated in 2% BSA for one hour with primary antibodies against B-Raf (Santa Cruz or Upstate), α-tubulin (Sigma) or Centrin (kindly provided by Jeffrey Salisbury at Mayo Clinic), washed 3X in PBS, incubated in 2% BSA for one hour with 488 or 594 Alexa Fluor secondary antibodies (Molecular Probes) and washed 3X in PBS. Cells were mounted with Prolong Gold containing DAPI (Molecular Probes).

To visualize B-Raf at the centrioles, cytoplasmic proteins were pre-extracted using 1% CHAPS in PHEM buffer containing protease and phosphatase inhibitors (60 mM Pipes, 25 mM Hepes pH 6.9, 10 mM EGTA, 4 mM $MgSO_4$, 1 µg/ml aprotenin, 1 µg/ml leupeptin, 1 µM pepstatin, 50 mM β-glycerophosphate, 200 µM $Na_3VO_4$) for 60 seconds at room temperature, fixed at 4º C in 4% paraformaldehyde and blocked in 2%

BSA. Pre-extracted cells were then incubated with a C-terminal peptide B-Raf polyclonal antibody (sc-166) obtained from Santa Cruz Biotechnology (Santa Cruz) and co-stained with a mouse monoclonal centrin antibody kindly provided by Jeffrey Salisbury (Mayo Clinic, Rochester) to visualize centrioles.

## Chromosome Isolations

Cells were treated with 1μg/mL colcemid for 2 hours, harvested by trypsinization and washed with PBS. Cells were swollen in 75mM KCL for 10 minutes at 37º and subsequently spun onto polylysine coated coverslips at 1800rpm for 8 minutes. Cells were immersed in KCM buffer containing 120mM KCl, 20mM NaCl, 10mM Tris-HCl ph7.5, 0.5mM EDTA and 0.1% Triton-X for 10 minutes at room temperature. Immunostaining was carried out at room temperature. Cells were exposed to primary antibodies against phospho-B-Raf (Santa Cruz) and CREST (Antibodies Incorporated) diluted in 2% BSA in KCM for one hour, washed twice with KCM followed by 488 or 594 Alexa Fluor secondary antibodies (Molecular Probes) and washed 2X with at room temperature. Immunostaining was performed as described above except BSA and antibodies were diluted KCM buffer and cells were washed in KCM buffer followed by one final wash with PBS prior to mounting coverslips as described above.

## Fluorescence *in situ* Hybridization (FISH) Analysis and Metaphase Spreads

Cells were treated with 1μg/mL colchicine for 2 hours, harvested by trypsinization and washed with PBS. Cells were swollen in 65mM KCL for 5 minutes at 37º, fixed in cold acetic acid/methanol for 5 minutes at 4º, dropped onto slides and dried

at room temperature. For metaphase spreads, cells were then stained with DAPI and viewed with a Nikon E800 fluorescence microscope with a 60x/1.40NA plan apo oil immersion objective. Images were captured with a Roper Coolsnap HQ CCD camera and processed with Metamorph 5.0 and Adobe Photoshop 6.0 software. FISH analysis on hTertHME1 and HEM cells were carried out 96 hours post-transfection. For FISH analysis, slides were stained with Cytocell enumeration probes against chromosomes 2 or 3, and 8 or 10, conjugated with FITC or Cy3.5, respectively (Rainbow Scientific). Staining was carried out according to the manufacturer's protocol. FISH samples were viewed with a fully automated, upright Zeiss Axio- ImagerZ.1 microscope with a 20X objective, and DAPI, FITC and Rhodamine filter cubes. Images were produced using the AxioCam MRm CCD camera and Axiovision version 4.5 software suite. P-values were calculated using a 2-sample test for equality of proportions with continuity correction.

**Microscopy**

Fluorescent images of mitotic figures were viewed with a Nikon E800 fluorescence microscope with a 60X/1.40NA plan Apo or 100X/1.3NA plan Fluor oil immersion objective. Images were captured with a Roper Coolsnap HQ CCD camera controlled with Metamorph software 5.0, saved as Tif. files, and transferred into Adobe Photoshop 8.0 software for final processing. Phospho-B-Raf images were viewed on a fully automated, upright Zeiss Axio-Imager Z.1 microscope with a 63X/1.40NA oil immersion objective and images were produced using the AxioCam MRm CCD camera and Axiovision version 4.5 software suite. Confocal images were captured through a 63X/1.40NA oil immersion objective using a DMI6000 inverted Leica TCS SP5 tandem

scanning microscope. Images and Z-stacks were produced with three cooled photomultiplier detectors and the LAS AF version 1.5.1.889 software suite. Phase contrast images of nocodazole-treated HeLa cells were acquired on a Nikon TE 2000-s microscope using a 20X objective lens.

Time-lapse live imaging of HeLa cells was performed with an inverted Nikon TE2000-S using a 20X 0.4NA Ph1 phase lens (Nikon). An FCS2 closed chamber system (Bioptechs, Inc., Butler, PA, USA) was used to infuse media and $CO_2$ at a rate of 5 mL per hour. Phase-contrast images were captured once per minute using a Retiga 1300 (QImaging Corporation, Canada) camera and IPLab 3.61 (BD Biosciences) software. Images were saved individually as Tif. files and incorporated into Image Pro Plus 6.2 (Media Cybernetics, Inc) to generate sequence file time lapse movies. The mass projections were 16 images taken through the Z dimension every 0.4um. Images were projected over one another in Maximum Projection to illustrate depth of field through the cell. The signal was enhanced using opacity (transparency) to demonstrate colocalization between B-Raf and microtubules.

The CENP-E, CREST mass projection was rendered 360 degrees around the y-axis to display colocalization in all 3 dimensions (x, y, z). For CENP-E, CREST colocalization, Samples were viewed with a Leica DMI6000 inverted microscope, TCS SP5 confocal scanner, and a 63X/1.40NA Plan Apochromat oil immersion objective (Leica Microsystems). 405 Diode, 488 Argon, and 594 HeNe laser lines were applied to excite the samples and tunable filters were used to minimize crosstalk between fluorochromes. Image sections at 0.5 µm were captured with photomultiplier detectors and prepared with the LAS AF software version 1.6.0 build 1016 (Leica Microsystems).

Images of colocalized pixels were prepared with LAS AF software and analyzed for CENPE intensity using Image Pro Plus 4.5 (Media Cybernetics, Maryland).

The Imaris deconvolution images were created by processing z stack images generated by the confocal microscope through AutoDeblur deconvolution software (Mediacybernetics Inc.) using default settings. The resulting z-stack images were then imported into Imaris version 5.5 (Bitplane Inc.). 3D isosurface renderings were created by adjusting the intensity thresholds for each color channel.

## Spindle Assembly in *Xenopus* Egg Extracts

Cytostatic factor (CSF) arrested extracts were prepared from unfertilized Xenopus eggs and spindle assembly reactions were preformed as described [347], except that extracts were cycled into mitosis using recombinant nondegradable cyclin B (75 nM final). Rhodamine-labeled bovine brain tubulin (Cytoskeleton) was added to a final concentration of 0.15 µg/µl in extracts to visualize microtubules. B-Raf (Santa Cruz) or IgG control (Sigma) antibodies were used for immunodepletions from CSF extracts prior to their activation and cycling. To monitor spindles and associated chromosomes, 2 µl of extract and 1 µl of Hoechst/fixative (25% glycerol, 7.4% formaldehyde, 0.1 mM Hepes pH 7.5, 4 µg/ml bisbenzimide) were applied to a microscope slide and examined by immunofluorescence.

## REFERENCES


1. Pines, J., and Rieder, C.L. (2001). Re-staging mitosis: a contemporary view of mitotic progression. Nature cell biology *3*, E3-6.
2. Fukasawa, K. (2002). Introduction. Centrosome. Oncogene *21*, 6140-6145.
3. Mitchison, T., Evans, L., Schulze, E., and Kirschner, M. (1986). Sites of microtubule assembly and disassembly in the mitotic spindle. Cell *45*, 515-527.
4. Kishimoto, T., Kuriyama, R., Kondo, H., and Kanatani, H. (1982). Generality of the action of various maturation-promoting factors. Experimental cell research *137*, 121-126.
5. Lohka, M.J. (1989). Mitotic control by metaphase-promoting factor and cdc proteins. Journal of cell science *92 ( Pt 2)*, 131-135.
6. Masui, Y., and Markert, C.L. (1971). Cytoplasmic control of nuclear behavior during meiotic maturation of frog oocytes. The Journal of experimental zoology *177*, 129-145.
7. Nurse, P. (1990). Universal control mechanism regulating onset of M-phase. Nature *344*, 503-508.
8. Sunkara, P.S., Wright, D.A., and Rao, P.N. (1979). Mitotic factors from mammalian cells induce germinal vesicle breakdown and chromosome condensation in amphibian oocytes. Proceedings of the National Academy of Sciences of the United States of America *76*, 2799-2802.
9. Wasserman, W.J., and Smith, L.D. (1978). The cyclic behavior of a cytoplasmic factor controlling nuclear membrane breakdown. The Journal of cell biology *78*, R15-22.
10. Kimura, K., Cuvier, O., and Hirano, T. (2001). Chromosome condensation by a human condensin complex in Xenopus egg extracts. The Journal of biological chemistry *276*, 5417-5420.
11. Kimura, K., Hirano, M., Kobayashi, R., and Hirano, T. (1998). Phosphorylation and activation of 13S condensin by Cdc2 in vitro. Science (New York, N.Y *282*, 487-490.
12. Kimura, K., and Hirano, T. (2000). Dual roles of the 11S regulatory subcomplex in condensin functions. Proceedings of the National Academy of Sciences of the United States of America *97*, 11972-11977.
13. Li, G., Sudlow, G., and Belmont, A.S. (1998). Interphase cell cycle dynamics of a late-replicating, heterochromatic homogeneously staining region: precise choreography of condensation/decondensation and nuclear positioning. The Journal of cell biology *140*, 975-989.

14. Dessev, G., Iovcheva-Dessev, C., Bischoff, J.R., Beach, D., and Goldman, R. (1991). A complex containing p34cdc2 and cyclin B phosphorylates the nuclear lamin and disassembles nuclei of clam oocytes in vitro. The Journal of cell biology *112*, 523-533.
15. Geoffrey M. Cooper, R.E.H. (2004). The Cell A Molecular Approach, 3rd Edition Edition, (Sunderland: Sinauer Associates, Inc.).
16. Rieder, C.L., Schultz, A., Cole, R., and Sluder, G. (1994). Anaphase onset in vertebrate somatic cells is controlled by a checkpoint that monitors sister kinetochore attachment to the spindle. The Journal of cell biology *127*, 1301-1310.
17. Hayden, J.H., Bowser, S.S., and Rieder, C.L. (1990). Kinetochores capture astral microtubules during chromosome attachment to the mitotic spindle: direct visualization in live newt lung cells. The Journal of cell biology *111*, 1039-1045.
18. Nasmyth, K., Peters, J.M., and Uhlmann, F. (2001). Splitting the chromosome: cutting the ties that bind sister chromatids. Novartis Foundation symposium *237*, 113-133; discussion 133-118, 158-163.
19. Panizza, S., Tanaka, T., Hochwagen, A., Eisenhaber, F., and Nasmyth, K. (2000). Pds5 cooperates with cohesin in maintaining sister chromatid cohesion. Curr Biol *10*, 1557-1564.
20. Waizenegger, I.C., Hauf, S., Meinke, A., and Peters, J.M. (2000). Two distinct pathways remove mammalian cohesin from chromosome arms in prophase and from centromeres in anaphase. Cell *103*, 399-410.
21. Hauf, S., Waizenegger, I.C., and Peters, J.M. (2001). Cohesin cleavage by separase required for anaphase and cytokinesis in human cells. Science (New York, N.Y *293*, 1320-1323.
22. Nasmyth, K., Peters, J.M., and Uhlmann, F. (2000). Splitting the chromosome: cutting the ties that bind sister chromatids. Science (New York, N.Y *288*, 1379-1385.
23. Uhlmann, F., Wernic, D., Poupart, M.A., Koonin, E.V., and Nasmyth, K. (2000). Cleavage of cohesin by the CD clan protease separin triggers anaphase in yeast. Cell *103*, 375-386.
24. Castro, A., Bernis, C., Vigneron, S., Labbe, J.C., and Lorca, T. (2005). The anaphase-promoting complex: a key factor in the regulation of cell cycle. Oncogene *24*, 314-325.
25. Yanagida, M. (2000). Cell cycle mechanisms of sister chromatid separation; roles of Cut1/separin and Cut2/securin. Genes Cells *5*, 1-8.
26. Luders, J., and Stearns, T. (2007). Microtubule-organizing centres: a re-evaluation. Nature reviews *8*, 161-167.
27. Mazia, D. (1984). Centrosomes and mitotic poles. Experimental cell research *153*, 1-15.
28. Moritz, M., Braunfeld, M.B., Guenebaut, V., Heuser, J., and Agard, D.A. (2000). Structure of the gamma-tubulin ring complex: a template for microtubule nucleation. Nature cell biology *2*, 365-370.
29. Oakley, B.R., Oakley, C.E., Yoon, Y., and Jung, M.K. (1990). Gamma-tubulin is a component of the spindle pole body that is essential for microtubule function in Aspergillus nidulans. Cell *61*, 1289-1301.

30. Bahe, S., Stierhof, Y.D., Wilkinson, C.J., Leiss, F., and Nigg, E.A. (2005). Rootletin forms centriole-associated filaments and functions in centrosome cohesion. The Journal of cell biology *171*, 27-33.
31. Bahmanyar, S., Kaplan, D.D., Deluca, J.G., Giddings, T.H., Jr., O'Toole, E.T., Winey, M., Salmon, E.D., Casey, P.J., Nelson, W.J., and Barth, A.I. (2008). beta-Catenin is a Nek2 substrate involved in centrosome separation. Genes & development *22*, 91-105.
32. Fry, A.M., Descombes, P., Twomey, C., Bacchieri, R., and Nigg, E.A. (2000). The NIMA-related kinase X-Nek2B is required for efficient assembly of the zygotic centrosome in Xenopus laevis. Journal of cell science *113 ( Pt 11)*, 1973-1984.
33. Fry, A.M., Meraldi, P., and Nigg, E.A. (1998). A centrosomal function for the human Nek2 protein kinase, a member of the NIMA family of cell cycle regulators. The EMBO journal *17*, 470-481.
34. Wiese, C., and Zheng, Y. (1999). Gamma-tubulin complexes and their interaction with microtubule-organizing centers. Current opinion in structural biology *9*, 250-259.
35. Zheng, Y., Wong, M.L., Alberts, B., and Mitchison, T. (1995). Nucleation of microtubule assembly by a gamma-tubulin-containing ring complex. Nature *378*, 578-583.
36. Moritz, M., Braunfeld, M.B., Fung, J.C., Sedat, J.W., Alberts, B.M., and Agard, D.A. (1995). Three-dimensional structural characterization of centrosomes from early Drosophila embryos. The Journal of cell biology *130*, 1149-1159.
37. Moritz, M., Braunfeld, M.B., Sedat, J.W., Alberts, B., and Agard, D.A. (1995). Microtubule nucleation by gamma-tubulin-containing rings in the centrosome. Nature *378*, 638-640.
38. Vogel, J.M., Stearns, T., Rieder, C.L., and Palazzo, R.E. (1997). Centrosomes isolated from Spisula solidissima oocytes contain rings and an unusual stoichiometric ratio of alpha/beta tubulin. The Journal of cell biology *137*, 193-202.
39. Karsenti, E. (1991). Mitotic spindle morphogenesis in animal cells. Seminars in cell biology *2*, 251-260.
40. Kirschner, M., and Mitchison, T. (1986). Beyond self-assembly: from microtubules to morphogenesis. Cell *45*, 329-342.
41. Wittmann, T., Hyman, A., and Desai, A. (2001). The spindle: a dynamic assembly of microtubules and motors. Nature cell biology *3*, E28-34.
42. Mastronarde, D.N., McDonald, K.L., Ding, R., and McIntosh, J.R. (1993). Interpolar spindle microtubules in PTK cells. The Journal of cell biology *123*, 1475-1489.
43. Biggins, S., and Walczak, C.E. (2003). Captivating capture: how microtubules attach to kinetochores. Curr Biol *13*, R449-460.
44. Rieder, C.L. (1982). The formation, structure, and composition of the mammalian kinetochore and kinetochore fiber. International review of cytology *79*, 1-58.
45. Kotwaliwale, C., and Biggins, S. (2006). Microtubule capture: a concerted effort. Cell *127*, 1105-1108.

46. Gorbsky, G.J., and Ricketts, W.A. (1993). Differential expression of a phosphoepitope at the kinetochores of moving chromosomes. The Journal of cell biology *122*, 1311-1321.
47. Rieder, C.L., Cole, R.W., Khodjakov, A., and Sluder, G. (1995). The checkpoint delaying anaphase in response to chromosome monoorientation is mediated by an inhibitory signal produced by unattached kinetochores. The Journal of cell biology *130*, 941-948.
48. Rieder, C.L., and Salmon, E.D. (1998). The vertebrate cell kinetochore and its roles during mitosis. Trends in cell biology *8*, 310-318.
49. Cimini, D., Moree, B., Canman, J.C., and Salmon, E.D. (2003). Merotelic kinetochore orientation occurs frequently during early mitosis in mammalian tissue cells and error correction is achieved by two different mechanisms. Journal of cell science *116*, 4213-4225.
50. Cimini, D. (2007). Detection and correction of merotelic kinetochore orientation by Aurora B and its partners. Cell cycle (Georgetown, Tex *6*, 1558-1564.
51. Girdler, F., Gascoigne, K.E., Eyers, P.A., Hartmuth, S., Crafter, C., Foote, K.M., Keen, N.J., and Taylor, S.S. (2006). Validating Aurora B as an anti-cancer drug target. Journal of cell science *119*, 3664-3675.
52. Hauf, S., Cole, R.W., LaTerra, S., Zimmer, C., Schnapp, G., Walter, R., Heckel, A., van Meel, J., Rieder, C.L., and Peters, J.M. (2003). The small molecule Hesperadin reveals a role for Aurora B in correcting kinetochore-microtubule attachment and in maintaining the spindle assembly checkpoint. The Journal of cell biology *161*, 281-294.
53. Kapoor, T.M., Lampson, M.A., Hergert, P., Cameron, L., Cimini, D., Salmon, E.D., McEwen, B.F., and Khodjakov, A. (2006). Chromosomes can congress to the metaphase plate before biorientation. Science (New York, N.Y *311*, 388-391.
54. Mistry, H.B., MacCallum, D.E., Jackson, R.C., Chaplain, M.A., and Davidson, F.A. (2008). Modeling the temporal evolution of the spindle assembly checkpoint and role of Aurora B kinase. Proceedings of the National Academy of Sciences of the United States of America *105*, 20215-20220.
55. Kelly, A.E., and Funabiki, H. (2009). Correcting aberrant kinetochore microtubule attachments: an Aurora B-centric view. Current opinion in cell biology *21*, 51-58.
56. Hardwick, K.G., Johnston, R.C., Smith, D.L., and Murray, A.W. (2000). MAD3 encodes a novel component of the spindle checkpoint which interacts with Bub3p, Cdc20p, and Mad2p. The Journal of cell biology *148*, 871-882.
57. May, K.M., and Hardwick, K.G. (2006). The spindle checkpoint. Journal of cell science *119*, 4139-4142.
58. Musacchio, A., and Salmon, E.D. (2007). The spindle-assembly checkpoint in space and time. Nature reviews *8*, 379-393.
59. Sudakin, V., Chan, G.K., and Yen, T.J. (2001). Checkpoint inhibition of the APC/C in HeLa cells is mediated by a complex of BUBR1, BUB3, CDC20, and MAD2. The Journal of cell biology *154*, 925-936.
60. Yen, T.J., and Kao, G.D. (2005). Mitotic checkpoint, aneuploidy and cancer. Advances in experimental medicine and biology *570*, 477-499.

61. Hoyt, M.A., Totis, L., and Roberts, B.T. (1991). S. cerevisiae genes required for cell cycle arrest in response to loss of microtubule function. Cell *66*, 507-517.
62. Johnson, V.L., Scott, M.I., Holt, S.V., Hussein, D., and Taylor, S.S. (2004). Bub1 is required for kinetochore localization of BubR1, Cenp-E, Cenp-F and Mad2, and chromosome congression. Journal of cell science *117*, 1577-1589.
63. Li, R., and Murray, A.W. (1991). Feedback control of mitosis in budding yeast. Cell *66*, 519-531.
64. Winey, M., Goetsch, L., Baum, P., and Byers, B. (1991). MPS1 and MPS2: novel yeast genes defining distinct steps of spindle pole body duplication. The Journal of cell biology *114*, 745-754.
65. Bharadwaj, R., and Yu, H. (2004). The spindle checkpoint, aneuploidy, and cancer. Oncogene *23*, 2016-2027.
66. Musacchio, A., and Hardwick, K.G. (2002). The spindle checkpoint: structural insights into dynamic signalling. Nature reviews *3*, 731-741.
67. Yu, H. (2002). Regulation of APC-Cdc20 by the spindle checkpoint. Current opinion in cell biology *14*, 706-714.
68. Chen, R.H., Shevchenko, A., Mann, M., and Murray, A.W. (1998). Spindle checkpoint protein Xmad1 recruits Xmad2 to unattached kinetochores. The Journal of cell biology *143*, 283-295.
69. Sharp-Baker, H., and Chen, R.H. (2001). Spindle checkpoint protein Bub1 is required for kinetochore localization of Mad1, Mad2, Bub3, and CENP-E, independently of its kinase activity. The Journal of cell biology *153*, 1239-1250.
70. Vigneron, S., Prieto, S., Bernis, C., Labbe, J.C., Castro, A., and Lorca, T. (2004). Kinetochore localization of spindle checkpoint proteins: who controls whom? Molecular biology of the cell *15*, 4584-4596.
71. Jones, M.H., Huneycutt, B.J., Pearson, C.G., Zhang, C., Morgan, G., Shokat, K., Bloom, K., and Winey, M. (2005). Chemical genetics reveals a role for Mps1 kinase in kinetochore attachment during mitosis. Curr Biol *15*, 160-165.
72. Winey, M., and Huneycutt, B.J. (2002). Centrosomes and checkpoints: the MPS1 family of kinases. Oncogene *21*, 6161-6169.
73. Zhao, Y., and Chen, R.H. (2006). Mps1 phosphorylation by MAP kinase is required for kinetochore localization of spindle-checkpoint proteins. Curr Biol *16*, 1764-1769.
74. De Antoni, A., Pearson, C.G., Cimini, D., Canman, J.C., Sala, V., Nezi, L., Mapelli, M., Sironi, L., Faretta, M., Salmon, E.D., et al. (2005). The Mad1/Mad2 complex as a template for Mad2 activation in the spindle assembly checkpoint. Curr Biol *15*, 214-225.
75. Howell, B.J., Moree, B., Farrar, E.M., Stewart, S., Fang, G., and Salmon, E.D. (2004). Spindle checkpoint protein dynamics at kinetochores in living cells. Curr Biol *14*, 953-964.
76. Shah, J.V., Botvinick, E., Bonday, Z., Furnari, F., Berns, M., and Cleveland, D.W. (2004). Dynamics of centromere and kinetochore proteins; implications for checkpoint signaling and silencing. Curr Biol *14*, 942-952.
77. Vink, M., Simonetta, M., Transidico, P., Ferrari, K., Mapelli, M., De Antoni, A., Massimiliano, L., Ciliberto, A., Faretta, M., Salmon, E.D., et al. (2006). In vitro

FRAP identifies the minimal requirements for Mad2 kinetochore dynamics. Curr Biol *16*, 755-766.
78. Yu, H. (2006). Structural activation of Mad2 in the mitotic spindle checkpoint: the two-state Mad2 model versus the Mad2 template model. The Journal of cell biology *173*, 153-157.
79. Hwang, L.H., Lau, L.F., Smith, D.L., Mistrot, C.A., Hardwick, K.G., Hwang, E.S., Amon, A., and Murray, A.W. (1998). Budding yeast Cdc20: a target of the spindle checkpoint. Science (New York, N.Y *279*, 1041-1044.
80. Fang, G. (2002). Checkpoint protein BubR1 acts synergistically with Mad2 to inhibit anaphase-promoting complex. Molecular biology of the cell *13*, 755-766.
81. Tang, Z., Bharadwaj, R., Li, B., and Yu, H. (2001). Mad2-Independent inhibition of APCCdc20 by the mitotic checkpoint protein BubR1. Developmental cell *1*, 227-237.
82. Karess, R. (2005). Rod-Zw10-Zwilch: a key player in the spindle checkpoint. Trends in cell biology *15*, 386-392.
83. Habu, T., Kim, S.H., Weinstein, J., and Matsumoto, T. (2002). Identification of a MAD2-binding protein, CMT2, and its role in mitosis. The EMBO journal *21*, 6419-6428.
84. Mapelli, M., Filipp, F.V., Rancati, G., Massimiliano, L., Nezi, L., Stier, G., Hagan, R.S., Confalonieri, S., Piatti, S., Sattler, M., et al. (2006). Determinants of conformational dimerization of Mad2 and its inhibition by p31comet. The EMBO journal *25*, 1273-1284.
85. Xia, G., Luo, X., Habu, T., Rizo, J., Matsumoto, T., and Yu, H. (2004). Conformation-specific binding of p31(comet) antagonizes the function of Mad2 in the spindle checkpoint. The EMBO journal *23*, 3133-3143.
86. D'Angiolella, V., Mari, C., Nocera, D., Rametti, L., and Grieco, D. (2003). The spindle checkpoint requires cyclin-dependent kinase activity. Genes & development *17*, 2520-2525.
87. Yudkovsky, Y., Shteinberg, M., Listovsky, T., Brandeis, M., and Hershko, A. (2000). Phosphorylation of Cdc20/fizzy negatively regulates the mammalian cyclosome/APC in the mitotic checkpoint. Biochemical and biophysical research communications *271*, 299-304.
88. Du, J., Cai, X., Yao, J., Ding, X., Wu, Q., Pei, S., Jiang, K., Zhang, Y., Wang, W., Shi, Y., et al. (2008). The mitotic checkpoint kinase NEK2A regulates kinetochore microtubule attachment stability. Oncogene *27*, 4107-4114.
89. Tang, J., Erikson, R.L., and Liu, X. (2006). Checkpoint kinase 1 (Chk1) is required for mitotic progression through negative regulation of polo-like kinase 1 (Plk1). Proceedings of the National Academy of Sciences of the United States of America *103*, 11964-11969.
90. Cimini, D., Howell, B., Maddox, P., Khodjakov, A., Degrassi, F., and Salmon, E.D. (2001). Merotelic kinetochore orientation is a major mechanism of aneuploidy in mitotic mammalian tissue cells. The Journal of cell biology *153*, 517-527.
91. Salmon, E.D., Cimini, D., Cameron, L.A., and DeLuca, J.G. (2005). Merotelic kinetochores in mammalian tissue cells. Philosophical transactions of the Royal Society of London *360*, 553-568.

92. English, J., Pearson, G., Wilsbacher, J., Swantek, J., Karandikar, M., Xu, S., and Cobb, M.H. (1999). New insights into the control of MAP kinase pathways. Experimental cell research *253*, 255-270.
93. Widmann, C., Gibson, S., Jarpe, M.B., and Johnson, G.L. (1999). Mitogen-activated protein kinase: conservation of a three-kinase module from yeast to human. Physiological reviews *79*, 143-180.
94. Siow, Y.L., Kalmar, G.B., Sanghera, J.S., Tai, G., Oh, S.S., and Pelech, S.L. (1997). Identification of two essential phosphorylated threonine residues in the catalytic domain of Mekk1. Indirect activation by Pak3 and protein kinase C. The Journal of biological chemistry *272*, 7586-7594.
95. Gartner, A., Nasmyth, K., and Ammerer, G. (1992). Signal transduction in Saccharomyces cerevisiae requires tyrosine and threonine phosphorylation of FUS3 and KSS1. Genes & development *6*, 1280-1292.
96. Pearson, G., Robinson, F., Beers Gibson, T., Xu, B.E., Karandikar, M., Berman, K., and Cobb, M.H. (2001). Mitogen-activated protein (MAP) kinase pathways: regulation and physiological functions. Endocrine reviews *22*, 153-183.
97. Dong, F., Gutkind, J.S., and Larner, A.C. (2001). Granulocyte colony-stimulating factor induces ERK5 activation, which is differentially regulated by protein-tyrosine kinases and protein kinase C. Regulation of cell proliferation and survival. The Journal of biological chemistry *276*, 10811-10816.
98. Kato, Y., Tapping, R.I., Huang, S., Watson, M.H., Ulevitch, R.J., and Lee, J.D. (1998). Bmk1/Erk5 is required for cell proliferation induced by epidermal growth factor. Nature *395*, 713-716.
99. Gille, H., Strahl, T., and Shaw, P.E. (1995). Activation of ternary complex factor Elk-1 by stress-activated protein kinases. Curr Biol *5*, 1191-1200.
100. Murphy, L.O., Smith, S., Chen, R.H., Fingar, D.C., and Blenis, J. (2002). Molecular interpretation of ERK signal duration by immediate early gene products. Nature cell biology *4*, 556-564.
101. Milne, D.M., Campbell, D.G., Caudwell, F.B., and Meek, D.W. (1994). Phosphorylation of the tumor suppressor protein p53 by mitogen-activated protein kinases. The Journal of biological chemistry *269*, 9253-9260.
102. Lin, L.L., Wartmann, M., Lin, A.Y., Knopf, J.L., Seth, A., and Davis, R.J. (1993). cPLA2 is phosphorylated and activated by MAP kinase. Cell *72*, 269-278.
103. Seger, R., and Krebs, E.G. (1995). The MAPK signaling cascade. Faseb J *9*, 726-735.
104. Yarden, Y., and Schlessinger, J. (1987). Self-phosphorylation of epidermal growth factor receptor: evidence for a model of intermolecular allosteric activation. Biochemistry *26*, 1434-1442.
105. Kolch, W. (2000). Meaningful relationships: the regulation of the Ras/Raf/MEK/ERK pathway by protein interactions. The Biochemical journal *351 Pt 2*, 289-305.
106. Wellbrock, C., Karasarides, M., and Marais, R. (2004). The RAF proteins take centre stage. Nature reviews *5*, 875-885.
107. Gotoh, Y., Moriyama, K., Matsuda, S., Okumura, E., Kishimoto, T., Kawasaki, H., Suzuki, K., Yahara, I., Sakai, H., and Nishida, E. (1991). Xenopus M phase

MAP kinase: isolation of its cDNA and activation by MPF. The EMBO journal *10*, 2661-2668.
108. Gotoh, Y., Nishida, E., Matsuda, S., Shiina, N., Kosako, H., Shiokawa, K., Akiyama, T., Ohta, K., and Sakai, H. (1991). In vitro effects on microtubule dynamics of purified Xenopus M phase-activated MAP kinase. Nature *349*, 251-254.
109. Minshull, J., Sun, H., Tonks, N.K., and Murray, A.W. (1994). A MAP kinase-dependent spindle assembly checkpoint in Xenopus egg extracts. Cell *79*, 475-486.
110. Takenaka, K., Gotoh, Y., and Nishida, E. (1997). MAP kinase is required for the spindle assembly checkpoint but is dispensable for the normal M phase entry and exit in Xenopus egg cell cycle extracts. The Journal of cell biology *136*, 1091-1097.
111. Roberts, E.C., Shapiro, P.S., Nahreini, T.S., Pages, G., Pouyssegur, J., and Ahn, N.G. (2002). Distinct cell cycle timing requirements for extracellular signal-regulated kinase and phosphoinositide 3-kinase signaling pathways in somatic cell mitosis. Molecular and cellular biology *22*, 7226-7241.
112. Shapiro, P.S., Vaisberg, E., Hunt, A.J., Tolwinski, N.S., Whalen, A.M., McIntosh, J.R., and Ahn, N.G. (1998). Activation of the MKK/ERK pathway during somatic cell mitosis: direct interactions of active ERK with kinetochores and regulation of the mitotic 3F3/2 phosphoantigen. J Cell Biol *142*, 1533-1545.
113. Willard, F.S., and Crouch, M.F. (2001). MEK, ERK, and p90RSK are present on mitotic tubulin in Swiss 3T3 cells: a role for the MAP kinase pathway in regulating mitotic exit. Cellular signalling *13*, 653-664.
114. Zecevic, M., Catling, A.D., Eblen, S.T., Renzi, L., Hittle, J.C., Yen, T.J., Gorbsky, G.J., and Weber, M.J. (1998). Active MAP kinase in mitosis: localization at kinetochores and association with the motor protein CENP-E. The Journal of cell biology *142*, 1547-1558.
115. Horne, M.M., and Guadagno, T.M. (2003). A requirement for MAP kinase in the assembly and maintenance of the mitotic spindle. The Journal of cell biology *161*, 1021-1028.
116. Zhang, W.L., Huitorel, P., Glass, R., Fernandez-Serra, M., Arnone, M.I., Chiri, S., Picard, A., and Ciapa, B. (2005). A MAPK pathway is involved in the control of mitosis after fertilization of the sea urchin egg. Developmental biology *282*, 192-206.
117. Wright, J.H., Munar, E., Jameson, D.R., Andreassen, P.R., Margolis, R.L., Seger, R., and Krebs, E.G. (1999). Mitogen-activated protein kinase kinase activity is required for the G(2)/M transition of the cell cycle in mammalian fibroblasts. Proceedings of the National Academy of Sciences of the United States of America *96*, 11335-11340.
118. Liu, X., Yan, S., Zhou, T., Terada, Y., and Erikson, R.L. (2004). The MAP kinase pathway is required for entry into mitosis and cell survival. Oncogene *23*, 763-776.
119. Guadagno, T.M., and Ferrell, J.E., Jr. (1998). Requirement for MAPK activation for normal mitotic progression in Xenopus egg extracts. Science (New York, N.Y *282*, 1312-1315.

120. Bitangcol, J.C., Chau, A.S., Stadnick, E., Lohka, M.J., Dicken, B., and Shibuya, E.K. (1998). Activation of the p42 mitogen-activated protein kinase pathway inhibits Cdc2 activation and entry into M-phase in cycling Xenopus egg extracts. Molecular biology of the cell *9*, 451-467.
121. Walter, S.A., Guadagno, T.M., and Ferrell, J.E., Jr. (1997). Induction of a G2-phase arrest in Xenopus egg extracts by activation of p42 mitogen-activated protein kinase. Molecular biology of the cell *8*, 2157-2169.
122. Walter, S.A., Guadagno, S.N., and Ferrell, J.E., Jr. (2000). Activation of Wee1 by p42 MAPK in vitro and in cycling xenopus egg extracts. Molecular biology of the cell *11*, 887-896.
123. Reszka, A.A., Seger, R., Diltz, C.D., Krebs, E.G., and Fischer, E.H. (1995). Association of mitogen-activated protein kinase with the microtubule cytoskeleton. Proceedings of the National Academy of Sciences of the United States of America *92*, 8881-8885.
124. Hoshi, M., Ohta, K., Gotoh, Y., Mori, A., Murofushi, H., Sakai, H., and Nishida, E. (1992). Mitogen-activated-protein-kinase-catalyzed phosphorylation of microtubule-associated proteins, microtubule-associated protein 2 and microtubule-associated protein 4, induces an alteration in their function. European journal of biochemistry / FEBS *203*, 43-52.
125. Ray, L.B., and Sturgill, T.W. (1987). Rapid stimulation by insulin of a serine/threonine kinase in 3T3-L1 adipocytes that phosphorylates microtubule-associated protein 2 in vitro. Proceedings of the National Academy of Sciences of the United States of America *84*, 1502-1506.
126. Verlhac, M.H., de Pennart, H., Maro, B., Cobb, M.H., and Clarke, H.J. (1993). MAP kinase becomes stably activated at metaphase and is associated with microtubule-organizing centers during meiotic maturation of mouse oocytes. Developmental biology *158*, 330-340.
127. Chau, A.S., and Shibuya, E.K. (1999). Inactivation of p42 mitogen-activated protein kinase is required for exit from M-phase after cyclin destruction. The Journal of biological chemistry *274*, 32085-32090.
128. Inoue, Y.H., and Glover, D.M. (1998). Involvement of the rolled/MAP kinase gene in Drosophila mitosis: interaction between genes for the MAP kinase cascade and abnormal spindle. Mol Gen Genet *258*, 334-341.
129. Chung, E., and Chen, R.H. (2003). Phosphorylation of Cdc20 is required for its inhibition by the spindle checkpoint. Nat Cell Biol *5*, 748-753.
130. Fukasawa, K., and Vande Woude, G.F. (1997). Synergy between the Mos/mitogen-activated protein kinase pathway and loss of p53 function in transformation and chromosome instability. Molecular and cellular biology *17*, 506-518.
131. Saavedra, H.I., Fukasawa, K., Conn, C.W., and Stambrook, P.J. (1999). MAPK mediates RAS-induced chromosome instability. The Journal of biological chemistry *274*, 38083-38090.
132. Warren, G. (1993). Membrane partitioning during cell division. Annual review of biochemistry *62*, 323-348.

133. Colanzi, A., Sutterlin, C., and Malhotra, V. (2003). RAF1-activated MEK1 is found on the Golgi apparatus in late prophase and is required for Golgi complex fragmentation in mitosis. The Journal of cell biology *161*, 27-32.
134. Harding, A., Giles, N., Burgess, A., Hancock, J.F., and Gabrielli, B.G. (2003). Mechanism of mitosis-specific activation of MEK1. J Biol Chem *278*, 16747-16754.
135. Acharya, U., Mallabiabarrena, A., Acharya, J.K., and Malhotra, V. (1998). Signaling via mitogen-activated protein kinase kinase (MEK1) is required for Golgi fragmentation during mitosis. Cell *92*, 183-192.
136. Sutterlin, C., Hsu, P., Mallabiabarrena, A., and Malhotra, V. (2002). Fragmentation and dispersal of the pericentriolar Golgi complex is required for entry into mitosis in mammalian cells. Cell *109*, 359-369.
137. Aebersold, D.M., Shaul, Y.D., Yung, Y., Yarom, N., Yao, Z., Hanoch, T., and Seger, R. (2004). Extracellular signal-regulated kinase 1c (ERK1c), a novel 42-kilodalton ERK, demonstrates unique modes of regulation, localization, and function. Mol Cell Biol *24*, 10000-10015.
138. Shaul, Y.D., and Seger, R. (2006). ERK1c regulates Golgi fragmentation during mitosis. J Cell Biol *172*, 885-897.
139. Chong, H., Lee, J., and Guan, K.L. (2001). Positive and negative regulation of Raf kinase activity and function by phosphorylation. The EMBO journal *20*, 3716-3727.
140. Chong, H., Vikis, H.G., and Guan, K.L. (2003). Mechanisms of regulating the Raf kinase family. Cellular signalling *15*, 463-469.
141. Daum, G., Eisenmann-Tappe, I., Fries, H.W., Troppmair, J., and Rapp, U.R. (1994). The ins and outs of Raf kinases. Trends in biochemical sciences *19*, 474-480.
142. Morrison, D.K., and Cutler, R.E. (1997). The complexity of Raf-1 regulation. Current opinion in cell biology *9*, 174-179.
143. Chuang, E., Barnard, D., Hettich, L., Zhang, X.F., Avruch, J., and Marshall, M.S. (1994). Critical binding and regulatory interactions between Ras and Raf occur through a small, stable N-terminal domain of Raf and specific Ras effector residues. Molecular and cellular biology *14*, 5318-5325.
144. Guan, K.L., Figueroa, C., Brtva, T.R., Zhu, T., Taylor, J., Barber, T.D., and Vojtek, A.B. (2000). Negative regulation of the serine/threonine kinase B-Raf by Akt. The Journal of biological chemistry *275*, 27354-27359.
145. Morrison, D.K., Heidecker, G., Rapp, U.R., and Copeland, T.D. (1993). Identification of the major phosphorylation sites of the Raf-1 kinase. The Journal of biological chemistry *268*, 17309-17316.
146. Zimmermann, S., and Moelling, K. (1999). Phosphorylation and regulation of Raf by Akt (protein kinase B). Science (New York, N.Y *286*, 1741-1744.
147. Michaud, N.R., Fabian, J.R., Mathes, K.D., and Morrison, D.K. (1995). 14-3-3 is not essential for Raf-1 function: identification of Raf-1 proteins that are biologically activated in a 14-3-3- and Ras-independent manner. Molecular and cellular biology *15*, 3390-3397.

148. Barnier, J.V., Papin, C., Eychene, A., Lecoq, O., and Calothy, G. (1995). The mouse B-raf gene encodes multiple protein isoforms with tissue-specific expression. The Journal of biological chemistry *270*, 23381-23389.
149. Papin, C., Eychene, A., Brunet, A., Pages, G., Pouyssegur, J., Calothy, G., and Barnier, J.V. (1995). B-Raf protein isoforms interact with and phosphorylate Mek-1 on serine residues 218 and 222. Oncogene *10*, 1647-1651.
150. Heidecker, G., Huleihel, M., Cleveland, J.L., Kolch, W., Beck, T.W., Lloyd, P., Pawson, T., and Rapp, U.R. (1990). Mutational activation of c-raf-1 and definition of the minimal transforming sequence. Molecular and cellular biology *10*, 2503-2512.
151. Jaumot, M., and Hancock, J.F. (2001). Protein phosphatases 1 and 2A promote Raf-1 activation by regulating 14-3-3 interactions. Oncogene *20*, 3949-3958.
152. Kubicek, M., Pacher, M., Abraham, D., Podar, K., Eulitz, M., and Baccarini, M. (2002). Dephosphorylation of Ser-259 regulates Raf-1 membrane association. The Journal of biological chemistry *277*, 7913-7919.
153. Nassar, N., Horn, G., Herrmann, C., Scherer, A., McCormick, F., and Wittinghofer, A. (1995). The 2.2 A crystal structure of the Ras-binding domain of the serine/threonine kinase c-Raf1 in complex with Rap1A and a GTP analogue. Nature *375*, 554-560.
154. Okada, T., Hu, C.D., Jin, T.G., Kariya, K., Yamawaki-Kataoka, Y., and Kataoka, T. (1999). The strength of interaction at the Raf cysteine-rich domain is a critical determinant of response of Raf to Ras family small GTPases. Molecular and cellular biology *19*, 6057-6064.
155. Vojtek, A.B., Hollenberg, S.M., and Cooper, J.A. (1993). Mammalian Ras interacts directly with the serine/threonine kinase Raf. Cell *74*, 205-214.
156. Diaz, B., Barnard, D., Filson, A., MacDonald, S., King, A., and Marshall, M. (1997). Phosphorylation of Raf-1 serine 338-serine 339 is an essential regulatory event for Ras-dependent activation and biological signaling. Molecular and cellular biology *17*, 4509-4516.
157. Fabian, J.R., Daar, I.O., and Morrison, D.K. (1993). Critical tyrosine residues regulate the enzymatic and biological activity of Raf-1 kinase. Molecular and cellular biology *13*, 7170-7179.
158. Mason, C.S., Springer, C.J., Cooper, R.G., Superti-Furga, G., Marshall, C.J., and Marais, R. (1999). Serine and tyrosine phosphorylations cooperate in Raf-1, but not B-Raf activation. The EMBO journal *18*, 2137-2148.
159. Marais, R., Light, Y., Paterson, H.F., and Marshall, C.J. (1995). Ras recruits Raf-1 to the plasma membrane for activation by tyrosine phosphorylation. The EMBO journal *14*, 3136-3145.
160. Zhang, B.H., and Guan, K.L. (2000). Activation of B-Raf kinase requires phosphorylation of the conserved residues Thr598 and Ser601. The EMBO journal *19*, 5429-5439.
161. Marais, R., Light, Y., Paterson, H.F., Mason, C.S., and Marshall, C.J. (1997). Differential regulation of Raf-1, A-Raf, and B-Raf by oncogenic ras and tyrosine kinases. The Journal of biological chemistry *272*, 4378-4383.

162. Berruti, G. (2000). A novel rap1/B-Raf/14-3-3 theta protein complex is formed in vivo during the morphogenetic differentiation of postmeiotic male germ cells. Experimental cell research *257*, 172-179.
163. Houslay, M.D., and Kolch, W. (2000). Cell-type specific integration of cross-talk between extracellular signal-regulated kinase and cAMP signaling. Molecular pharmacology *58*, 659-668.
164. Papin, C., Denouel, A., Calothy, G., and Eychene, A. (1996). Identification of signalling proteins interacting with B-Raf in the yeast two-hybrid system. Oncogene *12*, 2213-2221.
165. Vossler, M.R., Yao, H., York, R.D., Pan, M.G., Rim, C.S., and Stork, P.J. (1997). cAMP activates MAP kinase and Elk-1 through a B-Raf- and Rap1-dependent pathway. Cell *89*, 73-82.
166. Yamamori, B., Kuroda, S., Shimizu, K., Fukui, K., Ohtsuka, T., and Takai, Y. (1995). Purification of a Ras-dependent mitogen-activated protein kinase kinase kinase from bovine brain cytosol and its identification as a complex of B-Raf and 14-3-3 proteins. The Journal of biological chemistry *270*, 11723-11726.
167. York, R.D., Yao, H., Dillon, T., Ellig, C.L., Eckert, S.P., McCleskey, E.W., and Stork, P.J. (1998). Rap1 mediates sustained MAP kinase activation induced by nerve growth factor. Nature *392*, 622-626.
168. Rushworth, L.K., Hindley, A.D., O'Neill, E., and Kolch, W. (2006). Regulation and role of Raf-1/B-Raf heterodimerization. Molecular and cellular biology *26*, 2262-2272.
169. Bos, J.L., de Rooij, J., and Reedquist, K.A. (2001). Rap1 signalling: adhering to new models. Nature reviews *2*, 369-377.
170. Papin, C., Denouel-Galy, A., Laugier, D., Calothy, G., and Eychene, A. (1998). Modulation of kinase activity and oncogenic properties by alternative splicing reveals a novel regulatory mechanism for B-Raf. The Journal of biological chemistry *273*, 24939-24947.
171. Mizutani, S., Koide, H., and Kaziro, Y. (1998). Isolation of a new protein factor required for activation of Raf-1 by Ha-Ras: partial purification from rat brain cytosols. Oncogene *16*, 2781-2786.
172. Weber, C.K., Slupsky, J.R., Kalmes, H.A., and Rapp, U.R. (2001). Active Ras induces heterodimerization of cRaf and BRaf. Cancer research *61*, 3595-3598.
173. Wojnowski, L., Zimmer, A.M., Beck, T.W., Hahn, H., Bernal, R., Rapp, U.R., and Zimmer, A. (1997). Endothelial apoptosis in Braf-deficient mice. Nature genetics *16*, 293-297.
174. Wojnowski, L., Stancato, L.F., Larner, A.C., Rapp, U.R., and Zimmer, A. (2000). Overlapping and specific functions of Braf and Craf-1 proto-oncogenes during mouse embryogenesis. Mechanisms of development *91*, 97-104.
175. Storm, S.M., Cleveland, J.L., and Rapp, U.R. (1990). Expression of raf family proto-oncogenes in normal mouse tissues. Oncogene *5*, 345-351.
176. Wadewitz, A.G., Winer, M.A., and Wolgemuth, D.J. (1993). Developmental and cell lineage specificity of raf family gene expression in mouse testis. Oncogene *8*, 1055-1062.

177. Wixler, V., Smola, U., Schuler, M., and Rapp, U. (1996). Differential regulation of Raf isozymes by growth versus differentiation inducing factors in PC12 pheochromocytoma cells. FEBS letters *385*, 131-137.
178. MacNicol, M.C., and MacNicol, A.M. (1999). Nerve growth factor-stimulated B-Raf catalytic activity is refractory to inhibition by cAMP-dependent protein kinase. The Journal of biological chemistry *274*, 13193-13197.
179. Ohtsuka, T., Shimizu, K., Yamamori, B., Kuroda, S., and Takai, Y. (1996). Activation of brain B-Raf protein kinase by Rap1B small GTP-binding protein. The Journal of biological chemistry *271*, 1258-1261.
180. Borysov, S.I., Cheng, A.W., and Guadagno, T.M. (2006). B-Raf Is Critical For MAPK Activation during Mitosis and Is Regulated in an M Phase-dependent Manner in Xenopus Egg Extracts. J Biol Chem *281*, 22586-22596.
181. Borysov, S.I., and Guadagno, T.M. (2008). A novel role for Cdk1/cyclin B in regulating B-raf activation at mitosis. Molecular biology of the cell *19*, 2907-2915.
182. Cohen, S. (1965). The stimulation of epidermal proliferation by a specific protein (EGF). Developmental biology *12*, 394-407.
183. Cohen, S., Carpenter, G., and King, L., Jr. (1980). Epidermal growth factor-receptor-protein kinase interactions. Co-purification of receptor and epidermal growth factor-enhanced phosphorylation activity. The Journal of biological chemistry *255*, 4834-4842.
184. Yarden, Y., and Sliwkowski, M.X. (2001). Untangling the ErbB signalling network. Nature reviews *2*, 127-137.
185. Downward, J., Yarden, Y., Mayes, E., Scrace, G., Totty, N., Stockwell, P., Ullrich, A., Schlessinger, J., and Waterfield, M.D. (1984). Close similarity of epidermal growth factor receptor and v-erb-B oncogene protein sequences. Nature *307*, 521-527.
186. Lin, C.R., Chen, W.S., Kruiger, W., Stolarsky, L.S., Weber, W., Evans, R.M., Verma, I.M., Gill, G.N., and Rosenfeld, M.G. (1984). Expression cloning of human EGF receptor complementary DNA: gene amplification and three related messenger RNA products in A431 cells. Science (New York, N.Y *224*, 843-848.
187. Ullrich, A., Coussens, L., Hayflick, J.S., Dull, T.J., Gray, A., Tam, A.W., Lee, J., Yarden, Y., Libermann, T.A., Schlessinger, J., et al. (1984). Human epidermal growth factor receptor cDNA sequence and aberrant expression of the amplified gene in A431 epidermoid carcinoma cells. Nature *309*, 418-425.
188. Xu, Y.H., Ishii, S., Clark, A.J., Sullivan, M., Wilson, R.K., Ma, D.P., Roe, B.A., Merlino, G.T., and Pastan, I. (1984). Human epidermal growth factor receptor cDNA is homologous to a variety of RNAs overproduced in A431 carcinoma cells. Nature *309*, 806-810.
189. Ozanne, B., Richards, C.S., Hendler, F., Burns, D., and Gusterson, B. (1986). Over-expression of the EGF receptor is a hallmark of squamous cell carcinomas. The Journal of pathology *149*, 9-14.
190. Grandis, J.R., and Sok, J.C. (2004). Signaling through the epidermal growth factor receptor during the development of malignancy. Pharmacology & therapeutics *102*, 37-46.

191. Grandis, J.R., Zeng, Q., Drenning, S.D., and Tweardy, D.J. (1998). Normalization of EGFR mRNA levels following restoration of wild-type p53 in a head and neck squamous cell carcinoma cell line. International journal of oncology *13*, 375-378.
192. Moscatello, D.K., Holgado-Madruga, M., Godwin, A.K., Ramirez, G., Gunn, G., Zoltick, P.W., Biegel, J.A., Hayes, R.L., and Wong, A.J. (1995). Frequent expression of a mutant epidermal growth factor receptor in multiple human tumors. Cancer research *55*, 5536-5539.
193. Nishikawa, R., Ji, X.D., Harmon, R.C., Lazar, C.S., Gill, G.N., Cavenee, W.K., and Huang, H.J. (1994). A mutant epidermal growth factor receptor common in human glioma confers enhanced tumorigenicity. Proceedings of the National Academy of Sciences of the United States of America *91*, 7727-7731.
194. Rusch, V., Baselga, J., Cordon-Cardo, C., Orazem, J., Zaman, M., Hoda, S., McIntosh, J., Kurie, J., and Dmitrovsky, E. (1993). Differential expression of the epidermal growth factor receptor and its ligands in primary non-small cell lung cancers and adjacent benign lung. Cancer research *53*, 2379-2385.
195. Salomon, D.S., Brandt, R., Ciardiello, F., and Normanno, N. (1995). Epidermal growth factor-related peptides and their receptors in human malignancies. Critical reviews in oncology/hematology *19*, 183-232.
196. Gangarosa, L.M., Sizemore, N., Graves-Deal, R., Oldham, S.M., Der, C.J., and Coffey, R.J. (1997). A raf-independent epidermal growth factor receptor autocrine loop is necessary for Ras transformation of rat intestinal epithelial cells. The Journal of biological chemistry *272*, 18926-18931.
197. McCarthy, S.A., Samuels, M.L., Pritchard, C.A., Abraham, J.A., and McMahon, M. (1995). Rapid induction of heparin-binding epidermal growth factor/diphtheria toxin receptor expression by Raf and Ras oncogenes. Genes & development *9*, 1953-1964.
198. Schulze, A., Lehmann, K., Jefferies, H.B., McMahon, M., and Downward, J. (2001). Analysis of the transcriptional program induced by Raf in epithelial cells. Genes & development *15*, 981-994.
199. Mitin, N., Rossman, K.L., and Der, C.J. (2005). Signaling interplay in Ras superfamily function. Curr Biol *15*, R563-574.
200. Roberts, P.J., and Der, C.J. (2007). Targeting the Raf-MEK-ERK mitogen-activated protein kinase cascade for the treatment of cancer. Oncogene *26*, 3291-3310.
201. Bos, J.L. (1989). ras oncogenes in human cancer: a review. Cancer research *49*, 4682-4689.
202. Malumbres, M., and Barbacid, M. (2003). RAS oncogenes: the first 30 years. Nat Rev Cancer *3*, 459-465.
203. Wu, G.S. (2007). Role of mitogen-activated protein kinase phosphatases (MKPs) in cancer. Cancer metastasis reviews *26*, 579-585.
204. Loda, M., Capodieci, P., Mishra, R., Yao, H., Corless, C., Grigioni, W., Wang, Y., Magi-Galluzzi, C., and Stork, P.J. (1996). Expression of mitogen-activated protein kinase phosphatase-1 in the early phases of human epithelial carcinogenesis. The American journal of pathology *149*, 1553-1564.
205. Vicent, S., Garayoa, M., Lopez-Picazo, J.M., Lozano, M.D., Toledo, G., Thunnissen, F.B., Manzano, R.G., and Montuenga, L.M. (2004). Mitogen-

activated protein kinase phosphatase-1 is overexpressed in non-small cell lung cancer and is an independent predictor of outcome in patients. Clin Cancer Res *10*, 3639-3649.

206. Wang, H.Y., Cheng, Z., and Malbon, C.C. (2003). Overexpression of mitogen-activated protein kinase phosphatases MKP1, MKP2 in human breast cancer. Cancer letters *191*, 229-237.
207. Denkert, C., Schmitt, W.D., Berger, S., Reles, A., Pest, S., Siegert, A., Lichtenegger, W., Dietel, M., and Hauptmann, S. (2002). Expression of mitogen-activated protein kinase phosphatase-1 (MKP-1) in primary human ovarian carcinoma. International journal of cancer *102*, 507-513.
208. Manzano, R.G., Montuenga, L.M., Dayton, M., Dent, P., Kinoshita, I., Vicent, S., Gardner, G.J., Nguyen, P., Choi, Y.H., Trepel, J., et al. (2002). CL100 expression is down-regulated in advanced epithelial ovarian cancer and its re-expression decreases its malignant potential. Oncogene *21*, 4435-4447.
209. Rauhala, H.E., Porkka, K.P., Tolonen, T.T., Martikainen, P.M., Tammela, T.L., and Visakorpi, T. (2005). Dual-specificity phosphatase 1 and serum/glucocorticoid-regulated kinase are downregulated in prostate cancer. International journal of cancer *117*, 738-745.
210. Marchetti, S., Gimond, C., Roux, D., Gothie, E., Pouyssegur, J., and Pages, G. (2004). Inducible expression of a MAP kinase phosphatase-3-GFP chimera specifically blunts fibroblast growth and ras-dependent tumor formation in nude mice. Journal of cellular physiology *199*, 441-450.
211. Xu, S., Furukawa, T., Kanai, N., Sunamura, M., and Horii, A. (2005). Abrogation of DUSP6 by hypermethylation in human pancreatic cancer. Journal of human genetics *50*, 159-167.
212. Calogeraki, I., Barnier, J.V., Eychene, A., Felder, M.P., Calothy, G., and Marx, M. (1993). Genomic organization and nucleotide sequence of the coding region of the chicken c-Rmil(B-raf-1) proto-oncogene. Biochemical and biophysical research communications *193*, 1324-1331.
213. Eychene, A., Barnier, J.V., Apiou, F., Dutrillaux, B., and Calothy, G. (1992). Chromosomal assignment of two human B-raf(Rmil) proto-oncogene loci: B-raf-1 encoding the p94Braf/Rmil and B-raf-2, a processed pseudogene. Oncogene *7*, 1657-1660.
214. Jansen, H.W., Trachmann, C., and Bister, K. (1984). Structural relationship between the chicken protooncogene c-mil and the retroviral oncogene v-mil. Virology *137*, 217-224.
215. Sutrave, P., Bonner, T.I., Rapp, U.R., Jansen, H.W., Patschinsky, T., and Bister, K. (1984). Nucleotide sequence of avian retroviral oncogene v-mil: homologue of murine retroviral oncogene v-raf. Nature *309*, 85-88.
216. Davies, H., Bignell, G.R., Cox, C., Stephens, P., Edkins, S., Clegg, S., Teague, J., Woffendin, H., Garnett, M.J., Bottomley, W., et al. (2002). Mutations of the BRAF gene in human cancer. Nature *417*, 949-954.
217. Ciampi, R., and Nikiforov, Y.E. (2005). Alterations of the BRAF gene in thyroid tumors. Endocrine pathology *16*, 163-172.
218. Soares, P., Trovisco, V., Rocha, A.S., Feijao, T., Rebocho, A.P., Fonseca, E., Vieira de Castro, I., Cameselle-Teijeiro, J., Cardoso-Oliveira, M., and Sobrinho-

Simoes, M. (2004). BRAF mutations typical of papillary thyroid carcinoma are more frequently detected in undifferentiated than in insular and insular-like poorly differentiated carcinomas. Virchows Arch *444*, 572-576.
219. Trovisco, V., Vieira de Castro, I., Soares, P., Maximo, V., Silva, P., Magalhaes, J., Abrosimov, A., Guiu, X.M., and Sobrinho-Simoes, M. (2004). BRAF mutations are associated with some histological types of papillary thyroid carcinoma. The Journal of pathology *202*, 247-251.
220. Pollock, P.M., Harper, U.L., Hansen, K.S., Yudt, L.M., Stark, M., Robbins, C.M., Moses, T.Y., Hostetter, G., Wagner, U., Kakareka, J., et al. (2003). High frequency of BRAF mutations in nevi. Nat Genet *33*, 19-20.
221. Ciampi, R., Knauf, J.A., Rabes, H.M., Fagin, J.A., and Nikiforov, Y.E. (2005). BRAF kinase activation via chromosomal rearrangement in radiation-induced and sporadic thyroid cancer. Cell cycle (Georgetown, Tex *4*, 547-548.
222. Ciampi, R., Zhu, Z., and Nikiforov, Y.E. (2005). BRAF copy number gains in thyroid tumors detected by fluorescence in situ hybridization. Endocrine pathology *16*, 99-105.
223. Wellbrock, C., Ogilvie, L., Hedley, D., Karasarides, M., Martin, J., Niculescu-Duvaz, D., Springer, C.J., and Marais, R. (2004). V599EB-RAF is an oncogene in melanocytes. Cancer Res *64*, 2338-2342.
224. Wan, P.T., Garnett, M.J., Roe, S.M., Lee, S., Niculescu-Duvaz, D., Good, V.M., Jones, C.M., Marshall, C.J., Springer, C.J., Barford, D., et al. (2004). Mechanism of activation of the RAF-ERK signaling pathway by oncogenic mutations of B-RAF. Cell *116*, 855-867.
225. Calipel, A., Lefevre, G., Pouponnot, C., Mouriaux, F., Eychene, A., and Mascarelli, F. (2003). Mutation of B-Raf in human choroidal melanoma cells mediates cell proliferation and transformation through the MEK/ERK pathway. J Biol Chem *278*, 42409-42418.
226. Hingorani, S.R., Jacobetz, M.A., Robertson, G.P., Herlyn, M., and Tuveson, D.A. (2003). Suppression of BRAF(V599E) in human melanoma abrogates transformation. Cancer Res *63*, 5198-5202.
227. Patton, E.E., Widlund, H.R., Kutok, J.L., Kopani, K.R., Amatruda, J.F., Murphey, R.D., Berghmans, S., Mayhall, E.A., Traver, D., Fletcher, C.D., et al. (2005). BRAF mutations are sufficient to promote nevi formation and cooperate with p53 in the genesis of melanoma. Curr Biol *15*, 249-254.
228. Mercer, K., Giblett, S., Green, S., Lloyd, D., DaRocha Dias, S., Plumb, M., Marais, R., and Pritchard, C. (2005). Expression of endogenous oncogenic V600EB-raf induces proliferation and developmental defects in mice and transformation of primary fibroblasts. Cancer research *65*, 11493-11500.
229. Dankort, D., Curley, D.P., Cartlidge, R.A., Nelson, B., Karnezis, A.N., Damsky Jr, W.E., You, M.J., Depinho, R.A., McMahon, M., and Bosenberg, M. (2009). Braf(V600E) cooperates with Pten loss to induce metastatic melanoma. Nature genetics.
230. Dankort, D., Filenova, E., Collado, M., Serrano, M., Jones, K., and McMahon, M. (2007). A new mouse model to explore the initiation, progression, and therapy of BRAFV600E-induced lung tumors. Genes & development *21*, 379-384.

231. Knauf, J.A., Ma, X., Smith, E.P., Zhang, L., Mitsutake, N., Liao, X.H., Refetoff, S., Nikiforov, Y.E., and Fagin, J.A. (2005). Targeted expression of BRAFV600E in thyroid cells of transgenic mice results in papillary thyroid cancers that undergo dedifferentiation. Cancer research *65*, 4238-4245.
232. Lengauer, C., Kinzler, K.W., and Vogelstein, B. (1998). Genetic instabilities in human cancers. Nature *396*, 643-649.
233. Hsieh, P., and Yamane, K. (2008). DNA mismatch repair: molecular mechanism, cancer, and ageing. Mechanisms of ageing and development *129*, 391-407.
234. Wood, R.D. (1996). DNA repair in eukaryotes. Annual review of biochemistry *65*, 135-167.
235. Nowak, M.A., Komarova, N.L., Sengupta, A., Jallepalli, P.V., Shih Ie, M., Vogelstein, B., and Lengauer, C. (2002). The role of chromosomal instability in tumor initiation. Proceedings of the National Academy of Sciences of the United States of America *99*, 16226-16231.
236. Perucho, M. (1996). Cancer of the microsatellite mutator phenotype. Biological chemistry *377*, 675-684.
237. Jallepalli, P.V., and Lengauer, C. (2001). Chromosome segregation and cancer: cutting through the mystery. Nat Rev Cancer *1*, 109-117.
238. McNally, R.J., Rankin, J., Shirley, M.D., Rushton, S.P., and Pless-Mulloli, T. (2008). Space-time analysis of Down syndrome: results consistent with transient pre-disposing contagious agent. International journal of epidemiology *37*, 1169-1179.
239. Lengauer, C., Kinzler, K.W., and Vogelstein, B. (1997). Genetic instability in colorectal cancers. Nature *386*, 623-627.
240. Nowell, P.C. (1997). Genetic alterations in leukemias and lymphomas: impressive progress and continuing complexity. Cancer genetics and cytogenetics *94*, 13-19.
241. Bignold, L.P., Coghlan, B.L., and Jersmann, H.P. (2006). Hansemann, Boveri, chromosomes and the gametogenesis-related theories of tumours. Cell biology international *30*, 640-644.
242. Kops, G.J., Weaver, B.A., and Cleveland, D.W. (2005). On the road to cancer: aneuploidy and the mitotic checkpoint. Nat Rev Cancer *5*, 773-785.
243. Zhou, H., Kuang, J., Zhong, L., Kuo, W.L., Gray, J.W., Sahin, A., Brinkley, B.R., and Sen, S. (1998). Tumour amplified kinase STK15/BTAK induces centrosome amplification, aneuploidy and transformation. Nature genetics *20*, 189-193.
244. Fukasawa, K., Choi, T., Kuriyama, R., Rulong, S., and Vande Woude, G.F. (1996). Abnormal centrosome amplification in the absence of p53. Science (New York, N.Y *271*, 1744-1747.
245. Daniels, M.J., Wang, Y., Lee, M., and Venkitaraman, A.R. (2004). Abnormal cytokinesis in cells deficient in the breast cancer susceptibility protein BRCA2. Science (New York, N.Y *306*, 876-879.
246. Deng, C.X. (2002). Roles of BRCA1 in centrosome duplication. Oncogene *21*, 6222-6227.
247. Tutt, A., Gabriel, A., Bertwistle, D., Connor, F., Paterson, H., Peacock, J., Ross, G., and Ashworth, A. (1999). Absence of Brca2 causes genome instability by chromosome breakage and loss associated with centrosome amplification. Curr Biol *9*, 1107-1110.

248. Wang, R.H., Yu, H., and Deng, C.X. (2004). A requirement for breast-cancer-associated gene 1 (BRCA1) in the spindle checkpoint. Proceedings of the National Academy of Sciences of the United States of America *101*, 17108-17113.
249. McGrew, J.T., Goetsch, L., Byers, B., and Baum, P. (1992). Requirement for ESP1 in the nuclear division of Saccharomyces cerevisiae. Molecular biology of the cell *3*, 1443-1454.
250. Uzawa, S., Samejima, I., Hirano, T., Tanaka, K., and Yanagida, M. (1990). The fission yeast cut1+ gene regulates spindle pole body duplication and has homology to the budding yeast ESP1 gene. Cell *62*, 913-925.
251. Yamamoto, A., Guacci, V., and Koshland, D. (1996). Pds1p is required for faithful execution of anaphase in the yeast, Saccharomyces cerevisiae. The Journal of cell biology *133*, 85-97.
252. Jallepalli, P.V., Waizenegger, I.C., Bunz, F., Langer, S., Speicher, M.R., Peters, J.M., Kinzler, K.W., Vogelstein, B., and Lengauer, C. (2001). Securin is required for chromosomal stability in human cells. Cell *105*, 445-457.
253. Gassmann, R., Carvalho, A., Henzing, A.J., Ruchaud, S., Hudson, D.F., Honda, R., Nigg, E.A., Gerloff, D.L., and Earnshaw, W.C. (2004). Borealin: a novel chromosomal passenger required for stability of the bipolar mitotic spindle. The Journal of cell biology *166*, 179-191.
254. Fodde, R., Kuipers, J., Rosenberg, C., Smits, R., Kielman, M., Gaspar, C., van Es, J.H., Breukel, C., Wiegant, J., Giles, R.H., et al. (2001). Mutations in the APC tumour suppressor gene cause chromosomal instability. Nature cell biology *3*, 433-438.
255. Fodde, R., Smits, R., and Clevers, H. (2001). APC, signal transduction and genetic instability in colorectal cancer. Nat Rev Cancer *1*, 55-67.
256. Kaplan, K.B., Burds, A.A., Swedlow, J.R., Bekir, S.S., Sorger, P.K., and Nathke, I.S. (2001). A role for the Adenomatous Polyposis Coli protein in chromosome segregation. Nature cell biology *3*, 429-432.
257. Wassmann, K., and Benezra, R. (2001). Mitotic checkpoints: from yeast to cancer. Current opinion in genetics & development *11*, 83-90.
258. Michel, L.S., Liberal, V., Chatterjee, A., Kirchwegger, R., Pasche, B., Gerald, W., Dobles, M., Sorger, P.K., Murty, V.V., and Benezra, R. (2001). MAD2 haplo-insufficiency causes premature anaphase and chromosome instability in mammalian cells. Nature *409*, 355-359.
259. Dai, W., Wang, Q., Liu, T., Swamy, M., Fang, Y., Xie, S., Mahmood, R., Yang, Y.M., Xu, M., and Rao, C.V. (2004). Slippage of mitotic arrest and enhanced tumor development in mice with BubR1 haploinsufficiency. Cancer research *64*, 440-445.
260. Babu, J.R., Jeganathan, K.B., Baker, D.J., Wu, X., Kang-Decker, N., and van Deursen, J.M. (2003). Rae1 is an essential mitotic checkpoint regulator that cooperates with Bub3 to prevent chromosome missegregation. The Journal of cell biology *160*, 341-353.
261. Weaver, B.A., and Cleveland, D.W. (2007). Aneuploidy: instigator and inhibitor of tumorigenesis. Cancer research *67*, 10103-10105.

262. Weaver, B.A., Bonday, Z.Q., Putkey, F.R., Kops, G.J., Silk, A.D., and Cleveland, D.W. (2003). Centromere-associated protein-E is essential for the mammalian mitotic checkpoint to prevent aneuploidy due to single chromosome loss. The Journal of cell biology *162*, 551-563.
263. Weaver, B.A., Silk, A.D., Montagna, C., Verdier-Pinard, P., and Cleveland, D.W. (2007). Aneuploidy acts both oncogenically and as a tumor suppressor. Cancer cell *11*, 25-36.
264. Boveri, T. (1902). Ueber mehrpolige Mitosen als mittel zur Analyse des Zellkerns. Vehr. d. phys. med. Ges. zu Wurzburg NF *(available in English translation at http://8e.devbio.com/article.php?ch=4&id=24)*.
265. Boveri, T. (1914). Zur Frage der Entstehung maligner Tumoren. Translation Boveri M. The origin of malignant tumors. Baltimore: Williams and Wilkins; 1929.
266. Hansemann, D.v. (1890). Ueber asymmetrische Zelltheilung in Epithelkrebsen und deren biologische Bedeutung. Virchows Arch Path Anat *119*, 299-326.
267. Vogelstein, B., Fearon, E.R., Hamilton, S.R., Kern, S.E., Preisinger, A.C., Leppert, M., Nakamura, Y., White, R., Smits, A.M., and Bos, J.L. (1988). Genetic alterations during colorectal-tumor development. The New England journal of medicine *319*, 525-532.
268. Zimonjic, D., Brooks, M.W., Popescu, N., Weinberg, R.A., and Hahn, W.C. (2001). Derivation of human tumor cells in vitro without widespread genomic instability. Cancer research *61*, 8838-8844.
269. Duesberg, P., Li, R., Fabarius, A., and Hehlmann, R. (2006). Aneuploidy and cancer: from correlation to causation. Contributions to microbiology *13*, 16-44.
270. Li, R., Yerganian, G., Duesberg, P., Kraemer, A., Willer, A., Rausch, C., and Hehlmann, R. (1997). Aneuploidy correlated 100% with chemical transformation of Chinese hamster cells. Proceedings of the National Academy of Sciences of the United States of America *94*, 14506-14511.
271. Hahn, W.C., Counter, C.M., Lundberg, A.S., Beijersbergen, R.L., Brooks, M.W., and Weinberg, R.A. (1999). Creation of human tumour cells with defined genetic elements. Nature *400*, 464-468.
272. Loeb, L.A. (1991). Mutator phenotype may be required for multistage carcinogenesis. Cancer research *51*, 3075-3079.
273. Shih, I.M., Zhou, W., Goodman, S.N., Lengauer, C., Kinzler, K.W., and Vogelstein, B. (2001). Evidence that genetic instability occurs at an early stage of colorectal tumorigenesis. Cancer research *61*, 818-822.
274. Ried, T., Heselmeyer-Haddad, K., Blegen, H., Schrock, E., and Auer, G. (1999). Genomic changes defining the genesis, progression, and malignancy potential in solid human tumors: a phenotype/genotype correlation. Genes, chromosomes & cancer *25*, 195-204.
275. Mertens, F., Johansson, B., and Mitelman, F. (1994). Isochromosomes in neoplasia. Genes, chromosomes & cancer *10*, 221-230.
276. Cahill, D.P., Lengauer, C., Yu, J., Riggins, G.J., Willson, J.K., Markowitz, S.D., Kinzler, K.W., and Vogelstein, B. (1998). Mutations of mitotic checkpoint genes in human cancers. Nature *392*, 300-303.

277. Sotillo, R., Hernando, E., Diaz-Rodriguez, E., Teruya-Feldstein, J., Cordon-Cardo, C., Lowe, S.W., and Benezra, R. (2007). Mad2 overexpression promotes aneuploidy and tumorigenesis in mice. Cancer Cell *11*, 9-23.
278. Dominguez, A., Ramos-Morales, F., Romero, F., Rios, R.M., Dreyfus, F., Tortolero, M., and Pintor-Toro, J.A. (1998). hpttg, a human homologue of rat pttg, is overexpressed in hematopoietic neoplasms. Evidence for a transcriptional activation function of hPTTG. Oncogene *17*, 2187-2193.
279. Heaney, A.P., Singson, R., McCabe, C.J., Nelson, V., Nakashima, M., and Melmed, S. (2000). Expression of pituitary-tumour transforming gene in colorectal tumours. Lancet *355*, 716-719.
280. Saez, C., Japon, M.A., Ramos-Morales, F., Romero, F., Segura, D.I., Tortolero, M., and Pintor-Toro, J.A. (1999). hpttg is over-expressed in pituitary adenomas and other primary epithelial neoplasias. Oncogene *18*, 5473-5476.
281. Torii, S., Nakayama, K., Yamamoto, T., and Nishida, E. (2004). Regulatory mechanisms and function of ERK MAP kinases. J Biochem (Tokyo) *136*, 557-561.
282. Treisman, R. (1996). Regulation of transcription by MAP kinase cascades. Curr Opin Cell Biol *8*, 205-215.
283. Morice, C., Nothias, F., Konig, S., Vernier, P., Baccarini, M., Vincent, J.D., and Barnier, J.V. (1999). Raf-1 and B-Raf proteins have similar regional distributions but differential subcellular localization in adult rat brain. Eur J Neurosci *11*, 1995-2006.
284. Hayne, C., Tzivion, G., and Luo, Z. (2000). Raf-1/MEK/MAPK pathway is necessary for the G2/M transition induced by nocodazole. The Journal of biological chemistry *275*, 31876-31882.
285. Ziogas, A., Lorenz, I.C., Moelling, K., and Radziwill, G. (1998). Mitotic Raf-1 is stimulated independently of Ras and is active in the cytoplasm. The Journal of biological chemistry *273*, 24108-24114.
286. Hoffman, D.B., Pearson, C.G., Yen, T.J., Howell, B.J., and Salmon, E.D. (2001). Microtubule-dependent changes in assembly of microtubule motor proteins and mitotic spindle checkpoint proteins at PtK1 kinetochores. Molecular biology of the cell *12*, 1995-2009.
287. Kumar, R., Angelini, S., Czene, K., Sauroja, I., Hahka-Kemppinen, M., Pyrhonen, S., and Hemminki, K. (2003). BRAF mutations in metastatic melanoma: a possible association with clinical outcome. Clin Cancer Res *9*, 3362-3368.
288. Libra, M., Malaponte, G., Navolanic, P.M., Gangemi, P., Bevelacqua, V., Proietti, L., Bruni, B., Stivala, F., Mazzarino, M.C., Travali, S., et al. (2005). Analysis of BRAF mutation in primary and metastatic melanoma. Cell Cycle *4*, 1382-1384.
289. Nikiforova, M.N., Kimura, E.T., Gandhi, M., Biddinger, P.W., Knauf, J.A., Basolo, F., Zhu, Z., Giannini, R., Salvatore, G., Fusco, A., et al. (2003). BRAF mutations in thyroid tumors are restricted to papillary carcinomas and anaplastic or poorly differentiated carcinomas arising from papillary carcinomas. J Clin Endocrinol Metab *88*, 5399-5404.
290. Singer, G., Oldt, R., 3rd, Cohen, Y., Wang, B.G., Sidransky, D., Kurman, R.J., and Shih Ie, M. (2003). Mutations in BRAF and KRAS characterize the

development of low-grade ovarian serous carcinoma. J Natl Cancer Inst *95*, 484-486.
291. Young, J., Barker, M.A., Simms, L.A., Walsh, M.D., Biden, K.G., Buchanan, D., Buttenshaw, R., Whitehall, V.L., Arnold, S., Jackson, L., et al. (2005). Evidence for BRAF mutation and variable levels of microsatellite instability in a syndrome of familial colorectal cancer. Clin Gastroenterol Hepatol *3*, 254-263.
292. Satyamoorthy, K., Li, G., Gerrero, M.R., Brose, M.S., Volpe, P., Weber, B.L., Van Belle, P., Elder, D.E., and Herlyn, M. (2003). Constitutive mitogen-activated protein kinase activation in melanoma is mediated by both BRAF mutations and autocrine growth factor stimulation. Cancer Res *63*, 756-759.
293. Calipel, A., Lefevre, G., Pouponnot, C., Mouriaux, F., Eychene, A., and Mascarelli, F. (2003). Mutation of B-Raf in human choroidal melanoma cells mediates cell proliferation and transformation through the MEK/ERK pathway. J Biol Chem.
294. Karasarides, M., Chiloeches, A., Hayward, R., Niculescu-Duvaz, D., Scanlon, I., Friedlos, F., Ogilvie, L., Hedley, D., Martin, J., Marshall, C.J., et al. (2004). B-RAF is a therapeutic target in melanoma. Oncogene *23*, 6292-6298.
295. Hoeflich, K.P., Gray, D.C., Eby, M.T., Tien, J.Y., Wong, L., Bower, J., Gogineni, A., Zha, J., Cole, M.J., Stern, H.M., et al. (2006). Oncogenic BRAF is required for tumor growth and maintenance in melanoma models. Cancer Res *66*, 999-1006.
296. Sharma, A., Trivedi, N.R., Zimmerman, M.A., Tuveson, D.A., Smith, C.D., and Robertson, G.P. (2005). Mutant V599EB-Raf regulates growth and vascular development of malignant melanoma tumors. Cancer Res *65*, 2412-2421.
297. Bhatt, K.V., Hu, R., Spofford, L.S., and Aplin, A.E. (2007). Mutant B-RAF signaling and cyclin D1 regulate Cks1/S-phase kinase-associated protein 2-mediated degradation of p27Kip1 in human melanoma cells. Oncogene *26*, 1056-1066.
298. Bhatt, K.V., Spofford, L.S., Aram, G., McMullen, M., Pumiglia, K., and Aplin, A.E. (2005). Adhesion control of cyclin D1 and p27Kip1 levels is deregulated in melanoma cells through BRAF-MEK-ERK signaling. Oncogene *24*, 3459-3471.
299. Boisvert-Adamo, K., and Aplin, A.E. (2006). B-RAF and PI-3 kinase signaling protect melanoma cells from anoikis. Oncogene *25*, 4848-4856.
300. Boisvert-Adamo, K., and Aplin, A.E. (2008). Mutant B-RAF mediates resistance to anoikis via Bad and Bim. Oncogene *27*, 3301-3312.
301. Risques, R.A., Moreno, V., Ribas, M., Marcuello, E., Capella, G., and Peinado, M.A. (2003). Genetic pathways and genome-wide determinants of clinical outcome in colorectal cancer. Cancer research *63*, 7206-7214.
302. Zhou, W., Goodman, S.N., Galizia, G., Lieto, E., Ferraraccio, F., Pignatelli, C., Purdie, C.A., Piris, J., Morris, R., Harrison, D.J., et al. (2002). Counting alleles to predict recurrence of early-stage colorectal cancers. Lancet *359*, 219-225.
303. Fukasawa, K. (2007). Oncogenes and tumour suppressors take on centrosomes. Nat Rev Cancer *7*, 911-924.
304. Bastian, B.C., LeBoit, P.E., Hamm, H., Brocker, E.B., and Pinkel, D. (1998). Chromosomal gains and losses in primary cutaneous melanomas detected by comparative genomic hybridization. Cancer Res *58*, 2170-2175.

305. Bastian, B.C., Olshen, A.B., LeBoit, P.E., and Pinkel, D. (2003). Classifying melanocytic tumors based on DNA copy number changes. Am J Pathol *163*, 1765-1770.
306. Cui, Y., and Guadagno, T.M. (2008). B-Raf(V600E) signaling deregulates the mitotic spindle checkpoint through stabilizing Mps1 levels in melanoma cells. Oncogene *27*, 3122-3133.
307. Colanzi, A., Deerinck, T.J., Ellisman, M.H., and Malhotra, V. (2000). A specific activation of the mitogen-activated protein kinase kinase 1 (MEK1) is required for Golgi fragmentation during mitosis. The Journal of cell biology *149*, 331-339.
308. Wu, C., Lai, C.F., and Mobley, W.C. (2001). Nerve growth factor activates persistent Rap1 signaling in endosomes. J Neurosci *21*, 5406-5416.
309. Huo, L.J., Yu, L.Z., Liang, C.G., Fan, H.Y., Chen, D.Y., and Sun, Q.Y. (2005). Cell-cycle-dependent subcellular localization of cyclin B1, phosphorylated cyclin B1 and p34cdc2 during oocyte meiotic maturation and fertilization in mouse. Zygote *13*, 45-53.
310. Abrieu, A., Magnaghi-Jaulin, L., Kahana, J.A., Peter, M., Castro, A., Vigneron, S., Lorca, T., Cleveland, D.W., and Labbe, J.C. (2001). Mps1 is a kinetochore-associated kinase essential for the vertebrate mitotic checkpoint. Cell *106*, 83-93.
311. Stucke, V.M., Sillje, H.H., Arnaud, L., and Nigg, E.A. (2002). Human Mps1 kinase is required for the spindle assembly checkpoint but not for centrosome duplication. Embo J *21*, 1723-1732.
312. Borysova, M.K., Cui, Y., Snyder, M., and Guadagno, T.M. (2008). Knockdown of B-Raf impairs spindle formation and the mitotic checkpoint in human somatic cells. Cell Cycle *7*, 2894-2901.
313. Chen, R.H. (2004). Phosphorylation and activation of Bub1 on unattached chromosomes facilitate the spindle checkpoint. Embo J *23*, 3113-3121.
314. Diaz-Rodriguez, E., Sotillo, R., Schvartzman, J.M., and Benezra, R. (2008). Hec1 overexpression hyperactivates the mitotic checkpoint and induces tumor formation in vivo. Proceedings of the National Academy of Sciences of the United States of America *105*, 16719-16724.
315. Salvatore, G., De Falco, V., Salerno, P., Nappi, T.C., Pepe, S., Troncone, G., Carlomagno, F., Melillo, R.M., Wilhelm, S.M., and Santoro, M. (2006). BRAF is a therapeutic target in aggressive thyroid carcinoma. Clin Cancer Res *12*, 1623-1629.
316. Giancotti, F.G., and Tarone, G. (2003). Positional control of cell fate through joint integrin/receptor protein kinase signaling. Annual review of cell and developmental biology *19*, 173-206.
317. Frisch, S.M., and Francis, H. (1994). Disruption of epithelial cell-matrix interactions induces apoptosis. The Journal of cell biology *124*, 619-626.
318. Kunz, M., and Ibrahim, S.M. (2003). Molecular responses to hypoxia in tumor cells. Molecular cancer *2*, 23.
319. Kumar, S.M., Yu, H., Edwards, R., Chen, L., Kazianis, S., Brafford, P., Acs, G., Herlyn, M., and Xu, X. (2007). Mutant V600E BRAF increases hypoxia inducible factor-1alpha expression in melanoma. Cancer research *67*, 3177-3184.

320. Conner, S.R., Scott, G., and Aplin, A.E. (2003). Adhesion-dependent activation of the ERK1/2 cascade is by-passed in melanoma cells. The Journal of biological chemistry *278*, 34548-34554.
321. Vance, K.W., and Goding, C.R. (2004). The transcription network regulating melanocyte development and melanoma. Pigment cell research / sponsored by the European Society for Pigment Cell Research and the International Pigment Cell Society *17*, 318-325.
322. Goodall, J., Wellbrock, C., Dexter, T.J., Roberts, K., Marais, R., and Goding, C.R. (2004). The Brn-2 transcription factor links activated BRAF to melanoma proliferation. Molecular and cellular biology *24*, 2923-2931.
323. Bornstein, G., Bloom, J., Sitry-Shevah, D., Nakayama, K., Pagano, M., and Hershko, A. (2003). Role of the SCFSkp2 ubiquitin ligase in the degradation of p21Cip1 in S phase. The Journal of biological chemistry *278*, 25752-25757.
324. Carrano, A.C., Eytan, E., Hershko, A., and Pagano, M. (1999). SKP2 is required for ubiquitin-mediated degradation of the CDK inhibitor p27. Nature cell biology *1*, 193-199.
325. Kamura, T., Hara, T., Kotoshiba, S., Yada, M., Ishida, N., Imaki, H., Hatakeyama, S., Nakayama, K., and Nakayama, K.I. (2003). Degradation of p57Kip2 mediated by SCFSkp2-dependent ubiquitylation. Proceedings of the National Academy of Sciences of the United States of America *100*, 10231-10236.
326. Mendez, J., Zou-Yang, X.H., Kim, S.Y., Hidaka, M., Tansey, W.P., and Stillman, B. (2002). Human origin recognition complex large subunit is degraded by ubiquitin-mediated proteolysis after initiation of DNA replication. Molecular cell *9*, 481-491.
327. Nakayama, K., Nagahama, H., Minamishima, Y.A., Matsumoto, M., Nakamichi, I., Kitagawa, K., Shirane, M., Tsunematsu, R., Tsukiyama, T., Ishida, N., et al. (2000). Targeted disruption of Skp2 results in accumulation of cyclin E and p27(Kip1), polyploidy and centrosome overduplication. The EMBO journal *19*, 2069-2081.
328. Tsvetkov, L.M., Yeh, K.H., Lee, S.J., Sun, H., and Zhang, H. (1999). p27(Kip1) ubiquitination and degradation is regulated by the SCF(Skp2) complex through phosphorylated Thr187 in p27. Curr Biol *9*, 661-664.
329. Hu, R., and Aplin, A.E. (2008). Skp2 regulates G2/M progression in a p53-dependent manner. Molecular biology of the cell *19*, 4602-4610.
330. Hanahan, D., and Weinberg, R.A. (2000). The hallmarks of cancer. Cell *100*, 57-70.
331. Frasca, F., Nucera, C., Pellegriti, G., Gangemi, P., Attard, M., Stella, M., Loda, M., Vella, V., Giordano, C., Trimarchi, F., et al. (2008). BRAF(V600E) mutation and the biology of papillary thyroid cancer. Endocrine-related cancer *15*, 191-205.
332. Mesa, C., Jr., Mirza, M., Mitsutake, N., Sartor, M., Medvedovic, M., Tomlinson, C., Knauf, J.A., Weber, G.F., and Fagin, J.A. (2006). Conditional activation of RET/PTC3 and BRAFV600E in thyroid cells is associated with gene expression profiles that predict a preferential role of BRAF in extracellular matrix remodeling. Cancer research *66*, 6521-6529.

333. Coussens, L.M., Fingleton, B., and Matrisian, L.M. (2002). Matrix metalloproteinase inhibitors and cancer: trials and tribulations. Science (New York, N.Y *295*, 2387-2392.
334. Klein, R.M., Spofford, L.S., Abel, E.V., Ortiz, A., and Aplin, A.E. (2008). B-RAF regulation of Rnd3 participates in actin cytoskeletal and focal adhesion organization. Molecular biology of the cell *19*, 498-508.
335. *Cui, Y., *Borysova, M.E., Guadagno, T.M. (*authors contributed equally to this work) (Under Review). Oncogenic B-RafV600E induces spindle abnormalities, supernumerary centrosomes, and aneuploidy in human melanocytic cells. PNAS.
336. Mitsutake, N., Knauf, J.A., Mitsutake, S., Mesa, C., Jr., Zhang, L., and Fagin, J.A. (2005). Conditional BRAFV600E expression induces DNA synthesis, apoptosis, dedifferentiation, and chromosomal instability in thyroid PCCL3 cells. Cancer research *65*, 2465-2473.
337. Ford, J.H., Schultz, C.J., and Correll, A.T. (1988). Chromosome elimination in micronuclei: a common cause of hypoploidy. American journal of human genetics *43*, 733-740.
338. Denko, N.C., Giaccia, A.J., Stringer, J.R., and Stambrook, P.J. (1994). The human Ha-ras oncogene induces genomic instability in murine fibroblasts within one cell cycle. Proceedings of the National Academy of Sciences of the United States of America *91*, 5124-5128.
339. Saavedra, H.I., Knauf, J.A., Shirokawa, J.M., Wang, J., Ouyang, B., Elisei, R., Stambrook, P.J., and Fagin, J.A. (2000). The RAS oncogene induces genomic instability in thyroid PCCL3 cells via the MAPK pathway. Oncogene *19*, 3948-3954.
340. Hernando, E., Nahle, Z., Juan, G., Diaz-Rodriguez, E., Alaminos, M., Hemann, M., Michel, L., Mittal, V., Gerald, W., Benezra, R., et al. (2004). Rb inactivation promotes genomic instability by uncoupling cell cycle progression from mitotic control. Nature *430*, 797-802.
341. Michaloglou, C., Vredeveld, L.C., Mooi, W.J., and Peeper, D.S. (2008). BRAF(E600) in benign and malignant human tumours. Oncogene *27*, 877-895.
342. Michaloglou, C., Vredeveld, L.C., Soengas, M.S., Denoyelle, C., Kuilman, T., van der Horst, C.M., Majoor, D.M., Shay, J.W., Mooi, W.J., and Peeper, D.S. (2005). BRAFE600-associated senescence-like cell cycle arrest of human naevi. Nature *436*, 720-724.
343. Smalley, K.S., and Flaherty, K.T. (2009). Integrating BRAF/MEK inhibitors into combination therapy for melanoma. British journal of cancer *100*, 431-435.
344. da Rocha Dias, S., Friedlos, F., Light, Y., Springer, C., Workman, P., and Marais, R. (2005). Activated B-RAF is an Hsp90 client protein that is targeted by the anticancer drug 17-allylamino-17-demethoxygeldanamycin. Cancer research *65*, 10686-10691.
345. Fukuyo, Y., Inoue, M., Nakajima, T., Higashikubo, R., Horikoshi, N.T., Hunt, C., Usheva, A., Freeman, M.L., and Horikoshi, N. (2008). Oxidative stress plays a critical role in inactivating mutant BRAF by geldanamycin derivatives. Cancer research *68*, 6324-6330.

346. Gascoigne, K.E., and Taylor, S.S. (2008). Cancer cells display profound intra- and interline variation following prolonged exposure to antimitotic drugs. Cancer cell *14*, 111-122.
347. Desai, A., Murray, A., Mitchison, T.J., and Walczak, C.E. (1999). The use of Xenopus egg extracts to study mitotic spindle assembly and function in vitro. Methods Cell Biol *61*, 385-412.

## ABOUT THE AUTHOR

Meghan Borysova was born in Chicago, Illinois in 1973. She grew up in Michigan and in 1994, she moved to Tucson, Arizona where she began her scientific career. Meghan received her Bachelor's degree in Molecular and Cellular Biology from the University of Arizona where she worked as a researcher for eight years. In 2003, Meghan moved to Tampa entering Moffitt Cancer Center's Cancer Biology, Ph.D. program in 2004. Imaging is Meghan's favorite scientific medium.

Meghan is a wife and devoted mother. Meghan and her family enjoy long walks on the waterfront, gardening, and going to parks. Meghan and her husband enjoy the arts and exploring new foods. Meghan loves to bake, write in the children's journals, run a Mommy listserv, and read about science and politics.

Meghan's future plans are to develop a career in Cancer Imaging and to enjoy her enriching, fulfilling family life.